12-10-2018

# Ghrelin Regulates Energy Homeostasis Through Discrete Central and Peripheral Signaling Mechanisms

Michael Alex Thomas
*Georgia State University*

# GHRELIN REGULATES ENERGY HOMEOSTASIS THROUGH DISCRETE CENTRAL AND PERIPHERAL SIGNALING MECHANISMS

by

MICHAEL ALEX THOMAS

Under the Direction of Bingzhong Xue, PhD

## ABSTRACT

The obesity epidemic is a major health and economic burden in the United States with approximately 35% of the population classified as overweight or obese, and annual medical costs for obese persons is approximately 150% more relative to lean persons. Obesity can develop when energy intake exceeds energy expenditure, and the stomach-derived orexigenic hormone ghrelin has emerged as a key mediator of this balance in humans due to its increased circulating concentrations in obese persons and involvement in regulating ingestive behaviors and numerous metabolic processes. We and others have previously shown ghrelin is sufficient to drive both appetitive (i.e. the searching for and storage of food) and consummatory (i.e. the consumption of food) ingestive behaviors and metabolic processes such as gut motility, nutrient partitioning, glycemia, and body temperature. The ghrelin receptor, growth hormone secretagogue receptor

1a (GHSR), is widely expressed in the brain and on gastrointestinal vagal sensory neurons, and neuronal GHSR knockout affords protection against diet-induced obesity and glycemic dysregulation. Hence, the absence of ghrelin signaling results in a profoundly beneficial metabolic profile and elucidating the mechanisms through which ghrelin mediates ingestive behaviors and metabolic processes may provide novel obesity treatment options. Targeted central/peripheral ghrelin injections or neuronal-specific GHSR restoration in otherwise GHSR-null mice has provided mounting evidence for discrete neuroanatomical mechanisms regulating ghrelin's behavioral and metabolic effects, yet a thorough interrogation of these distributed signaling pathways in the context of ghrelin-mediated ingestive behaviors or metabolism has yet to be conducted. Here, we utilize two rodent models (Siberian hamsters and mice) to examine the mechanisms through which ghrelin regulates ingestive behaviors and overall metabolic homeostasis. We find that central ghrelin signaling is necessary and sufficient to drive appetitive and consummatory ingestive behaviors and that hypothalamic agouti-related peptide is critical for ghrelin-induced appetitive, but not consummatory, behaviors. In addition, we identify a novel, peripheral sensory neuron ghrelin signaling pathway that is critical for regulating energy expenditure and metabolic homeostasis. Thus, this dissertation provides a significant step forward for our understanding of ghrelin signaling and the discrete mechanisms through which it mediates behaviors and metabolic processes.

INDEX WORDS: Ghrelin, Metabolism, Appetitive, Consummatory, Dorsal root ganglia, Knockout mouse, Energy homeostasis, GHSR1a

# GHRELIN REGULATES METABOLIC HOMEOSTASIS THROUGH DISCRETE CENTRAL AND PERIPHERAL SIGNALING MECHANISMS

by

MICHAEL ALEX THOMAS

A Dissertation Submitted in Partial Fulfillment of the Requirements for the Degree of

Doctor of Philosophy

in the College of Arts and Sciences

Georgia State University

2018

# GHRELIN REGULATES METABOLIC HOMEOSTASIS THROUGH DISCRETE CENTRAL AND PERIPHERAL SIGNALING MECHANISMS

by

MICHAEL ALEX THOMAS

Committee Chair: Bingzhong Xue

Committee: Bingzhong Xue

Hang Shi

Christoph Buettner

Electronic Version Approved:

Office of Graduate Studies

College of Arts and Sciences

Georgia State University

December, 2018

## DEDICATION

This dissertation is dedicated to my wife, family and friends who never hesitated in their love and support for me and provided the daily motivation that facilitated this journey. Without them I would not have been able to complete any facet of this work, and I am grateful beyond words for all that you have done for me.

# ACKNOWLEDGEMENTS

I would like to acknowledge and thank the countless professors and scientists that have been integral in my completion of this degree and development as a scientist. I am eternally grateful to Dr. Timothy Bartness and Dr. Bingzhong Xue for sharing their immense knowledge, expertise, and wisdom for both science and life. I am also thankful to my other committee members, Dr. Christoph Buettner and Dr. Hang Shi, for providing their time, knowledge, and insights at every step along this journey.

I would also like to thank past and present Bartness and Xue lab members who have served as both friends and mentors throughout my time as a graduate student. In particular, Dr. Johnny Garretson, Dr. Ngoc Ly Nguyen, Dr. Laura Szymanski, Dr. Brett Tuebner, Dr. Qiang Cao, Dr. Xin Cui, Dr. Jia Jing, Dr. Fenfen Li, and Dr. Emily Bruggeman.

Lastly, I am grateful for past professors who helped instill a scientific mindset and provided the foundation through which I developed as a scientist. Dr. Andrei Barkovskii, Dr. William Walthall, Dr. Vincent Rehdar, Dr. Paul Ulrich, Nancy Russell, and Dr. David Blaustein. Finally, I thank Georgia State University and the NIH for awarding me the 2CI Obesity Reversal Fellowship and NRSA F31 Predoctoral Fellowship respectively. Without these awards I would not have had the funding necessary to complete this work.

# TABLE OF CONTENTS

## LIST OF FIGURES

# LIST OF ABBREVIATIONS

3V, third ventricle

ACOX1, acyl-CoA oxidase 1

AgRP, agouti related protein

Arc, arcuate nucleus

β3AR, β3 adrenergic receptor

BAT, brown adipose tissue

BM, body mass

CIDEA, cell death-inducing DFFA-like effector A

CPT1B, carnitine palmitoyltransferase 1B

CCK, cholecystokinin

COX1, cyclooxygenase 1

DEPC, diethylpyrocarbonate

DIO2, iodothyronine deiodinase 2

DMH, dorsomedial hypothalamus

DMV, dorsal motor vagus

DRG, dorsal root ganglia

DsiRNA, DICER small interfering RNA

ELOVL3, ELOVL fatty acid elongase 3

eWAT, epididymal white adipose tissue

FD, food deprivation

FF, food foraging

FH, food hoarding

FI, food intake

GABA, gamma-aminobutyric acid

GHSR, growth hormone secretagogue receptor 1a

GI, gastrointestinal

GLP-1, glucagon-like peptide-1

GOAT, ghrelin *O*-acyl-transferase

ICV, intracerebroventricular

iBAT, interscapular brown adipose tissue

iWAT, inguinal white adipose tissue

ip, intraperitoneal

ir, immunoreactivity

MC3R, melanocortin 3 receptor

MC4R, melanocortin 4 receptor

NPY, neuropeptide Y

NTS, nucleus tractus solitarius

PPAR-α, peroxisome proliferator activated receptor alpha

PPAR- γ, peroxisome proliferator activated receptor gamma

PGC-1β, PPARG coactivator 1 beta

PRDM16, PR domain containing 16

POMC, pro-opiomelanocortin

PVH, paraventricular hypothalamus

PYY, peptide YY

qPCR, quantitative polymerase chain reaction

RFI, relative fluorescent intensity

S.C., subcutaneous

scRNA, scrambled RNA

SNS, sympathetic nervous system

UCP-1, uncoupling protein 1

UCP-3, uncoupling protein 3

VMH, ventromedial hypothalamus

VTA, ventral tegmental area

# 1 INTRODUCTION

## 1.1 Global rise of the Obesity Epidemic

Over 1.4 billion people worldwide are classified as overweight or obese with the number of affected persons nearly doubling in developed countries and tripling in developing countries since 1980 [1]. As obesity is closely associated with a myriad of secondary health consequences including diabetes, stroke, and some types of cancers, the resulting annual medical costs for obese persons is approximately 42% higher than lean persons [2]. The dramatic increase in obesity rates and resultant economic impact is due, in part, to an increasingly sedentary lifestyle coupled with the prevalence of inexpensive, calorically dense foods with long shelf lives. To this end, obesity can develop when energy intake exceeds energy expenditure, and there are multiple behavioral and metabolic factors that contribute to this imbalance and can compound the effects of consuming energy rich foods and a sedentary lifestyle. Daily fluctuations in orexigenic (e.g. the stomach derived hormone ghrelin [3]) or satiety hormones (e.g. leptin [4]) correspond with physiological changes that mediate the searching for and storage of food, energy conservation, or the liberation of energy stores [5-11]. Hence, a comprehensive interrogation of the ethological, genetic, and neuroanatomical mechanism through which animals (including humans) regulate energy homeostasis is critical for stopping the obesity epidemic.

Previous work on the neuroendocrine control of energy homeostasis has largely focused on uncovering the central (i.e. brain) mechanisms regulating food intake and peripheral metabolism and, in the process, identified a detailed neuroanatomical framework regulating these outputs. However, both central and peripheral endocrine signaling is critical for metabolic

control, and uncovering the distributed systems regulating excessive weight gain through behavioral and non-behavioral mechanisms will inevitably lead to better treatment options to reduce the obesity epidemic. Therefore, the overall goal of this dissertation is to investigate how discrete central and peripheral neuroendocrine signaling regulates behavior and metabolism, with a focus on the orexigenic hormone ghrelin which has been identified as a key mediator of energy homeostasis.

## 1.2 Ethological and Neuroendocrine Control of Body Mass

Obese and lean animals, including humans, have clear differences in the physiological mechanisms regulating metabolism and ingestive behaviors [12, 13], yet previous studies examining the neuroendocrine control of energy homeostasis have primarily focused on food intake and largely ignored the appetitive behaviors that bring animals into contact with food. To this end, humans invariably search (forage) for food (e.g. at grocery stores and restaurants) prior to consumption, and numerous studies have suggested overweight and obese persons purchase more calorically dense foods and store these foods (hoard) for longer periods of time compared with lean persons (e.g. in cupboards and refrigerators) [14-17]. In an evolutionary context, an adaptive response to energetic challenges in which animals increase food hoarding, rather than overeat, upon locating food would prove beneficial for two reasons: first, a surplus of stored food would allow an animal to expend minimal energy to acquire the next meal and thus expedite the replenishment of lost calories; second, the long-term storage of food would mitigate the potential for future negative energy balances. Caloric restriction is the most potent stimulator of food foraging and food hoarding in humans and laboratory rodents, and it elicits a profoundly negative valence signal mediated, in part, through neuroendocrine signaling that drives energy conservation and food seeking behaviors to prevent starvation and replenish energy stores [18,

19]. These energy stores are maintained through a tightly regulated network involving the brain and periphery, and peripheral organs such as the stomach and adipose tissue can communicate with central nuclei through neuronal and/or endocrine signaling mechanisms [11, 20, 21]. Indeed, we and others have previously identified numerous peripheral endocrine signals, whose circulating concentrations are dependent on caloric state, that are sufficient to modulate ingestive behaviors, adipose tissue metabolism, and energy expenditure through activation of brain nuclei [22-26]. This behavioral and metabolic response to caloric deficiency would increase the survival probability of ancestral humans, but when coupled with the advent of calorically dense foods with long shelf-lives it directly contributes to the obesity epidemic in contemporary society.

As the behavioral and metabolic parameters regulating energy homeostasis are often mediated by the same neuroendocrine mechanisms, it is logical to classify the concomitant responses to caloric imbalance as either behavioral or metabolic. At the most basic level, maintaining energy homeostasis necessitates central and peripheral mechanisms that relay nutrient state to avoid overeating or starvation. For instance, ghrelin promotes caloric intake and adiposity through a marked increase in food foraging, food hoarding, and food intake (i.e. a behavioral response) while simultaneously decreasing fatty acid utilization and liberation (i.e. a metabolic response) [22, 27-31]. In the context of adipose tissue metabolism and energy expenditure, this ghrelin signal → central/peripheral nuclei → adipose metabolic response can manifest through altered sympathetic nervous system (SNS) outflow [32-36]. The SNS is the primary driver of lipolysis, and changes to SNS outflow is sufficient to modulate whole body energy expenditure [33, 37-43]. Indeed, central ghrelin injections that circumvent peripheral receptors are sufficient to mediate both ingestive behaviors and sympathetic outflow [35, 44-47],

yet emerging evidence suggests these responses are mediated by a complex, distributed ghrelin signaling network. Direct brain activation can occur directly through humoral circulating [48-51], and numerous central nuclei critical for metabolic control are circumventricular organs exposed to circulating ghrelin [51-55]. By contrast, ghrelin responsive enteric sensory neurons emanating from the vagus nerve and dorsal root ganglia (DRGs) can facilitate rapid crosstalk with the brain [56-59], and previous work has demonstrated ghrelin activation of hindbrain or vagal sensory neurons is sufficient to mediate food intake, energy expenditure, and adipose tissue metabolism [60-62]. These vagal and DRG sensory neurons can synapse with hindbrain nuclei that project to, and receive projections from, numerous hypothalamic nuclei critical for both ingestive behaviors and metabolic control [63-66], and presence of multiple pathways regulating energy homeostasis may provide the basis through which peripheral endocrine signals drive behaviors and/or metabolic processes. In support of this, ghrelin microinjections into hypothalamic nuclei is sufficient to drive a rapid, robust increase in ingestive behaviors, whereas microinjections into the hindbrain can decrease SNS outflow and energy expenditure independent of food intake effects [47, 67-72]. As previous work has predominantly focused on a single experimental outcome (i.e. food intake or augmented metabolic processes), an approach that examines both behavioral and non-behavioral control of whole-body energy homeostasis represents a novel paradigm to combat the obesity epidemic.

### *1.2.1 Siberian hamsters as a model to study ingestive behaviors*

Animal models used to study obesity have largely consisted of mice and rats, and the advent of genetic modification in these animals has provided a paradigm shift in how we can interrogate the neuroendocrine mechanisms regulating metabolism. However, genetic mutations account for less than 5% of obesity cases in people [73], and mice and rats have limited use for

obesity related behavioral studies because they do not naturally hoard food. By contrast, Siberian hamsters (*Phodopus sungorus*), like humans, are natural and prodigious food hoarders [74-76]. Siberian hamsters housed in short day photoperiod (8 hours light) accumulate up to 50% body mass (a state that would be considered morbidly obese in humans) and simultaneously increase the amount of food hoarded [74, 76-78]. Hence, these animals provide an ideal model to study ingestive behaviors in the context of obesity as they display similar changes in food intake, food foraging, and food hoarding as obese humans.

Interrogating the mechanisms regulating appetitive and consummatory behaviors necessitates the use of a unique experimental set up in which food foraging, food hoarding, and food intake can be delineated. To accomplish this, we have previously developed a novel foraging/hoarding apparatus consisting of a transparent foraging cage, in which food is earned through wheel running, and an opaque hoarding cage in which the animal sleeps and stores food (**Fig. 1.1**) [79]. In brief, a running wheel present in the top, foraging cage is fitted with a magnet and a magnet detector connected to a computer is placed on the metal cage lid. For every 10-wheel revolutions, a food pellet is dispensed and the animal can either 1) immediately consume the

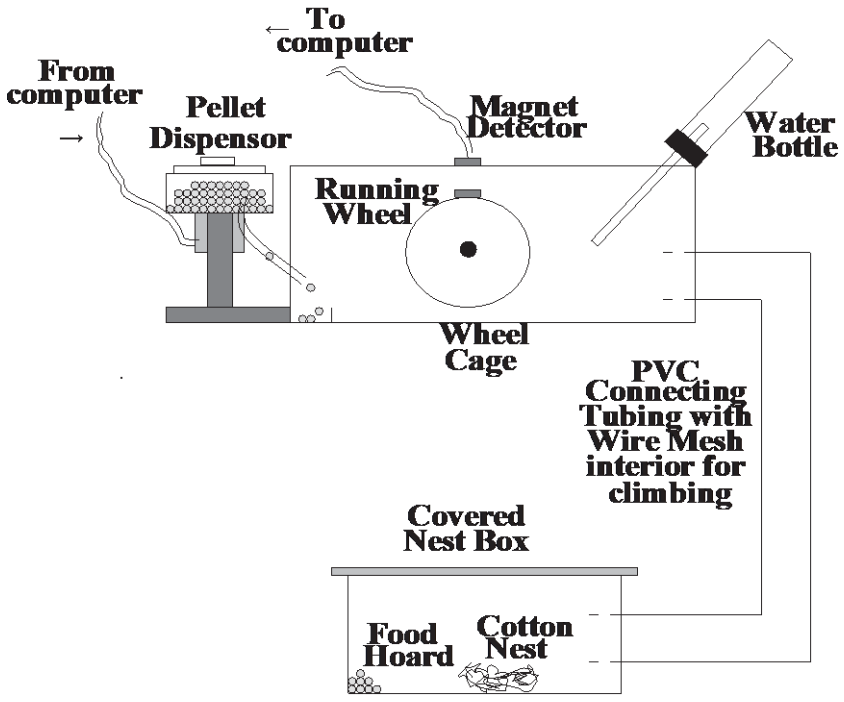


**Fig. 1.1** Diagram of foraging and hoarding apparatus.

pellet, 2) leave the pellet in the foraging cage, or 3) take the pellet from the foraging cage through PVC tubing down to the bottom, hoarding cage for storage. Wheel revolutions (foraging), food intake, and food hoarding is then measured daily for all animals. Using Siberian hamsters and our unique foraging/hoarding apparatus, we have begun to identify a detailed neuroendocrine framework driving appetitive and consummatory ingestive behaviors [76-78].

### 1.3 Ghrelin Regulates Ingestive Behaviors and Metabolism

Ghrelin is a peptide hormone released by X/A-like stomach cells, and has received considerable attention for its role in obesity development as it is the only known peripheral orexigenic signal [3, 80, 81]. Pre-pro-ghrelin is modified into its active, acylated form acyl-ghrelin (henceforth referred to as ghrelin) by the protein ghrelin *O*-acyl-transferase (GOAT) [3, 82]. Unacylated ghrelin, des-acyl-ghrelin, has limited biological functionality in the context of ingestive behaviors and appears to signal through an alternate mechanism than acylated ghrelin (for review see [83]). Circulating ghrelin levels rise pre-prandially (i.e. during fasting) and decrease post-prandially, and the rise and fall of ghrelin concentrations is suggested as a contributor to normal energy homeostasis and overall metabolic health [84, 85]. Elevated ghrelin levels underlie pathologies including Prader-Willi Syndrome that are characterized by obesity, unrestrained feeding and hoarding of food and food-related objects indicating an important link between obesity and atypical ingestive behaviors [86, 87]. The marked increase in appetitive and consummatory behaviors following fasting corresponds with elevated plasma ghrelin concentrations [84, 88], and we have previously demonstrated an exogenous ghrelin challenge drives food foraging, hoarding, and intake in Siberian hamsters [22]. Fasting or an exogenous ghrelin challenge acutely increases food intake, but results in a rapid and prolonged increase in food hoarding behavior (5-7 days) [22]. This long-term behavioral adaptation to

caloric deficiency is of particular importance as it, in part, underlies the frequent weight regain following caloric restriction (e.g. during a diet), and understanding the mechanism through which long-term behavioral responses are regulated is critical for sustained weight loss. To this end, there are presently several pharmacological treatments aimed at blocking either the ghrelin peptide directly or GOAT, the enzyme responsible for the conversion into its active, acylated form [82, 89]. Ghrelin blockade with a single anti-ghrelin Spiegelmer injection blocks acute fasting-induced ingestive behaviors but has no effect on food foraging and hoarding past 48 hours due to compensatory increases in circulating ghrelin [90]. By contrast, blockade of ghrelin acylation by GO-CoA-Tat-mediated GOAT inhibition significantly decreases food intake and the long-term (2-3 day) increase in food hoarding following an overnight fast [91]. This sustained attenuation of food hoarding is notable in that GOAT inhibition persists for only 6 hours [92], suggesting an initial blockade of ghrelin signaling is sufficient to inhibit the chronic increases in appetitive behaviors following energetic challenges.

In addition to driving ingestive behaviors, ghrelin markedly increases adiposity through its effects on numerous metabolic processes. Central ghrelin administration activates key enzymes promoting fatty acid storage while simultaneously inhibiting fat oxidation in an SNS dependent manner, independent of food intake or energy expenditure [93]. Moreover, central ghrelin infusion inhibits glucose-stimulated insulin secretion and impairs glucose tolerance in healthy humans, and the ghrelin system has in turn been proposed as a possible target for diabetes treatment [70, 94]. The dual role of ghrelin in driving appetitive behaviors, which require energy expenditure, and promoting energy conservation must therefore be balanced. A possible mechanism underlying this balance is the presence of multiple signaling pathways that mediate the discrete ingestive and metabolic effects of ghrelin. Although this hypothesis has not

been directly tested, several independent studies strongly point to discrete systems regulating ghrelin's effects on ingestive behaviors and metabolic processes. Ghrelin microinjections into several hypothalamic nuclei including the hypothalamic arcuate nucleus (Arc) or paraventricular hypothalamus (PVH) are sufficient to drive food intake and decrease energy expenditure whereas hindbrain microinjections into the caudal brainstem are sufficient to regulate energy expenditure and, to a lesser extent, food intake [68, 69]. It should be noted that within the Arc, ghrelin activates neurons that broadly project to hindbrain nuclei and may therefore mediate energy expenditure through these pathways and food intake through separate projections [95]. Indeed, only a subset of Arc, ghrelin sensitive neuronal projections is sufficient to drive food intake, but the function of the remaining projections remains unclear [95].

### *1.3.1 The ghrelin receptor*

In addition to circulating ghrelin levels, fasting markedly increases expression of its receptor, growth hormone secretagogue receptor 1a (GHSR) [96, 97]. GHSRs are broadly expressed in the brain and on gastrointestinal vagal sensory neurons [98, 99], and the orexigenic effects of ghrelin are entirely mediated through GHSRs as exogenous ghrelin fails to induce food intake in rodents lacking this receptor [100, 101]. Moreover, pharmacologic activation of GHSRs, independent of ghrelin manipulation, markedly increase ingestive behaviors indicating GHSR signaling is sufficient to mediate appetitive and consummatory feeding behaviors [102]. In line with the pharmacological approaches targeting the ghrelin peptide directly, several GHSR antagonists have been developed including MK-0677, L692,585, and [d-Lys3]-growth hormone-releasing peptide-6 (Dlys), JMV2959, and [d-Arg(1),d-Phe(5),d-Trp(7, 9),Leu(11)]-substance P (SP-analog) [103]. Of these GHSR antagonists, JMV2959 is highly selective and has proven effective at reducing ghrelin- and food deprivation-induced food intake in rodents as well as

food-based reward behaviors [103-106]. Although GHSR antagonism is sufficient to acutely reduce food intake, the long-term effects of GHSR antagonist administration, the specific mechanisms through which this antagonism mediates its effects, and it's potential to inhibit or attenuate ghrelin- or food deprivation-induced food foraging and food hoarding remains unclear.

### *1.3.2 Metabolic effects of ghrelin or GHSR knockout*

Following the discovery of ghrelin by Kojima et al., several ghrelin-deficient rodent models have been developed. Whole body *ghrelin* or *ghsr* deletion imparts a profoundly beneficial metabolic phenotype in high-fat-diet fed mice [100, 107]. As ghrelin was initially identified as an appetite stimulating hormone, it would be logical that *ghrelin* or *ghsr* knockout models would resist obesity development through decreased food intake. However, these knockout mice have comparable food intake with wild type littermates, yet they have markedly reduced body mass on high fat diet due to increased energy expenditure and a shift toward higher lipid utilization [108, 109]. In addition, these mice have improved glucose disposal and insulin sensitivity compared with high-fat-diet fed wild type controls suggesting the absence of ghrelin protects against Type 2 Diabetes development [108]. The comparable food intake of *ghrelin* or *ghsr* deficient and wild type mice strongly suggests ghrelin is not an essential meal initiation hormone and supports the presence of multiple mechanisms through which ghrelin can regulate caloric intake and metabolic processes. To this end, numerous central and peripheral ghrelin signaling pathways have been identified (see below), and deconstructing these discrete pathways has revealed a complex network regulating ghrelin's effects. Selective Arc *ghsr* restoration in otherwise *ghsr*-null mice restores ghrelin-induced food intake and partially regulates glycemic dysregulation, yet selective restoration in hindbrain *Phox2b* neurons is sufficient to restore glycemic control only [70, 110]. The sufficiency of hindbrain *ghsr* restoration to mediate

glycemic control is notable as *Phox2b* neurons are present in the periphery therefore suggests peripheral ghrelin signaling is involved in glycemic control whereas Arc signaling drives food intake [111, 112]. Moreover, the authors did not examine the mechanisms through which Arc ghrelin signaling regulates glycemia, but emerging evidence suggests these neurons act through downstream nuclei in the hindbrain. In particular, the nucleus tractus solitarius (NTS) and dorsal motor vagus (DMV) have been recognized for their role in ghrelin-mediated energy homeostasis [55, 113]. These studies collectively indicate clear physiological roles for ghrelin in regulating body mass and adiposity, and it is increasingly evident that ghrelin's diverse metabolic effects are mediated through a complex, distributed system that remains to be fully elucidated.

### 1.4 Ghrelin Signals Through Discrete Central and Peripheral Pathways

The broad central and peripheral GHSR expression evident in laboratory rodents strongly suggests the diverse effects of ghrelin are mediated through discrete tissues and signaling pathways. In the context of obesity, neuronal ghrelin signaling is necessary for obesity development and glycemic dysregulation during high fat diet feeding [107]. Initial GHSR characterization identified the vagus nerve, which densely innervates the gastrointestinal system, as the primary ghrelin signaling pathway and critical for ghrelin's metabolic effects [57, 114, 115]. However, further studies found that a subdiaphragmatic vagotomy has no effect on ghrelin-induced food intake or gastric motility suggesting that either brain GHSRs or non-vagal sensory neurons are sufficient to mediate ghrelin's effects independent of the vagus nerve [116, 117 , 118, 119]. To this end, central GHSR expressing neurons have been identified in diverse areas including the hippocampus, ventral tegmental area, hypothalamus, and dorsal motor vagus (DMV), and several studies have identified non-vagal sensory neurons within the gut, likely emanating from DRGs, as ghrelin responsive [117, 120]. Although these studies have begun to

elucidate the separate and shared mechanisms through which central and peripheral GHSR signaling regulates energy homeostasis, it remains unclear whether sensory neurons (i.e. both vagal and non-vagal) are necessary for ghrelin's effects, whether central GHSR activation is necessary for appetitive behaviors in addition to consummatory behaviors, and the central/peripheral mechanisms through which ghrelin drives acute and chronic changes in ingestive behaviors and peripheral metabolic processes.

### *1.4.1 Ghrelin signaling in the brain*

#### *1.4.1.1 Hypothalamic arcuate nucleus*

Numerous studies have implicated the Arc as a key regulator of metabolism and food intake [11, 27, 121, 122]. The Arc contains more than 50 unique neuronal populations, many of which are critical for food intake regulation [123-125], and it has been hypothesized as a key link between central and peripheral endocrine signaling due to the absence of a normal blood brain barrier [126]. Within the Arc, GHSRs are most strongly expressed on neurons that co-release the neurotransmitters agouti-related protein (AgRP) and neuropeptide Y (NPY)- AgRP neurons [110]. Arc ablation in adult animals blocks the orexigenic action of a peripheral ghrelin challenge and results in profound hypophagia leading to death [127, 128]. In the context of appetitive behaviors, neonatal Arc destruction in Siberian hamsters has no effect on baseline food foraging or food hoarding [129], yet food deprivation in these animals markedly increases food hoarding upon refeeding suggesting compensatory mechanisms are sufficient to maintain basal appetitive behaviors independent of the Arc [129]. However, it should be noted that Arc destruction following NPY-saporin or monosodium glutamate treatment is unable to completely ablate all Arc neurons [129], and recent work has demonstrated as few as 400 AgRP neurons are

sufficient to drive food intake in mice [95]. Therefore, even in the absence of compensatory mechanisms, the intact AgRP/NPY neurons not destroyed by saporin or monosodium glutamate may be sufficient to regulate appetitive behaviors.

Exogenous ghrelin markedly increases AgRP/NPY expression and AgRP neuron c-Fos-immunoreactivity (-ir), a marker of neuronal activation [122, 130], and central administration of AgRP and NPY significantly increases both appetitive and consummatory ingestive behaviors in Siberian hamsters [131-133]. The integral role of Arc AgRP ghrelin signaling is further supported by the findings that 1) pharmacogenetic or optogenetic AgRP neuron activation drives a rapid and robust food intake response [134, 135], 2) mice lacking AgRP/NPY do not increase food intake in response to an exogenous ghrelin challenge [136], and 3) selective reexpression of GHSRs on AgRP neurons in otherwise *ghsr*-null mice restores ghrelin's orexigenic effects [110]. These results collectively indicate the Arc is the primary regulator of ghrelin-induced appetitive and consummatory ingestive behaviors, and AgRP neurons are necessary for ghrelin's orexigenic actions in adult animals. Recent advances in neuron-specific circuit mapping has elucidated numerous downstream nuclei that control AgRP-induced ingestive behaviors. Discrete activation of AgRP→anterior bed nucleus of the stria terminalis, AgRP→PVH, or AgRP→lateral hypothalamus neurons drive food intake comparable to total Arc AgRP activation indicating the presence of parallel pathways mediating, at the very least, food intake [95, 134]. By contrast, AgRP→parabrachial nucleus, periaqueductal gray, or central amygdala projections have no effect on food intake, and may therefore regulate energy expenditure rather than food intake [95]. This hypothesis is supported by the findings that many of these hindbrain nuclei also express the GHSRs and are involved in sympathetic outflow to adipose tissues [120, 137]. While the role of these parallel pathways in the context of energy expenditure and food foraging

and food hoarding remains relatively unstudied, AgRP→PVH projections have received considerable attention for their role in driving appetitive behaviors [28, 138-141]. Indeed, we have previously demonstrated the PVH is integral in regulating food foraging, food hoarding, and food intake in Siberian hamsters [28], and the discrete mechanism through which the PVH regulates these behaviors is actively being investigated.

Although AgRP neuron activation rapidly drives food intake in satiated animals, NPY and AgRP peptide signaling appears to mediate ingestive behaviors through discrete temporal mechanisms. Studies in mice have demonstrated that NPY promotes rapid, but transient increases in food intake while AgRP drives food intake in a delayed, but prolonged, manner [134, 142]. In Siberian hamsters, intracerebroventricular NPY results in a pronounced (~500%-1000%), but transient (<48h), increase in ingestive behaviors whereas AgRP drives long-term (~7D) food hoarding to a greater extent than food intake. The robust, delayed effects on food hoarding following a central AgRP challenge closely mimics the timeframe in which the maximal increase in food hoarding is seen following exogenous ghrelin or food deprivation [22, 28]. It is thus likely that the long-term increases in food hoarding following food deprivation or a peripheral ghrelin challenge are due to AgRP signaling, and the acute increases in food intake, food foraging, and food hoarding are regulated by NPY. In addition, recently developed mouse models allowing for real-time neuronal recording have demonstrated Arc AgRP neurons are rapidly modulated by sensory detection of food independent of caloric intake [143]. In a calorically depleted state, in which AgRP neuron activity is markedly increased relative to a satiated state, sensory detection of food rapidly inhibits AgRP activity (within seconds) prior to caloric intake [143]. This inhibition is reversed if food is removed prior to consumption suggesting the modulation of AgRP neurons following food presentation is a mechanism to stop

foraging and promote feeding. Moreover, as hunger (and, hence, increased AgRP neuron activity) imparts a profoundly negative valence teaching signal [18], inhibiting AgRP neurons upon food discovery may be due to a learned correlation between finding food and consuming or storing the food for future meals.

#### *1.4.1.2 Midbrain nuclei*

In addition to forebrain Arc AgRP neurons, GHSRs are strongly expressed in midbrain [98]. The midbrain ventral tegmental area (VTA) is recognized as a key regulator of the reward system and is characterized by its dense dopaminergic neuron population [144, 145]. Many of these dopaminergic neurons express GHSRs, and ghrelin has been proposed as a mediator of food-related reward and motivation [106, 146, 147]. Indeed, ghrelin microinjections into the VTA markedly increase sucrose self-administration and food intake [105, 148], and ablating VTA dopaminergic neurons blocks ghrelin's ability to elicit food-reinforced behavior [149]. In an evolutionary context, it is logical for ghrelin to increase the motivation to find food (i.e. foraging behavior) and mediate the subsequent reward signals once the food is found. Caloric depletion is an inherently negative valence signal that drives an animal to search for food (see above), and concomitant reward circuitry activation by ghrelin would help ensure an animal continues to forage for food to prevent starvation. It is notable that the VTA, unlike the Arc, is not recognized as a circumventricular organ exposed to circulating nutrients or endocrine signals, and it is therefore unclear how endogenous ghrelin activates these neurons. To this end, ghrelin mRNA has been localized to periventricular neurons adjacent to the Arc that project to AgRP neurons [29], but whether the VTA is a downstream target of these neurons was not investigated. Future studies are clearly needed to elucidate the mechanism through which ghrelin activates VTA neurons and would provide further insight into ghrelin’s effects on the reward system.

#### *1.4.1.3 Hindbrain nuclei*

GHSR-positive neurons have been identified in hindbrain nuclei including the DMV, NTS, and area postrema [120], and 4$^{th}$ ventricular ghrelin injection induces food intake and cFos expression in these areas [67, 68, 150]. Converging evidence suggest these hindbrain GHSR-positive nuclei can function independently of the forebrain. 3$^{rd}$ ventricular ghrelin infusion is sufficient to drive food intake and induce hindbrain cFos, yet 4$^{th}$ ventricular ghrelin injections increase food intake but not forebrain cFos [67, 68, 150]. In addition, glutamatergic neuronal stimulation in the lateral hypothalamus activates NTS GHSR-positive neurons and promotes gastric motility [151]. Hence, current evidence suggests the presence of discrete forebrain and hindbrain ghrelin signaling pathways such that hypothalamic GHSR activation can elicit effects locally and in downstream hindbrain nuclei, but hindbrain GHSR activation may only act locally. To this end, GHSR restoration in hindbrain *Phox2b* expressing neurons is sufficient to restore ghrelin's glucoregulatory, but not food intake, effects [70], but GHSR restoration in AgRP neurons is sufficient to partially restore both ghrelin-induced food intake and glycemic regulation [110]. A notable limitation of these studies is 1) *Phox2b* is expressed in both hindbrain and vagal sensory neurons which precludes specificity [111, 112], and 2) hypothalamic GHSR-positive neurons project to hindbrain nuclei and it is therefore unclear where these effects are being mediated [95].

NTS and DMV neurons act as a critical relay between visceral stimuli and central integration, and crosstalk between these nuclei is sufficient to regulate neuronal efferent activity [152, 153]. Gastric afferents synapse in both the DMV and NTS, and GABAergic NTS neurons tonically inhibit DMV efferents [154-156]. Because GHSRs are distributed on multiple NTS neuron types including GABAergic and noradrenergic neurons [157, 158], it is likely ghrelin's

discrete hindbrain effects (i.e. gastric motility or food intake) are mediated through spatially unique neurons and downstream targets. Indeed, NTS GHSR-positive neurons are segregated and would provide a neuroanatomical basis for this functional distribution. Caudal $GHSR^{NTS}$ neurons respond to gastric mechanostimuli whereas rostral $GHSR^{NTS}$ neurons respond to energetic challenges including fasting or HFD feeding [157]. However, the mechanism through which peripheral ghrelin activates or inhibits hindbrain nuclei and which hindbrain GHSR signaling pathways regulate specific metabolic effects remains unclear and requires additional studies.

### *1.4.2 Peripheral ghrelin signaling*

The peripheral mechanisms regulating ghrelin's effects have received considerably less attention compared with the central mechanisms. Peripheral sensory neurons that innervate the gastrointestinal system provide a rapid signaling pathway through which viscerosensory information and gut endocrine signals can be relayed to the brain. The gut is highly innervated by vagal and non-vagal sensory neurons emanating from DRGs, yet few studies have interrogated the role of ghrelin signaling in these neurons [59]. Activation of vagal sensory neurons that detect gastric nutrients or stretching decreases food intake [60, 61] and increases energy expenditure and brown adipose tissue (BAT) thermogenesis [62]. Ghrelin directly inhibits these vagal neurons indicating an important link between the gastrointestinal system, ghrelin signaling, and energy homeostasis control [57]. Enteroendocrine sensory integration can occur in hindbrain nuclei, such as the NTS and DMV, that regulate metabolic processing of food, nutrient partitioning, and behavioral outputs [159-163]. Moreover, these hindbrain nuclei project to, and receive projections from, numerous hypothalamic nuclei critical for ingestive behaviors

including the Arc and PVH [63-66]. In addition to the vagus, sensory neurons that detect gastric stimuli and endocrine signals also emanate from DRGs [59], and total sensory neuron ablation following capsaicin treatment, but not vagotomy alone, impairs cold-induced thermogenic responses, adipose tissue metabolism, and, at the very least, ghrelin-induced gut motility indicating sensory nerves are mandatory for metabolic control [119, 164, 165]. Indeed, previous work has suggested non-vagal sensory neurons regulate exogenous ghrelin-induced gut motility and decreased energy expenditure [117, 166], yet the mechanism through which these non-vagal sensory neurons regulate ghrelin-induced ingestive behaviors and/or metabolic homeostasis remains unclear.

Previous work on peripheral ghrelin signaling has predominantly focused on gut motility as the peptide was initially characterized by its effects on gastric acid secretion and motility in humans and rodents [116, 167-169]. Fujino and colleagues demonstrated peripheral ghrelin-induced gut motility is not affected by vagotomy alone, but this motility is blocked when ghrelin is co-injected with a GHSR antagonist in vagotomized animals [170, 171]. In addition, the same study found central GHSR antagonism had no effect on peripheral ghrelin-induced gut motility in either normal or vagotomized animals suggesting redundant peripheral mechanisms mediate ghrelin-induced gut motility independent of the brain [170]. Although peripheral ghrelin has clear effects on gut motility, few studies have investigated its role in regulating energy expenditure. In lean humans and rodents, activation of gastric stretch or nutrient receptors promotes satiety [60, 172, 173], and their activity is directly enhanced by anorectic gut hormones including CCK and GLP-1and inhibited by ghrelin [61, 174]. *in vivo* auricular vagus nerve stimulation or intra-duodenal vagal lipid receptor activation increases sympathetic outflow and brown adipose tissue (BAT) thermogenesis [62, 175], a key mediator of whole-body energy

expenditure and adiposity [43, 176]. Currently, no studies have interrogated ghrelin's role in activating or inhibiting these neurons, but the presence of GHSRs on these sensory neurons and the sufficiency of ghrelin to mediate their activity would suggest a role in regulating energy expenditure. Discrete peripheral ghrelin signaling mechanisms that regulate metabolism independent of food intake is further evidenced by *in vitro* studies demonstrating that 1) exogenous ghrelin markedly increases electrically evoked cholinergic neural responses in rat stomach strips [117, 177], 2) GHSRs are present in a subset of guinea pig myenteric neurons [178], and 3) ghrelin evokes calcium efflux through GHSR activation in a subset of myenteric neurons [179]. These studies collectively suggest peripheral ghrelin signaling on gastrointestinal vagal and non-vagal sensory neurons is an important mediator of energy homeostasis.

## 1.5 Dissertation Goals

The goals of this dissertation are to target the separate and shared mechanisms through which ghrelin regulates metabolic homeostasis. Our overarching question for this dissertation is: are there discrete mechanisms through which ghrelin regulates acute and chronic appetitive and consummatory ingestive behaviors, and through what mechanism does ghrelin regulate metabolic homeostasis independent of food intake. We hypothesize that central ghrelin signaling primarily through Arc AgRP neurons is the major regulator of ingestive behaviors whereas peripheral ghrelin signaling regulates energy expenditure and adiposity independent of food intake.

These dissertation goals were tested across three major experiments. We first examined whether central or peripheral ghrelin is necessary and sufficient to regulate food foraging, food hoarding, and food intake using Siberian hamsters in our foraging and hoarding apparatus.

Hamsters were given either central or peripheral ghrelin in conjunction with a novel ghrelin receptor antagonist (JMV2915) and food foraging, hoarding, and intake measurements taken daily. In addition, we characterized the central neuronal activity following an exogenous ghrelin challenge and JMV2959 administration to uncover the central nuclei involved in the behavioral phenotype. We next examined the mechanisms through which central ghrelin regulates ingestive behavior by focusing on Arc AgRP neurons as they are necessary and sufficient for ghrelin-induced food intake. We tested whether Arc AgRP, but not NPY, knockdown was sufficient to block ghrelin- or food deprivation-induced increases in appetitive and/or consummatory ingestive behaviors using Siberian hamsters in our foraging and hoarding apparatus. Finally, we examined the role of peripheral ghrelin signaling in regulating metabolic homeostasis using a GHSR-GFP transgenic mouse and by generating a novel, sensory neuron specific GHSR knockout mouse. We identified the inherent function of these neurons using energetic challenges that increase circulating ghrelin (e.g. food deprivation) and characterized the necessity of ghrelin signaling on these neurons for the development of diet-induced obesity.

Collectively, this dissertation serves as a critical step in our understanding of ghrelin and the mechanisms through which it regulates metabolic homeostasis. In conjunction with previous research, this work provides complementary evidence to ghrelin's role in driving food intake while simultaneously uncovering the mechanisms through which ghrelin regulates food foraging and food hoarding independent of food intake. Moreover, this work identifies a novel mechanism through which peripheral ghrelin signaling regulates metabolic homeostasis through peripheral sensory neuron signaling.

# 2 CENTRAL GHRELIN INCREASES FOOD FORAGING/HOARDING THAT IS BLOCKED BY GHSR ANTAGONISM AND ATTENUATES HYPOTHALAMIC PARAVENTRICULAR NUCLEUS NEURONAL ACTIVATION

## 2.1 Abstract

The stomach-derived "hunger hormone" ghrelin increases in circulation in direct response to time since the last meal, increasing preprandially and falling immediately following food consumption. We found previously that peripheral injection of ghrelin potently stimulates food foraging (FF), food hoarding (FH) and food intake (FI) in Siberian hamsters. It remains, however, largely unknown if central ghrelin stimulation is necessary/sufficient to increase these behaviors regardless of peripheral stimulation of the ghrelin receptor [growth hormone secretagogue receptor (GHSR)]. We injected three doses (0.01 µg, 0.1 µg, and 1.0 µg) of ghrelin into the third ventricle (3V) of Siberian hamsters and measured changes in FF, FH, and FI. To test the effects of 3V ghrelin receptor blockade, we used the potent GHSR antagonist JMV2959 to block these behaviors in response to food deprivation or a peripheral ghrelin challenge. Finally, we examined neuronal activation in the arcuate nucleus (Arc) and paraventricular hypothalamic nucleus (PVH) in response to peripheral ghrelin administration and 3V GHSR antagonism. Third ventricular ghrelin injection significantly increased FI through 24 h and FH through Day 4. Pretreatment with 3V JMV2959 successfully blocked peripheral ghrelin-induced increases in FF, FH and FI at all time points and food deprivation-induced increases in FF, FH and FI up to 4h. c-Fos-immunoreactivity was significantly reduced in the PVH, but not the Arc following pretreatment with i.p. JMV2959 and ghrelin. Collectively, these data suggest central GHSR activation is both necessary and sufficient to increase appetitive and consummatory behaviors in Siberian hamsters.

## 2.2 Introduction

Obesity is a primary health concern affecting both developed and developing countries worldwide with an incidence rate of 34.9% in the United States as of 2008 [1]. Comorbidities associated with obesity include type 2 diabetes, stroke, heart disease, and some cancers [2-7]. As a result of the increasing rate of obesity and its comorbidities, the health costs associated with treatment has reached $147 billion [8], making obesity a major health and economic burden. Many factors, including genetics, contribute to excess weight gain but the primary cause is a surplus of energy intake compared with energy expenditure. This is compounded by the problem of easy access to calorically dense, cheap food as well as the ability to store more of these items for longer periods of time. Thus, understanding the underlying behaviors and neuroanatomical pathways involved in weight gain is critical to find novel treatments.

Appetitive behaviors include driving to/ shopping for food (foraging) and the storing (hoarding) of food in cupboards, refrigerators, freezers, and pantries, whereas consummatory behavior involves the consumption of food [9]. The research to date in the field has largely focused on consummatory behavior (food intake) in mice and rats, and in the process uncovered detailed central and peripheral pathways controlling this behavior . Although considerable attention has been paid to consummatory appetitive behavior, little attention has been paid to appetitive behaviors such as the hoarding of food and foraging [for review see Ref. 10]. Food restriction and deprivation in laboratory rats and mice trigger subsequent increases in FI upon re-exposure to food [for review see Rev.11]; by contrast, humans and hamsters, contrary to popular belief and personal anecdotes, instead ‘overhoard,’ storing considerably more food than normal, but do not overeat [12-15]. Furthermore, when faced with extended food deprivation (~24-48 h) humans and Siberian hamsters do not exhibit prolonged overeating. Rather than increasing FI

for extended periods, humans and Siberian hamsters increase FH [12, 14, 16-21]. In both humans and rodents, periods of negative energy balance directly correlate with increases in circulating concentration of the endocrine hormone ghrelin [22-24]. Furthermore, peripheral administration of ghrelin mimics the substantial increases in FF, FH and FI after a 56 h food deprivation in Siberian hamsters [25, 26] indicating its importance in driving both appetitive and consummatory behaviors.

Ghrelin acts on its receptor (GHSR) in diverse central and peripheral areas including the arcuate nucleus (Arc) [for review see Ref. 27], ventral tegmental area [for review see Ref. 28], suprachiasmatic nucleus [29, 30], paraventricular hypothalamic nucleus (PVH) [31], and vagus nerve [32]. Within the Arc, ghrelin activates agouti related protein (AgRP) / neuropeptide Y neurons to increase food intake [27, 33], and the co-administration of these peptides into the 3V increases FF, FH and FI in Siberian hamsters [34]. Ghrelin-sensitive neurons in the Arc project to diverse brain areas including the PVH [35, 36] and parabrachial nucleus [37, 38] to stimulate FI, and peripheral administration of ghrelin triggers c-Fos expression (a marker of neuronal activation [39, 40]) in these areas [30, 31]. Together these data demonstrate a varied and multifaceted role of ghrelin in driving appetitive and consummatory behaviors.

The development of direct and indirect ghrelin antagonists have shed light on the physiological role of ghrelin in rodents. Peripheral administration of an anti-ghrelin Spieglemer compound [41], as well as inhibition of ghrelin octanoylation, and thus its conversion into its active form [42], blocks exogenous ghrelin-induced neural activation both peripherally and centrally (given its route of administration peripherally) and short-term (<48 h) increases in FF, FI, and FH; however; long term (>48 h) appetitive and consummatory behaviors remain unchanged. In addition to ghrelin-peptide antagonists, the development of the specific GHSR

antagonist JMV2959 [43, 44] allows for site-specific studies of ghrelin activity throughout the brain [45-47]. These studies have partially elucidated the role of ghrelin in Siberian hamsters and other rodent models, but it remains unclear if central GHSR activation is necessary and sufficient to drive appetitive ingestive behaviors independent of peripheral GHSR blockade.

Here, we tested the sufficiency of 3V central ghrelin to increase FF, FI, and FH in Siberian hamsters. After confirming the sufficiency of 3V ghrelin to drive these behaviors, we then tested the effects of 3V GHSR blockade by administering the GHSR antagonist JMV2959 followed by: 1) a 48 h food deprivation challenge and 2) a peripheral ghrelin challenge. Finally, we examined neuronal activation as seen by c-Fos immunoreactivity (-ir; [40]) in the Arc and PVH following peripheral ghrelin administration and 3V GHSR antagonism to further clarify neuronal activity from two structures implicated in driving appetitive behaviors in Siberian hamsters.

## 2.3 Materials and Methods

### *2.3.1 Animals*

Adult male Siberian hamsters (*Phodopus sungorus; n* = 39) were obtained from our breeding colony. Hamsters were housed in same same-sex groups in polypropylene cages (48 X 27 X 15cm), given ad libitum access to food (5001, Purina, St. Louis, MO) and water, and raised in a long-day photoperiod (16:8-h light-dark cycle; light offset 1800) from birth until used in the following experiment. Room temperature was maintained at 21.0 ± 2.0˚C. At ~2.5-3.0 mo, animals were transferred and singly housed in polypropylene cages (27.8 X 17.5 X 13.0 cm) with Alpha-Dri (Specialty Papers, Kalamazoo, MI) bedding and one cotton Nestlet (Ancare, Belmore, NY). Animals were given *ad libitum* access to the experimental, pelleted test diet (DPPs, Purified 75 mg pellets; Bio-Serve, Frenchtown, NJ) and water and housed at 21.0 ± 2.0 ˚C with

50% humidity ± 10 in 16L:8D (light offset 1300) for two weeks to acclimate to the new light offset. All procedures were approved by the Georgia State University Institutional Animal Care and Use Committee and were in accordance with Public Health Service and United States Department of Agriculture guidelines.

### *2.3.2 Foraging and hoarding apparatus*

Hamsters were acclimated for 1 wk before and after cannula implantation in specially designed foraging/hoarding set up as previously described [48]. In brief, two cages were connected using convoluted polyvinylchloride tubing (38.1 mm inner diameter and ~1.5 m long) with 3 bends containing wire mesh to allow for vertical and horizontal climbing between each cage. The top, foraging cage was 456 X 234 X 200 mm (length X width X height) and equipped with a pellet dispenser, running wheel (524 mm circumference), and water bottle. The bottom, hoarding cage was 290 X 180 X 130 mm (length X width X height) and contained Alpha-Dri bedding and 1 cotton Nestlet. In order to mimic the darkness of a burrow, the hoarding cage was opaque and covered with an aluminum pan throughout the duration of the experiment. Wheel revolutions were measured using a magnetic detection system connected to a computer with monitoring software (Med Associates, Georgia,VT). Food was available *ad libitum* for 2 d following introduction to the foraging and hoarding apparatus. Subsequent to this initial training period, access to food was removed and all food had to be earned (1 pellet/10 wheel revolutions) for 5 d, during which time wheel revolutions, FI, pellets earned (FF), food hoarding (FH), and body mass were measured daily. Following 1 wk acclimation period, animals were placed back into cages with *ad libitum* access to food and further used for cannulation surgery.

### *2.3.3 Measurement of FF, FH, and FI*

FF was defined as the number of pellets earned following completion of the required 10 wheel revolutions. FH was defined as the number of pellets collected in the bottom, burrowing cage as well as pellets removed from cheek pouches. FI was defined as the total number of pellets earned, minus the number of pellets left in the top cage and pellets hoarded. An electronic balance set to parts measurement was used to count pellets (75 mg = 1 pellet). All whole and fractions of food pellets were recovered from each cage and hamster food pouches daily (0900) then quantified as whole pellets using a precision balance set to 'parts' whereby one 75 mg food pellet = 1 and fractions of pellets computed by the balance. FF, FH, and FI was measured daily at 0900 for the duration of the experiment.

### *2.3.4 Cannula implantation, injections, and verification*

Cannulas were stereotaxically implanted into 3V under isoflurane (Aerrane; Baxter Healthcare, Deerfield, IL) with anesthesia as previously described [49]. In brief, each animal was anesthetized and head shaved to expose the skull. A guide cannula (26-gauge stainless steel; Plastics One, Roanoke, VA) was lowered stereotaxically (coordinates: anterior-posterior from bregma 0 mm, medial-lateral from midsaggital sinus 0 mm, and dorsal-ventral from the top of the skull -5.5 mm) targeted for the 3V. Cannula were secured to the skull using cyanoacrylate ester gel, 3/16 mm jeweler's screws, and dental acrylic. A removable dummy cannula was used to seal the opening of the guide cannula throughout the experiment. Animals received ketofen (5 mg/kg; s.c; Fort Dodge Animal Health, Fort Dodge, IA) to minimize postoperative discomfort and an apple slice to facilitate food and water intake for the first 2-3 days postsurgery. Animals were kept in shoebox-type caging for 2 wk post-surgery for recovery.

One wk before each test d, each animal was lightly handled for 1 min and the dummy cannula removed and replaced to acclimate the animal to the injection protocol. On test days, an injection cannulae (33-gauge stainless steel; Plastics One) extending 0.5 mm beyond the guide cannula was connected to a microsyringe via PE-20 tubing and inserted into the guide cannula. All hamsters were injected with 400 nl of ghrelin, JMV2959 or saline vehicle over the course of 30 s and the injector was left in place for 30 s to minimize reflux up the sides of the cannula before removal as previously described [49].

Following the last behavioral test in *Experiment 3*, an injection of 400 nl of bromophenol blue dye was given to each animal to confirm placement of the cannula in the 3V. Animals were then given an overdose of pentobarbital sodium (100 mg/kg), transcardially perfused with 100 ml heparinized saline followed by 125 ml of 4% paraformaldehyde in phosphate buffered saline (PBS; pH = 7.4). Brains were then removed and post fixed in 4% paraformaldehyde for 2 d followed by a 30% sucrose solution until sectioning. Brains were sectioned on a freezing microtome at 80 $\mu$m and cannulae placement was verified using light microscopy. Cannulae were considered a hit if blue dye was visible in any part of the ventricle and only these animals were included in the analysis.

### *2.3.5 Experiment 1: Does 3V injection of ghrelin increase FF, FI, and FH in Siberian hamsters?*

Following the initial acclimation period, all hamsters were assigned to 4 groups counterbalanced for body mass, FI, FF, and FH levels. On test days, animals were provided with a clean burrowing cage and blocked from accessing the top cage to prevent feeding 2 h before injections. Animals were injected at light-offset with one of four 3V injections: *1)* 0.01 µg ghrelin, *2)* 0.1 µg ghrelin, *3)* 1.0 µg ghrelin, or *4)* vehicle and access to food was returned.

Following these injections, FI, FF (wheel revolutions), and FH was recorded at 2 h, 4 h, 24 h post injection and then daily for 8 d. After a 1 wk washout period, a length of time previously determined to yield a return to baseline, the same protocol was repeated until each animal had received all 4 treatments (n = 30).

#### *2.3.5.1 Measurement of circulating plasma ghrelin concentrations*

To ensure 3V administered ghrelin does not cross the blood brain barrier, a separate cohort of 36 adult male hamsters were obtained from our breeding colony and singly housed in polypropylene cages with Alpha-Dri bedding and one cotton Nestlet. Cannula were implanted as described above and animals were allowed to recover for two weeks with *ad libitum* food. Daily food intake and body mass were recorded. Following recovery, animals were counterbalanced for daily food intake and body mass and, finally, assigned into four groups: *1)* 0.01 µg ghrelin, *2)* 0.1 µg ghrelin, *3)* 1.0 µg ghrelin, or *4)* vehicle. Third ventricular injections were given at light-offset and retro-orbital blood was taken from anesthetized animals according to our previously published method [42] at 2 h, 4 h, and 24 h post-injection. Circulating acylated ghrelin concentrations were measured using ELISA (Mouse/Rat Acylated Ghrelin ELISA; Caymen Chemical) according to manufacturer's instructions and previously published methods [50]. In brief, 500 µl of blood was collected using heparinized Natelson tubes, transferred to pre-chilled BD microtainers containing EDTA (Franklin Lakes, NJ), and inverted ten times. Subsequently, 300 µl of blood was immediately transferred from EDTA tubes to pre-chilled microcentrifuge tubes containing 300 µl of the transfer buffer (1.2 % 10 N NaOH, 2 mM p-hydroxymercuribenzoic acid, 500 mM NaCl, and 25 mM EDTA in deionized water), mixed thoroughly by gentle inversion, and spun at 5,000 rpm at 4˚C for 10 min. Next, 300 µl of plasma

was transferred to prechilled microcentrifuge tubes, acidified with 1 N HCl (1 µl HCl/10 µl plasma), spun at 5,000 rpm at 4˚C for 5 min andstored at -20˚C until assayed.

### *2.3.6 Experiment 2: Does 3V injections of a GHSR antagonist JMV2959 prevent ghrelin-induced increases in FF, FI, and FH in Siberian hamsters*

Following a 10 d washout period after the final test day of *Experiment 1*, animals were assigned to 4 new treatment groups counterbalanced for body mass, FI, FF, and FH levels. In our pilot studies and based on Jerlhag *et al*. [51] and Skibicka *et al.* [51, 52], we determined that 10 µg of the GHSR antagonist JMV2959 was effective in blocking the effects of exogenous ghrelin while not adversely affecting locomotor activity (M. A. Thomas and T. J. Bartness, unpublished observations); we thus chose this dose to use throughout the experiment. Treatment groups consisted of: *1)* intraperitoneal (i.p.) Saline + 3V saline, *2)* i.p. saline + 3V JMV2959 (10 µg) *3)* i.p. ghrelin (30 µg/kg body mass) + 3V JMV2959 (10 µg), and *4)* i.p. ghrelin (30 µg/kg body weight) + 3V saline. On test days, animals were provided with a clean burrowing cage and prevented from accessing the top cage in the same manner as *Experiment 1*. All injections were given concurrently at light-offset and access to food returned. Following these injections, FI, FF, and FH was recorded at 2 h, 4 h, 24 h, and then daily for 8 d. Following a 1 wk washout period, the same injection protocol was repeated until each animal had received all treatments (n=20).

### *2.3.7 Experiment 3: Does 3V injections of a GHSR antagonist block food deprivation-induced increases in FF, FI, and FH?*

Following a 10 d washout period after the final test day of *Experiment 2*, animals were divided into 2 groups counterbalanced for body mass, FI, FF, and FH levels. Treatment groups consisted of *1)* 3V saline and *2)* 3V JMV3959 (10 $\mu$g). Animals received injections of either saline or JMV2959 at the onset of food deprivation (time (T) = 0), T + 24 h, and T + 48 h.

Following the final injection, access to food was returned and FF, FI, and FH were recorded at 2 h, 4 h, 24 h, and then daily until animals returned to behavioral baseline. After returning to baseline, animals were transferred to shoebox cages and brain tissue was processed as above to verify cannulae location (n=20).

### *2.3.8 Experiment 4: Does 3V injection of a GHSR antagonist prevent ghrelin-induced increases in c-Fos expression?*

Twenty Siberian hamsters were selected from the breeding colony and housed individually in shoebox cages before and after 3V cannula implantation. A separate, age-matched cohort of animals was used for *Experiment 4* due to the within-subject design of *Experiments 1, 2,* and *3* not allowing for unconfounded test of neural activation. Animals were divided into 4 treatment groups: *1)* i.p. saline + 3V saline, *2)* i.p. saline + 3V JMV2959 (10 µg), *3)* i.p. ghrelin (30 µg/ kg body mass) + 3V saline, and *4)* i.p. ghrelin (30 µg/ kg body mass) + 3V JMV2959 (10 µg). Animals were injected at light offset and perfused 2 h later. This time point was chosen because preliminary data showed the largest increases in FF, FI and FH occurring between 2-4 h [25, 41]. Brains were sectioned at 40 $\mu$m on a freezing microtome. For immunohistochemistry, free-floating brain sections were rinsed in 0.1 M PBS (2 x 15 min) followed by 30 min incubation in a blocking and permiablization solution consisting of 10.0 % normal goat serum (NGS) and 0.3 % Triton X-100 in 0.1 M PBS. Sections were incubated overnight with rabbit anti-c-Fos antiserum (1:800; sc-52, Santa Cruz Biotechnology, Santa Cruz, CA) in 0.1 M PBS with 0.5 % NGS. For immunohistological controls, the primary antibody was either omitted or preadsorbed with the immunizing peptide overnight at 4 °C resulting in abolished immunostaining. Subsequently, sections were washed in 0.1 M PBS (2 x 15 min) and incubated with biotinylated goat anti-rabbit antibody (1:200; Vector Laboratories, Burlingame,

CA, USA) for 2 h. Bound secondary antibody was then amplified with the Vector Elite ABC kit (1:800; Vector Laboratories, Burlingame, CA, USA) and antibody complexes were visualized by 0.05 % diaminobenzidine reaction. After mounting, sections were dehydrated and cleared through a series of ethanol, isopropanol and xylene solutions. Cleared slides were immediately mounted with Permount (Thermo Fisher Scientific, Waltham, MA, USA) and cover slipped.

### *2.3.9 Quantitative and statistical analysis*

Images were viewed and captured using 100x and 200x magnification with an Olympus DP73 imaging photomicroscope (Olympus, Tokyo, Japan). The PVH- and Arc-c-Fos-ir images were evaluated with the aid of CellSens (Olympus) and the Adobe Photoshop CS5 (Adobe Systems, San Jose, CA) software. The Arc and PVH were chosen for quantification because previous studies showed increased neuronal activity in these areas in response to ghrelin [41, 53]. The c-Fos-ir neurons were considered positively labeled based on the nuclei size and shape. Exhaustive counts of c-Fos positive neurons at the same anatomical level in all animals were then averaged across all animals within each experimental group. A mouse brain atlas [Paxinos and Franklin, 2007] was used to identify brain areas because no Siberian hamster brain atlas is available and because of the similarity in size and shape of most of the brain structures between Siberian hamsters and mice that are much more similar than the commercially available Syrian hamster stereotaxic atlas. For the preparation of the photomicrographs, we used Adobe Photoshop CS5 (Adobe Systems) only to adjust the brightness and contrast, and to remove artifactual obstacles (*i.e.*, obscuring bubbles) to make the composite plates.

In *Experiment 1* and *2*, raw behavioral data for each individual animal were transformed into percent change from saline control before statistical analysis according to the formula: [((X-vehicle)/vehicle) x 100], where X is equal to the measured value in response to experimental

treatment and vehicle is equal to the value measured for the individual following control injection (*Experiment 1* = 3V saline; *Experiment 2* = IP saline + 3V saline). Thus, each animal serves as its own control and data are reported as a percent change from baseline measurements. No statistical comparisons were made across the time intervals due to the unequal duration of the intervals. Behavioral data were analyzed using one-way repeated measures ANOVA across all treatments within each time point followed by the post-hoc Bonferroni's test using NCSS (version 2009, Kaysville, UT). For all measures of foraging, intake, and hoarding in *Experiment 1* and *Experiment 2*, data were reported as the mean percent difference from vehicle control (100%) ± SEM. Circulating acyl-ghrelin concentrations in *experiment 1* were analyzed using one-way ANOVA at each time point. For *Experiment 3*, data were not transformed into percent change because animals were only food deprived once and, therefore, cannot serve as their own control because Siberian hamsters do not overeat after food deprivation and therefore take weeks to return to their initial body mass readily. Raw data for FF, FI, and FH were analyzed using Mann-Whitney U test. For *Experiment 4*, c-Fos-ir for all groups was analyzed using one-way ANOVA. Exact probabilities and test values were omitted for simplicity and clarity of presentation. Differences were considered statistically significant if $P < 0.05$.

## 2.4 Results

### *2.4.1 Experiment 1: Does 3V injection of ghrelin increase FF, FI, and FH?*

#### *2.4.1.1 FF*

No significant increase in FF was seen across all three doses of 3V ghrelin at all time points examined compared with saline controls (**Fig. 2.1A**). A trend of increased FF was observed at the 2-4 h post injection for both 0.1 µg and 1.0 µg ghrelin doses, but only reached a maximum increase of ~160 % compared with saline ($P = 0.10$; **Fig. 2.1A**).

#### *2.4.1.2 FI*

FI was significantly increased by ~200% of control at 2-4 h post injection for the 1.0 µg ghrelin dose ($P < 0.05$ vs. 3V Saline; **Fig. 2.1B**). No significant increase was seen for 3V injection of either the 0.01 µg or 0.1 µg ghrelin doses at any time point examined (**Fig. 2.1B**).

#### *2.4.1.3 FH*

3V ghrelin significantly increased FH at 0-2 h through Day 4 for the 1.0 µg dose ($P < 0.05$ vs. 3V Saline; **Fig. 2.1C**). FH reached a maximum of ~600% following 1 µg ghrelin compared with control values at 48 h post injection and gradually declined to baseline at Day 5. 0.1 µg ghrelin significantly increased FH at 2-4 h and Day 3, reaching a maximum increase of ~400% ($P < 0.05$ vs. 3V Saline; **Fig. 2.1C**). No increase was observed at any time point for the 0.01 µg ghrelin dose (**Fig. 2.1C**) compared with the saline control.

#### *2.4.1.4 Circulating acyl-ghrelin concentrations*

To ensure 3V administered ghrelin was not crossing the blood brain barrier, we repeated *experiment 1* and measured peripheral circulating acyl-ghrelin concentrations at 2 h, 4 h, and 24 h post-injection. No dose of 3V administered ghrelin significantly affected peripheral circulating acyl-ghrelin concentrations at any time point examined (**Fig. 2.2**).

### *2.4.2 Experiment 2: Does 3V injection of a GHSR antagonist JMV2959 prevent peripheral ghrelin-induced increases in FF, FI, and FH in Siberian hamsters?*

#### *2.4.2.1 FF*

FF was significantly increased at the 4-24 h time point for the IP ghrelin + 3V saline group ($P < 0.05$ vs. IP Saline + 3V Saline; **Fig. 2.3A**) by ~350% compared with the control group. Foraging was attenuated at the 4-24 h time point in animals receiving IP ghrelin + 3V JMV2959 treatment, reaching a maximum of ~200% compared with saline ($P = 0.28$; **Fig. 2.3A**).

No change from the control treatment was seen across all time points in animals receiving IP saline + 3V JMV2959 (**Fig. 2.3A**). Foraging returned to baseline at 48 h for all groups (**Fig. 2.3A**).

#### *2.4.2.2 FI*

FI was significantly increased by ~200% of control at the 0-2 h time point for animals receiving IP ghrelin + 3V saline ($P < 0.05$ vs. IP Saline + 3V Saline; **Fig. 2.3B**). FI was attenuated at 0-2 h and 2-4 h following IP ghrelin + 3V JMV2959 treatment and reached a maximum of ~160% at 4-24 h ($P < 0.05$ vs. IP Saline + 3V Saline). No change in pellets eaten was observed following IP saline + 3V JMV2959 treatment (**Fig. 2.3B**).

#### *2.4.2.3 FH*

Pellets hoarded were significantly increased at all time points, except for 48 hs, examined through Day 5 in animals receiving IP ghrelin + 3V saline ($P < 0.05$ vs. IP Saline + 3V Saline; **Fig. 2.3C**), and reaching a maximum of ~400% at Day 5. FH was attenuated in animals receiving IP ghrelin + 3V JMV2959 treatment at all time points and reaching a maximum of ~200% at Day 5; however, without statistical significance ($P = 0.16$; **Fig. 2.3C**). No change in pellets hoarded was observed for the IP saline + 3V JMV2959 treatment group at all time points.

### *2.4.3 Experiment 3: Does 3V injection of a GHSR antagonist block food deprivation-induced increases in FF, FI, and FH in Siberian hamsters?*

#### *2.4.3.1 FF*

FF was significantly decreased in animals receiving 3V JMV2959 0-2 h and 2-4 h time points post injection compared with 3V saline control ($P < 0.05$; **Fig. 2.4A**). No difference was observed between the two groups 4-24 h or 48 h post injection (**Fig. 2.4A**).

#### *2.4.3.2 FI*

Pellets eaten was significantly decreased in animals receiving 3V JMV2959 at 0-2 h post injection compared with 3V saline control ($P < 0.05$; **Fig. 2.4B**). No difference in pellets eaten was observed 2-4 h, 4-24 h, and 48 h post injection (**Fig. 2.4B**).

#### *2.4.3.3 FH*

FH was significantly decreased in animals receiving 3V JMV2959 0-2 h and 2-4 h post injection compared with 3V saline control ($P < 0.05$; **Fig. 2.4C**). No difference in pellets hoarded was observed at the 4-24 h through Day 7 for both groups (**Fig. 2.4C**). Animals receiving 3V JMV2959 displayed a trend of increased food hoarding following the 48 h time point, although never reaching statistical significance (**Fig. 2.4C**).

### *2.4.4 Experiment 4: Does 3V injection of a GHSR antagonist prevent ghrelin-induced increases in c-Fos expression?*

IP ghrelin significantly increased c-Fos-ir in the Arc compared with IP saline controls ($P < 0.05$; **Fig. 2.5A, c**); however, 3V JMV2959 failed to block ghrelin-induced Arc neuronal activation (**Fig. 2.5A, d**). IP ghrelin (30 µg/kg body weight) + 3V saline significantly increased c-Fos-ir in the PVH ($P < 0.05$; **Fig. 2.5B, g**) 2 h postinjection compared with IP saline and JMV2959 blocked this effect ($P < 0.05$; **Fig. 2.5B, h**).

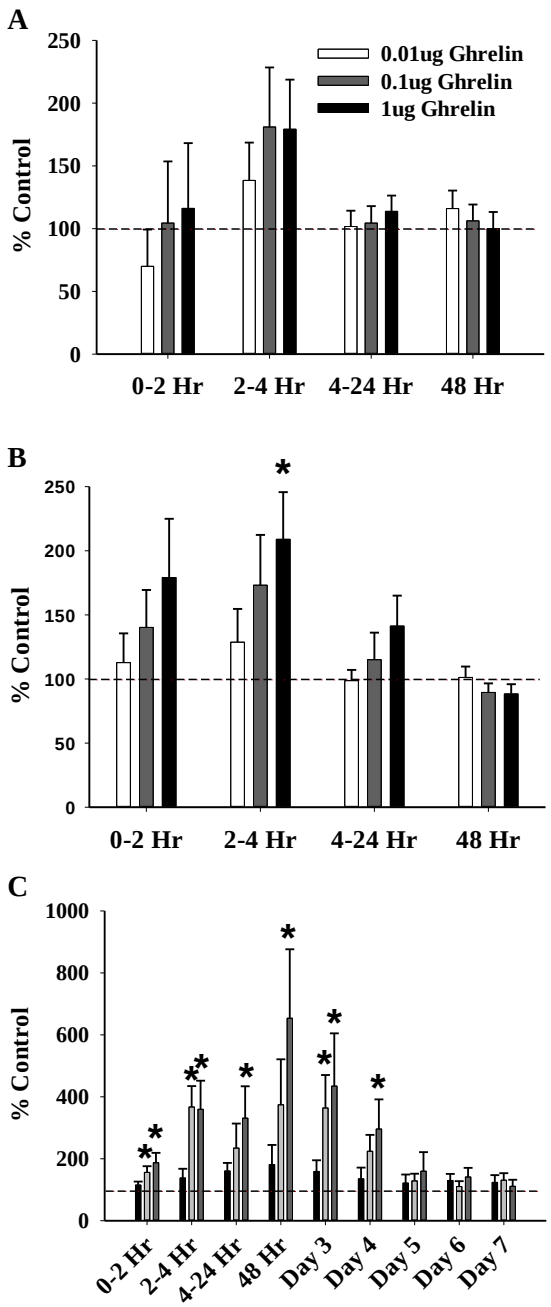


**Fig. 2.1** 3V ghrelin drives FF, FI, and FH.
Mean ± SE % difference in FF (A), FI (B), and FH (C) in response to 3V injection of 0.01 µg ghrelin (white bars), 0.1 µg ghrelin (grey bars), or 1.0 µg ghrelin (black bars). *$p<0.05$ compared with saline controls; n = 30 for each group.

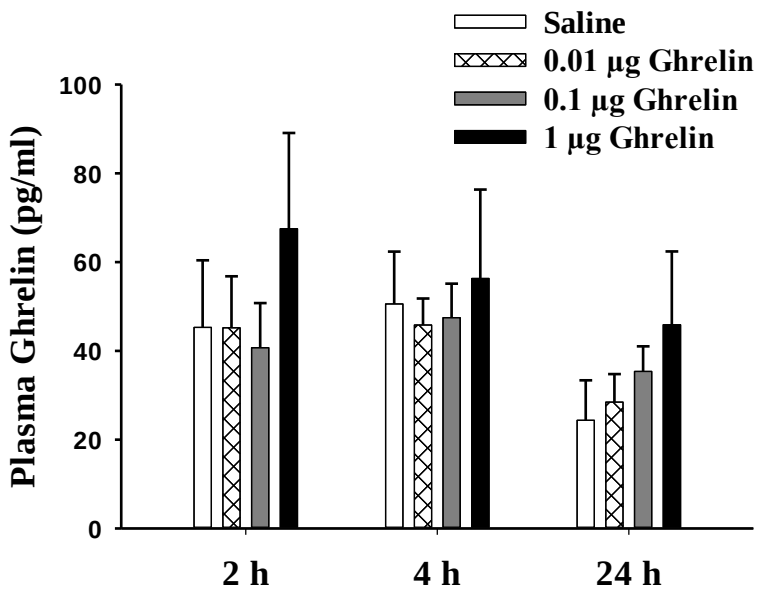


**Fig. 2.2** 3V ghrelin has no effect on plasma ghrelin concentrations.
Mean ± SE of plasma acyl-ghrelin concentrations in animals receiving 3V injection of saline (white bars), 0.01 µg ghrelin (white, crossed bars), 0.1 µg ghrelin (grey bars), or 1.0 µg ghrelin (black bars). n= 9 for each group.

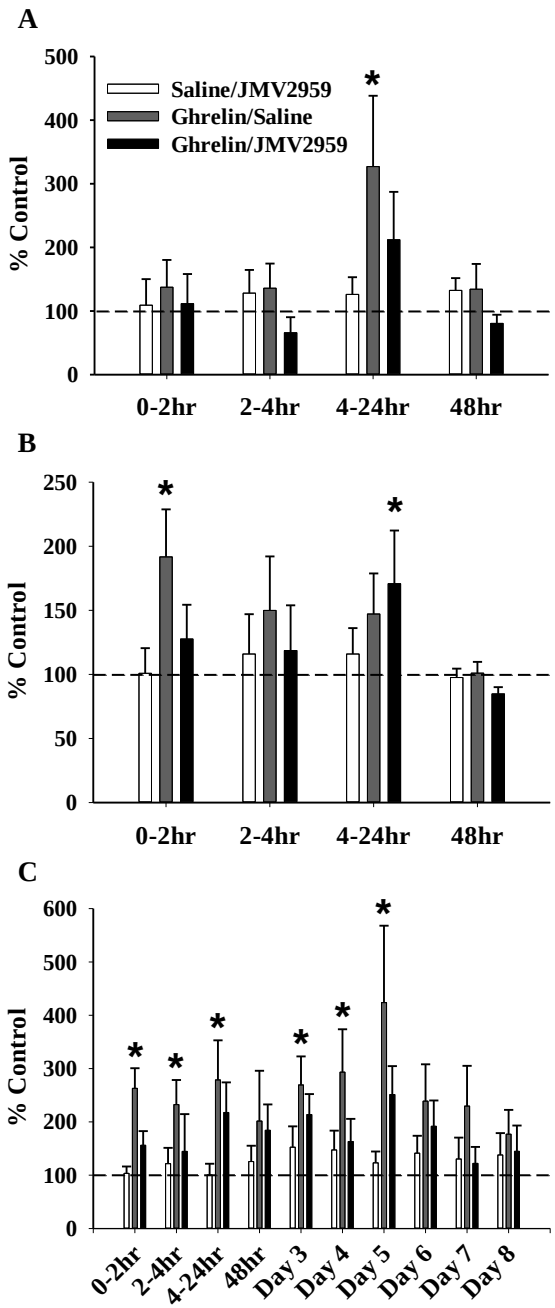


**Fig. 2.3** Central GHSR antagonism blocks peripheral ghrelin-induced FF, FI, and FH. Mean ± SE % difference in FF (A), FI (B), and FH (C) in response to i.p. saline + 10 µg 3V JMV2959 (white bars), 30 µg/kg i.p. ghrelin + 10 µg 3V JMV2959 (grey bars), or 30 µg/kg i.p. ghrelin + 3V saline (black bars). *$p<0.05$ compared with i.p. saline + 3V saline controls; n = 21 for each group.

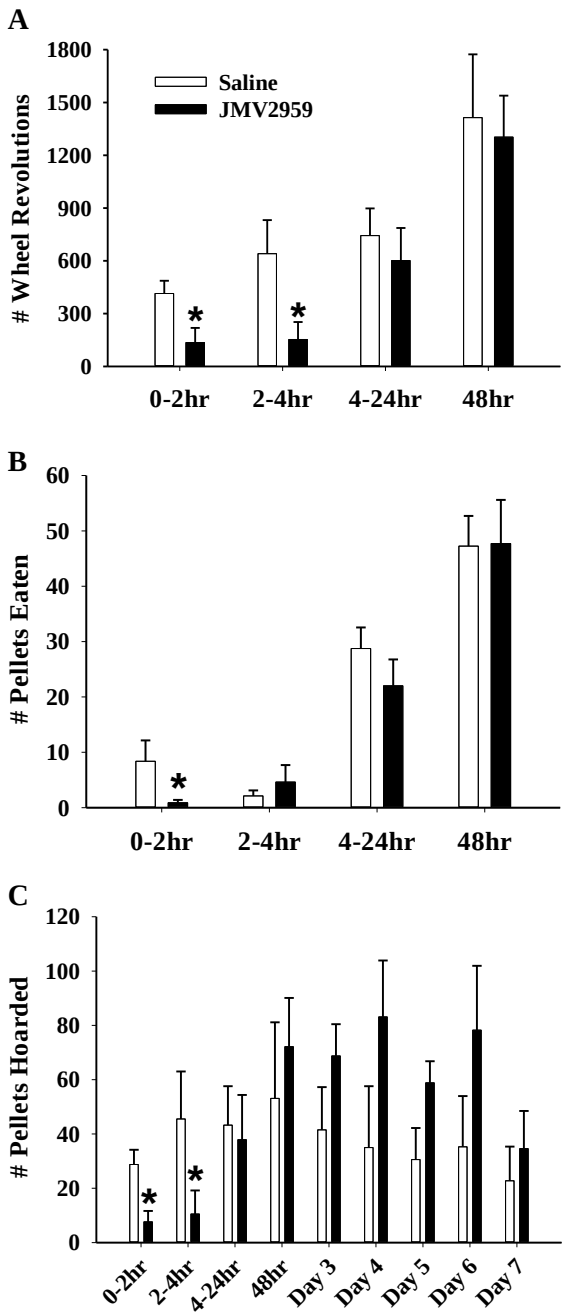


**Fig. 2.4** Central GHSR antagonism blocks food deprivation-induced FF, FI, and FH. Mean ± SE number of wheel revolutions (A), pellets eaten (B), and pellets hoarded (C) following 48 h food deprivation and 3V injection of saline (white bars) or JMV2959 (black bars). *$p<0.05$ compared with saline control; n = 10 for each group.

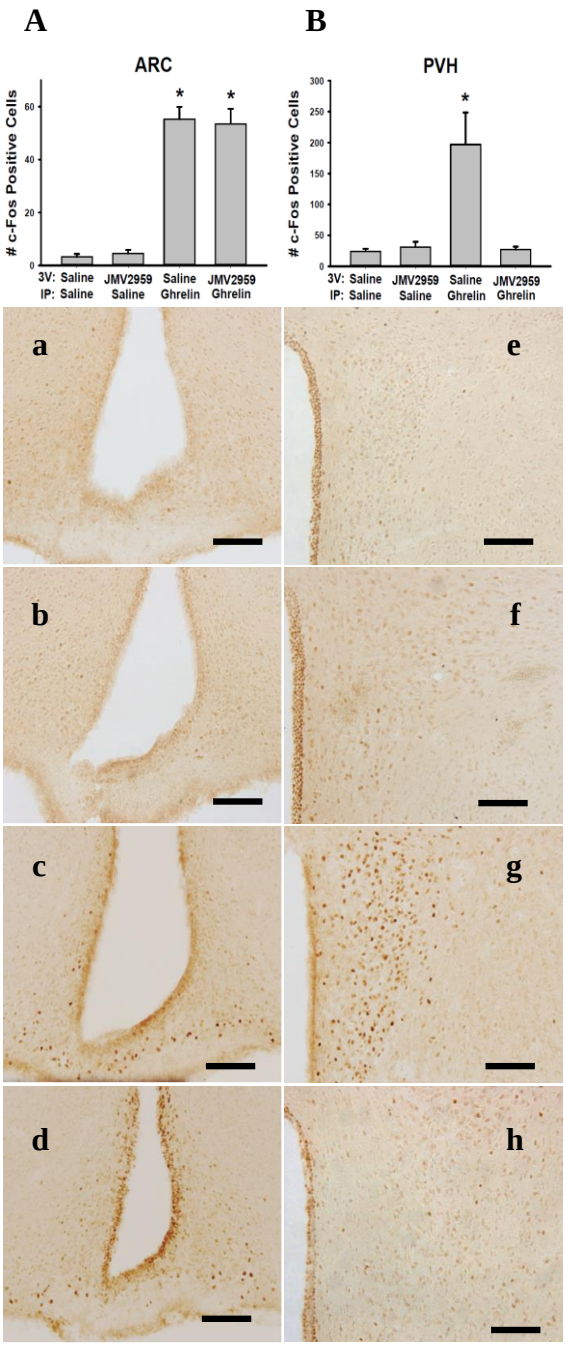


**Fig. 2.5** Central GHSR antagonism blocks peripheral ghrelin-induced c-Fos in the PVH. Mean ± SE number of c-Fos-ir cells and representative photographs in the Arc (*A*, *a-d*) and the PVH (*B*, *e-h*) in response to i.p. saline + 3V saline (*a*, *e*), i.p. saline + 10 µg 3V JMV2959 (*b*, *f*), 30 µg/kg i.p. ghrelin + 3V saline (*c*,*g*), or 30 µg/kg i.p. ghrelin + 10 µg 3V JMV2959 (*d*,*h*). *p<0.05 compared with i.p. saline + 3V saline controls; Scale bar= 100 µm. n = 5 for each group.

## 2.5 Discussion

The current study was designed to test the sufficiency and necessity of central and peripheral GHSR activation to increase appetitive and consummatory behaviors in Siberian hamsters. Similar to previous reports in laboratory mice and rats [26, 54-56], 3V administration of ghrelin was sufficient to increase FI in ad libitum fed Siberian hamsters. We showed here for the first time however that 3V ghrelin is sufficient to increase appetitive and consummatory behaviors independent of peripheral GSHR stimulation/blockade. We next tested the hypothesis that central GHSR activation mediates the appetitive and consummatory response to peripheral ghrelin. The GHSR antagonist JMV2959 successfully blocked exogenous ghrelin-induced increases in FF, FI and attenuated FH from the first time point measured post injection (2 h) through the end of the study (8 d). To further elucidate the neuronal mechanism underlying this effect, we measured c-Fos-ir in the Arc and PVH following administration of 3V JMV2959 and i.p. ghrelin. Pretreatment with JMV2959 significantly decreased c-Fos positive cells in the PVH but not in the Arc following a peripheral ghrelin challenge, suggesting peripheral ghrelin-induced increases in FF, FI and FH are mediated by neuronal activity in the PVH rather than the Arc.

In line with previous experiments testing the effects of peripheral ghrelin, 3V ghrelin potently stimulated both appetitive and consummatory behaviors in Siberian hamsters. By contrast to i.p. injections [25, 41], 3V administration circumvents possible peripherally mediated mechanisms driving appetitive and consummatory behavior. For instance, activation of the stomach-vagal-hindbrain-midbrain axis [32, 57, 58] increases FI whereas 3V administration prevents peripheral GHSR involvement. 3V ghrelin potently stimulated FF, FI, and FH for both 0.1 µg and 1.0 µg (Fig. 2.1A-C). Furthermore, 3V ghrelin administration closely mimicked the

drastic increases in FH observed following i.p. injection reaching an apex of ~600% (Fig. 2.1C). We thus hypothesize that centrally mediated ghrelin activity is sufficient to induce appetitive and consummatory behaviors independent of peripheral GHSR stimulation/blockade. This is further supported by our finding that 3V ghrelin does not significantly affect peripheral circulating ghrelin concentrations and indicates 3V ghrelin does not cross the blood brain barrier. The marked increase in ghrelin plasma concentration following an exogenous ghrelin challenge or prolonged food deprivation activates peripheral and central GHSRs and markedly increases FF, FI, and FH [25]; however, by circumventing peripheral GHSR involvement we have for the first time directly examined the discrete role of central GHSR activation in driving appetitive and consummatory behaviors in Siberian hamsters. The central and peripheral distribution of GHSRs suggests the effects of ghrelin are mediated by a number of distinct areas [59]. Furthermore, our findings here that 3V ghrelin markedly increases FF, FI, and FH independent of peripheral GHSR activation further supports the presence of multiple, redundant systems mediating appetitive and consummatory behaviors [60]. Overall, we demonstrated that 3V ghrelin is sufficient to increase both appetitive and consummatory behaviors independent of peripheral GHSR1a activation.

Our previous tests on the necessity of ghrelin focused on peripheral mechanisms to block ghrelin directly [41] or prevent its conversion into its physiological active form [42] without directly blocking its receptor. We therefore tested the necessity of central GHSR activation to increase FF, FI, and FH in response to a peripheral ghrelin challenge using the potent GHSR antagonist JMV2959. JMV2959 administration attenuates FI [61] and ghrelin-induced operant responding for food reward in rodents [45]. Here, 3V injection of JMV2959 abolished the ghrelin-induced increases in both appetitive and consummatory behavior at all time points

examined (Fig. 2.3A-C). Furthermore, 3V JMV2959 + IP saline did not affect FF compared with 3V saline + IP saline indicating the blockade of FF, FI and FH is not due to non-specific effects on locomotor activity. The inhibition observed following central GHSR antagonism is in contrast to previous work with Siberian hamsters attempting to block the appetitive and consummatory effects of exogenous ghrelin, both directly and indirectly [41, 42, 62, 63], in that there was a complete blockade of both appetitive and consummatory behaviors throughout the duration of the experiment. Furthermore, direct 3V administration of JMV2959 circumvents peripheral GHSR manipulation and therefore directly tests the discrete role of central GHSR activation. The blockade of appetitive behaviors in response to a peripheral ghrelin challenge suggests central GHSR activation is integral for these effects and could in turn be a more useful clinical treatment option if the mechanism for this complete blockade could be discerned. It remains unclear however the exact ghrelin-dependent pathway being inhibited as 3V administration of JMV2959 blocks GHSR activation throughout the brain and future studies are needed to delineate the precise pathways driving appetitive and consummatory behaviors. We have collectively demonstrated for the first time that central GHSR activation is integral in driving appetitive and consummatory behaviors in Siberian hamsters.

To further examine the ability of JMV2959 to block ghrelin-induced increases in appetitive and consummatory behaviors, we chronically injected JMV2959 throughout a 48 h food deprivation, which has previously been shown to potently increase FF, FI and FH and circulating ghrelin levels in Siberian hamsters [18, 19, 64-66]. We chose to repeatedly inject JMV2959 in 12 h increments to block GHSR activation throughout food deprivation in line with previous experiments [41] because ghrelin is continuously released in response to the negative energy balance that would occur during the 48 h food deprivation. 3V treatment with JMV2959

blocked FF and FI through 2 h and FH through 4 h post refeeding (Fig. 2.4A-C). By contrast to a single peripheral ghrelin challenge, food deprivation chronically increases circulating ghrelin concentrations. In turn, acute GHSR antagonism is able to block exogenous ghrelin, but not food deprivation-induced increases in both long-term appetitive and consummatory behaviors. These data suggest that JMV2959 blocks the effects of ghrelin throughout food deprivation, but once its effectiveness is diminished the food deprivation-induced circulating ghrelin begins to drive the appetitive ingestive behaviors. Taken together, Experiment 2 and Experiment 3 demonstrate that central activation of GHSR is necessary for exogenous ghrelin-induced increases in FF, FI, and FH, but not for long-term food deprivation-induced increases. This result supports previous reports suggesting ghrelin is integral in food deprivation increases in appetitive behavior, but not necessary due to the abundance of other physiological mechanisms compensating in its absence , that is the multiple redundant systems driving ingestive behaviors [60, 67].

In order to determine brain areas involved in ghrelin-induced changes in appetitive and consummatory behaviors in a preliminary examination, c-Fos-ir in the Arc and PVH was quantified following exogenous ghrelin treatment and 3V administration of JMV2959. We chose these areas due to previous work indicating significantly increased neuronal activity following peripheral ghrelin injection [41, 53]. Here, and in previous reports, exogenous ghrelin potently increased FI and FH 0-4 h post injection [25, 41, 62]. We therefore examined c-Fos-ir in the Arc and PVH at 2 h following identical treatments as in Experiment 2. Increased c-Fos-ir in response to exogenous ghrelin was observed in the Arc and PVH 2 h postinjection in line with previous reports [31, 41, 68]. Pretreatment with JMV2959 blocked neuronal activation in the PVH following exogenous ghrelin, but, interestingly, the Arc was unaffected (Fig. 2.5A-B). Approximately 94% of AgRP neurons express GHSRs [69] and exogenous ghrelin markedly

increases AgRP/NPY expression [70]. Moreover, subthreshold injection of AgRP and NPY increases FF, FI, and FH in Siberian hamsters [34]. AgRP neurons project to a number of downstream nuclei including the PVH [35, 71], where it antagonizes melanocortin receptors 3 and 4 (MC3R and MC4R) to promote food intake. In addition, AgRP neurons directly inhibit neighboring POMC neurons [72, 73]. As GHSR antagonism predominantly affects AgRP neurons, one potential explanation for our finding is GHSR blockade disinhibits POMC neurons and in turn, ghrelin-induced c-Fos-ir is comparable in the Arc regardless of GHSR antagonism. GHSR antagonism may therefore attenuate ghrelin-induced FF, FI, and FH through blockade of AgRP  PVH neuron signaling, and thereby inhibit PVH c-Fos-ir, while other Arc neurons remain active. However, as the identity of these c-Fos-positive neurons remains a mystery, we can only speculate as to the reasoning for this finding.

Ghrelin acts primarily in the Arc to promote food intake [56, 59]; however, GHSRs are expressed in a number of brain nuclei including the PVH [59]. We hypothesize however that GHSR blockade attenuates FF, FI, and FH in an Arc-dependent manner based on the following data: 1) peripheral ghrelin administration markedly increases Arc AgRP expression and these neurons project to the PVH [53, 72, 74], 2) Complete Arc or NPY neuron ablation markedly decreases both central and peripheral ghrelin-induced food intake [75, 76] indicating Arc activation mediates ghrelin-induced food intake, and 3) photostimulation of AgRP neurons markedly increases food intake [37, 77] whereas concurrent AgRP photostimulation and AgRP  PVH chemoinhibition attenuates this increase [37] indicating AgRP  PVH activation primarily drives food intake. Collectively, these data indicate the inhibition of PVH neuronal activity here is due to downstream effects of Arc GHSR blockade. Based on behavioral results in Experiment 2, we hypothesize that peripheral ghrelin may increase appetitive behaviors in the

very least in a PVH-involved mechanism and GHSR blockade attenuates ghrelin-induced neuronal activity of PVH inputs. It remains unclear, however, if PVH activity is in response to hindbrain activity (or vice versa), other brain areas, or both and future experiments will expand on this question. We are aware of the circumstantial evidence provided by c-Fos-ir in that the absence of neuronal activity in the PVH does not necessarily indicate the absence of activity as some neurons use other immediate-early genes [40]. We therefore interpret these findings as being suggestive of a possible PVH involved mechanism driving appetitive behaviors in Siberian hamsters.

These data collectively indicate central activation of GHSR by exogenous ghrelin is integral in driving appetitive and consummatory behaviors in Siberian hamsters. In addition, central GHSR antagonism is able to block food deprivation-induced short term increases in appetitive behaviors, but not long term due to the continued release of ghrelin (e.g., food deprivation). The blockade of appetitive behaviors in response to GHSR antagonism and a peripheral ghrelin challenge appear to involve the PVH which receives projections from a number of discrete brain areas including the Arc. Although GHSR antagonism successfully blocked ghrelin-induced increases in appetitive and consummatory behaviors, future studies are needed to delineate the precise pathways involved.

### 2.6 Perspective and Significance

Understanding the complex relationship of central integration of peripheral satiety signals is an important step in the development of clinically useful obesity treatment options. We have developed a novel model to study human food foraging and food hoarding, a relatively unstudied facet of obesity, in Siberian hamsters. Here, we show for the first time central blockade of GHSRs prevents the marked increase in both short-term and long-term food

foraging, food hoarding, and food intake following a peripheral ghrelin challenge. In addition, we show for the first time this blockade prevents neuronal activation of the PVH, but not the Arc, suggesting PVH activity is integral in driving both appetitive and consummatory behaviors.

## 2.7 Acknowledgements

This work is dedicated to the memory of our friend and mentor, Dr. Timothy J. Bartness. The authors would like to thank Babette Aicher (AeternaZentaris, Inc) for the GHSR antagonist JMV2959, and Johnny Garretson and Fardowsa Robow for their continued help in data collection.

## 2.8 Disclosures

The authors have nothing to disclose.

## 2.9 References

[1] Ogden, C. L., Carroll, M. D. Prevalence of Overweight, Obesity, and Extreme Obesity Among Adults: United States, Trends 1960-1962 Through 2007-2008. 2010.

[2] Calle, E. E., Rodriguez, C., Walker-Thurmond, K., Thun, M. J. Overweight, obesity, and mortality from cancer in a prospectively studied cohort of U.S. adults. N.Engl.J Med. 2003,348:1625-38.

[3] Goldstein, L. B., Bushnell, C. D., Adams, R. J., Appel, L. J., Braun, L. T., Chaturvedi, S., et al. Guidelines for the primary prevention of stroke: a guideline for healthcare professionals from the American Heart Association/American Stroke Association. Stroke. 2011,42:517-84.

[4] Harvey, A. E., Lashinger, L. M., Hursting, S. D. The growing challenge of obesity and cancer: an inflammatory issue. Ann.N.Y.Acad.Sci. 2011,1229:45-52.

[5] Rao, G. H., Thethi, I., Fareed, J. Vascular disease: obesity and excess weight as modulators of risk. Expert.Rev.Cardiovasc.Ther. 2011,9:525-34.

[6] Vague, J., Vague, P., Tramoni, M., Vialettes, B., Mercier, P. Obesity and diabetes. Acta Diabetol.Lat. 1980,17:87-99.

[7] Zalesin, K. C., Franklin, B. A., Miller, W. M., Peterson, E. D., McCullough, P. A. Impact of obesity on cardiovascular disease. Med.Clin.North Am. 2011,95:919-37.

[8] Finkelstein, E. A., Trogdon, J. G., Cohen, J. W., Dietz, W. Annual medical spending attributable to obesity: payer-and service-specific estimates. Health Aff.(Millwood.). 2009,28:822-31.

[9] Craig, W. Appetites and aversions as constituents of instincts. Biol.Bull. 1918,34:91-107.

[10] Bartness, T. J., Demas, G. E. Comparative studies of food intake: Lessons from non-traditionally studied species. In: Stricker EM, Woods SC, eds. Food and Fluid Intake. New York: Plenum; 2004. p. 423-67.

[11] Bartness, T. J., Day, D. E. Food hoarding: a quintessential anticipatory appetitive behavior. Progress in Psychobiology and Physiological Psychology. 2003,18:69-100.

[12] Dodd, D. K., Stalling, R. B., Bedell, J. Grocery purchases as a function of obesity and assumed food deprivation. Int.J Obes. 1977,1:43-7.

[13] Hetherington, M. M., Stoner, S. A., Andersen, A. E., Rolls, B. J. Effects of acute food deprivation on eating behavior in eating disorders. Int.J Eat.Disord. 2000,28:272-83.

[14] Mela, D. J., Aaron, J. I., Gatenby, S. J. Relationships of consumer characteristics and food deprivation to food purchasing behavior. Physiol Behav. 1996,60:1331-5.

[15] Levitsky, D. A., DeRosimo, L. One day of food restriction does not result in an increase in subsequent daily food intake in humans. Physiol Behav. 2010,99:495-9.

[16] Bartness, T. J., Keen-Rhinehart, E., Dailey, M. J., Teubner, B. J. Neural and hormonal control of food hoarding. Am.J Physiol. 2011,301:R641-R55.

[17] Beneke, W. M., Davis, C. H. Relationship of hunger, use of a shopping list and obesity to food purchases. Int.J.Obes. 1985,9:391-9.

[18] Wood, A. D., Bartness, T. J. Food deprivation-induced increases in hoarding by Siberian hamsters are not photoperiod-dependent. Physiol Behav. 1996,60:1137-45.

[19] Bartness, T. J., Clein, M. R. Effects of food deprivation and restriction, and metabolic blockers on food hoarding in Siberian hamsters. Am.J.Physiol. 1994,266:R1111-R7.

[20] Day, D. E., Bartness, T. J. Fasting-induced increases in hoarding are dependent on the foraging effort level. Physiology and Behavior. 2003,78:655-68.

[21] Garretson, J. T., Bartness, T. J. Dynamic modification of hoarding in response to hoard size manipulation. Physiol Behav. 2014,127:8-12.

[22] Kojima, M., Hosoda, H., Date, Y., Nakazato, M., Matsuo, H., Kangawa, K. Ghrelin is a growth-hormone-releasing acylated peptide from stomach. Nature. 1999,402:656-60.

[23] Wren, A. M., Seal, L. J., Cohen, M. A., Brynes, A. E., Frost, G. S., Murphy, K. G., et al. Ghrelin enhances appetite and increases food intake in humans. J.Clin.Endocrinol.Metab. 2001,86:5992.

[24] Toshinai, K., Mondal, M. S., Nakazato, M., Date, Y., Murakami, N., Kojima, M., et al. Upregulation of ghrelin expression in the stomach upon fasting, insulin- induced hypoglycemia, and leptin administration. Biochemical and Biophysical Research Communications. 2001,281:1220-5.

[25] Keen-Rhinehart, E., Bartness, T. J. Peripheral ghrelin injections stimulate food intake, foraging and food hoarding in Siberian hamsters. Am.J.Physiol. 2005,288:R716-R22.

[26] Tschop, M., Smiley, D. L., Heiman, M. L. Ghrelin induces adiposity in rodents. Nature. 2000,407:908-13.

[27] Andrews, Z. B. Central mechanisms involved in the orexigenic actions of ghrelin. Peptides. 2011,32:2248-55.

[28] Dickson, S. L., Egecioglu, E., Landgren, S., Skibicka, K. P., Engel, J. A., Jerlhag, E. The role of the central ghrelin system in reward from food and chemical drugs. Mol.Cell Endocrinol. 2011,340:80-7.

[29] Yannielli, P. C., Molyneux, P. C., Harrington, M. E., Golombek, D. A. Ghrelin effects on the circadian system of mice. J Neurosci. 2007,27:2890-5.

[30] Bradley, S. P., Pattullo, L. M., Patel, P. N., Prendergast, B. J. Photoperiodic regulation of the orexigenic effects of ghrelin in Siberian hamsters. Hormones and Behavior. 2010,58:647-52.

[31] Kobelt, P., Wisser, A. S., Stengel, A., Goebel, M., Inhoff, T., Noetzel, S., et al. Peripheral injection of ghrelin induces Fos expression in the dorsomedial hypothalamic nucleus in rats. Brain Res. 2008,1204:77-86.

[32] Date, Y., Murakami, N., Toshinai, K., Matsukura, S., Niijima, A., Matsuo, H., et al. The role of the gastric afferent vagal nerve in ghrelin-induced feeding and growth hormone secretion in rats. Gastroenterology. 2002,123:1120-8.

[33] Bradley, S. P., Pattullo, L. M., Patel, P. N., Prendergast, B. J. Photoperiodic regulation of the orexigenic effects of ghrelin in Siberian hamsters. Horm.Behav. 2010.

[34] Teubner, B. J., Keen-Rhinehart, E., Bartness, T. J. Third ventricular coinjection of subthreshold doses of NPY and AgRP stimulate food hoarding and intake and neural activation. Am.J.Physiol Regul.Integr.Comp Physiol. 2012,302:R37-R48.

[35] Cowley, M. A., Pronchuk, N., Fan, W., Dinulescu, D. M., Colmers, W. F., Cone, R. D. Integration of NPY, AGRP, and melanocortin signals in the hypothalamic paraventricular nucleus: evidence of a cellular basis for the adipostat. Neuron. 1999,24:155-63.

[36] Krashes, M. J., Shah, B. P., Madara, J. C., Olson, D. P., Strochlic, D. E., Garfield, A. S., et al. An excitatory paraventricular nucleus to AgRP neuron circuit that drives hunger. Nature. 2014,507:238-42.

[37] Wu, Q., Boyle, M. P., Palmiter, R. D. Loss of GABAergic signaling by AgRP neurons to the parabrachial nucleus leads to starvation. Cell. 2009,137:1225-34.

[38] Wu, Q., Palmiter, R. D. GABAergic signaling by AgRP neurons prevents anorexia via a melanocortin-independent mechanism. Eur.J Pharmacol. 2011,660:21-7.

[39] Verbalis, J. G., Stricker, E. M., Robinson, A. G., Hoffman, G. E. Cholecystokinin activates cFos expression in hypothalamic oxytocin and corticotropin releasing hormone neurons. Journal of Neuroendocrinology. 1991,3:205-13.

[40] Hoffman, G. E., Smith, M. S., Verbalis, J. G. c-Fos and related immediate early gene products as markers of activity in neuroendocrine systems. Frontiers in Neuroendocrinology. 1993,14:173-213.

[41] Teubner, B. J., Bartness, T. J. Anti-ghrelin Spiegelmer inhibits exogenous ghrelin-induced increases in food intake, hoarding, and neural activation, but not food deprivation-induced increases. Am.J.Physiol Regul.Integr.Comp Physiol. 2013,305:R323-R33.

[42] Teubner, B. J., Garretson, J. T., Hwang, Y., Cole, P. A., Bartness, T. J. Inhibition of ghrelin O-acyltransferase attenuates food deprivation-induced increases in ingestive behavior. Horm.Behav. 2013,63:667-73.

[43] Moulin, A., Demange, L., Berge, G., Gagne, D., Ryan, J., Mousseaux, D., et al. Toward potent ghrelin receptor ligands based on trisubstituted 1,2,4-triazole structure. 2. Synthesis and pharmacological in vitro and in vivo evaluations. Journal of medicinal chemistry. 2007,50:5790-806.

[44] Moulin, A., Brunel, L., Boeglin, D., Demange, L., Ryan, J., M'Kadmi, C., et al. The 1,2,4-triazole as a scaffold for the design of ghrelin receptor ligands: development of JMV 2959, a potent antagonist. Amino acids. 2013,44:301-14.

[45] Skibicka, K. P., Hansson, C., Egecioglu, E., Dickson, S. L. Role of ghrelin in food reward: impact of ghrelin on sucrose self-administration and mesolimbic dopamine and acetylcholine receptor gene expression. Addict.Biol. 2011.

[46] Salome, N., Hansson, C., Taube, M., Gustafsson-Ericson, L., Egecioglu, E., Karlsson-Lindahl, L., et al. On the central mechanism underlying ghrelin's chronic pro-obesity effects in rats: new insights from studies exploiting a potent ghrelin receptor antagonist. J Neuroendocrinol. 2009,21:777-85.

[47] Sarvari, M., Kocsis, P., Deli, L., Gajari, D., David, S., Pozsgay, Z., et al. Ghrelin modulates the fMRI BOLD response of homeostatic and hedonic brain centers regulating energy balance in the rat. PloS one. 2014,9:e97651.

[48] Day, D. E., Bartness, T. J. Effects of foraging effort on body fat and food hoarding by Siberian hamsters. J.Exp.Zool. 2001,289:162-71.

[49] Dailey, M. J., Bartness, T. J. Appetitive and consummatory ingestive behaviors stimulated by PVH and perifornical area NPY injections. Am.J.Physiol Regul.Integr.Comp Physiol. 2009,296:R877-R92.

[50] Barnett, B. P., Hwang, Y., Taylor, M. S., Kirchner, H., Pfluger, P. T., Bernard, V., et al. Glucose and weight control in mice with a designed ghrelin O-acyltransferase inhibitor. Science. 2010,330:1689-92.

[51] Jerlhag, E., Egecioglu, E., Landgren, S., Salome, N., Heilig, M., Moechars, D., et al. Requirement of central ghrelin signaling for alcohol reward. Proc Natl Acad Sci U S A. 2009,106:11318-23.

[52] Skibicka, K. P., Hansson, C., Egecioglu, E., Dickson, S. L. Role of ghrelin in food reward: impact of ghrelin on sucrose self-administration and mesolimbic dopamine and acetylcholine receptor gene expression. Addiction biology. 2012,17:95-107.

[53] Cowley, M. A., Smith, R. G., Diano, S., Tschop, M., Pronchuk, N., Grove, K. L., et al. The distribution and mechanism of action of ghrelin in the CNS demonstrates a novel hypothalamic circuit regulating energy homeostasis. Neuron. 2003,37:649-61.

[54] Wren, A. M., Small, C. J., Ward, H. L., Murphy, K. G., Dakin, C. L., Taheri, S., et al. The novel hypothalamic peptide ghrelin stimulates food intake and growth hormone secretion. Endocrinology. 2000,141:4325-8.

[55] Kamegai, J., Tamura, H., Shimizu, T., Ishii, S., Sugihara, H., Wakabayashi, I. Central effect of ghrelin, an endogenous growth hormone secretagogue, on hypothalamic peptide gene expression. Endocrinology. 2000,141:4797-800.

[56] Wren, A. M., Small, C. J., Abbott, C. R., Dhillo, W. S., Seal, L. J., Cohen, M. A., et al. Ghrelin causes hyperphagia and obesity in rats. Diabetes. 2001,50:2540-7.

[57] Date, Y. Ghrelin and the vagus nerve. Methods in enzymology. 2012,514:261-9.

[58] Date, Y., Shimbara, T., Koda, S., Toshinai, K., Ida, T., Murakami, N., et al. Peripheral ghrelin transmits orexigenic signals through the noradrenergic pathway from the hindbrain to the hypothalamus. Cell Metab. 2006,4:323-31.

[59] Zigman, J. M., Jones, J. E., Lee, C. E., Saper, C. B., Elmquist, J. K. Expression of ghrelin receptor mRNA in the rat and the mouse brain. J.Comp Neurol. 2006,494:528-48.

[60] Grill, H. J. Distributed neural control of energy balance: contributions from hindbrain and hypothalamus. Obesity (Silver.Spring). 2006,14 Suppl 5:216S-21S.

[61] Gomez, J. L., Ryabinin, A. E. The effects of ghrelin antagonists [D-Lys(3) ]-GHRP-6 or JMV2959 on ethanol, water, and food intake in C57BL/6J mice. Alcoholism, clinical and experimental research. 2014,38:2436-44.

[62] Keen-Rhinehart, E., Bartness, T. J. MTII attenuates ghrelin- and food deprivation-induced increases in food hoarding and food intake. Hormones and Behavior. 2007,52:612-20.

[63] Keen-Rhinehart, E., Bartness, T. J. NPY Y1 receptor is involved in ghrelin- and fasting-induced increases in foraging, food hoarding, and food intake. Am.J Physiol Regul.Integr.Comp Physiol. 2007,292:R1728-R37.

[64] Bartness, T. J., Morley, J. E., Levine, A. S. Effects of food deprivation and metabolic fuel utilization on the photoperiodic control of food intake in Siberian hamsters. Physiology and Behavior. 1995,57:61-8.

[65] Day, D. E., Mintz, E. M., Bartness, T. J. Diet self-selection and food hoarding after food deprivation by Siberian hamsters. Physiology and Behavior. 1999,68:187-94.

[66] Tups, A., Helwig, M., Khorooshi, R. M., Archer, Z. A., Klingenspor, M., Mercer, J. G. Circulating ghrelin levels and central ghrelin receptor expression are elevated in response to food deprivation in a seasonal mammal (Phodopus sungorus). J.Neuroendocrinol. 2004,16:922-8.

[67] Billington, C. J., Levine, A. S. Appetite regulation: Shedding new light on obesity. Current Biology. 1996,6:920-3.

[68] Ruter, J., Kobelt, P., Tebbe, J. J., Avsar, Y. Y., Veh, R., Wang, L., et al. Intraperitoneal injection of ghrelin induces Fos expression in the paraventricular nucleus of the hypothalamus in rats. Brain Res. 2003,991:26-33.

[69] Willesen, M. G., Kristensen, P., Romer, J. Co-localization of growth hormone secretagogue receptor and NPY mRNA in the arcuate nucleus of the rat. Neuroendocrinology. 1999,70:306-16.

[70] Dickson, S. L., Luckman, S. M. Induction of c-fos messenger ribonucleic acid in neuropeptide Y and growth hormone (GH)-releasing factor neurons in the rat arcuate nucleus following systemic injection of the GH secretagogue, GH-releasing peptide-6. Endocrinology. 1997,138:771-7.

[71] Bagnol, D., Lu, X. Y., Kaelin, C. B., Day, H. E., Ollmann, M., Gantz, I., et al. Anatomy of an endogenous antagonist: relationship between Agouti- related protein and proopiomelanocortin in brain. Journal of Neuroscience. 1999,19:RC26.

[72] Atasoy, D., Betley, J. N., Su, H. H., Sternson, S. M. Deconstruction of a neural circuit for hunger. Nature. 2012,488:172-7.

[73] Cowley, M. A., Smart, J. L., Rubinstein, M., Cerdan, M. G., Diano, S., Horvath, T. L., et al. Leptin activates anorexigenic POMC neurons through a neural network in the arcuate nucleus. Nature. 2001,411:480-4.

[74] Nakazato, M., Murakami, N., Date, Y., Kojima, M., Matsuo, H., Kangawa, K., et al. A role for ghrelin in the central regulation of feeding. Nature. 2001,409:194-8.

[75] Tamura, H., Kamegai, J., Shimizu, T., Ishii, S., Sugihara, H., Oikawa, S. Ghrelin Stimulates GH But Not Food Intake in Arcuate Nucleus Ablated Rats. Endocrinology. 2002,143:3268-75.

[76] Bugarith, K., Dinh, T. T., Li, A. J., Speth, R. C., Ritter, S. Basomedial hypothalamic injections of neuropeptide Y conjugated to saporin selectively disrupt hypothalamic controls of food intake. Endocrinology. 2005,146:1179-91.

[77] Aponte, Y., Atasoy, D., Sternson, S. M. AGRP neurons are sufficient to orchestrate feeding behavior rapidly and without training. Nat Neurosci. 2011,14:351-5.

# 3 AGRP KNOCKDOWN BLOCKS LONG-TERM APPETITIVE, BUT NOT CONSUMMATORY, FEEDING BEHAVIORS IN SIBERIAN HAMSTERS

## 3.1 Abstract

Arcuate hypothalamus-derived agouti-related protein (AgRP) and neuropeptide Y (NPY) are critical for maintaining energy homeostasis. Fasting markedly upregulates AgRP/NPY expression and circulating ghrelin, and exogenous ghrelin treatment robustly increases acute food foraging and food intake, and chronic food hoarding behaviors in Siberian hamsters. We previously demonstrated that 3rd ventricular AgRP injection robustly stimulates acute and chronic food hoarding, largely independent of food foraging and intake. By contrast, 3rd ventricular NPY injection increases food foraging, food intake, and food hoarding, but this effect is transient and gone by 24 h post-injection. Because of this discrepancy in AgRP/NPY-induced ingestive behaviors, we tested whether selective knockdown of AgRP blocks fasting and ghrelin-induced increases in food hoarding. AgRP gene knockdown by a novel DICER small interfering RNA (AgRP-DsiRNA) blocked food-deprivation induced increases in AgRP expression, but had no effect on NPY expression. AgRP-DsiRNA attenuated acute (1 day), and significantly decreased chronic (4-6 days), food deprivation-induced increases in food hoarding. In addition, AgRP-DsiRNA treatment blocked exogenous ghrelin-induced increases in food hoarding through day 3, but had no effect on basal food foraging, food intake, or food hoarding prior to ghrelin treatment. Lastly, chronic AgRP knockdown had no effect on body mass, fat mass, or lean mass in either food deprived or *ad libitum* fed hamsters. These data collectively suggest that the prolonged increase in food hoarding behavior following energetic challenges, and food deprivation especially, is primarily regulated by downstream AgRP signaling.

## 3.2 Introduction

Obesity is a critical health concern facing both developed and developing countries worldwide due to its many secondary comorbidities including stroke, type 2 diabetes, cardiovascular disease, and cancer [1-5]. Energy intake that exceeds energy expenditure is the primary cause of obesity, and the prevalence of readily accessible, calorically dense foods contributes to a state of chronic energy surplus in obese persons [6]. Previous research on ingestive behaviors has largely focused on uncovering the neuroendocrine mechanisms governing food intake using laboratory mice and rats, yet in humans the search for food (i.e. food shopping/foraging) invariably precedes the immediate consumption or long-term storage (i.e. in refrigerators, freezers, and pantries) or hoarding of food. Hence, ingestive behaviors are more accurately dichotomized as appetitive behaviors that bring animals into contact with food (i.e. food foraging and food hoarding) and consummatory behaviors in which animals consume food [7]. Previous studies have suggested obese or food deprived persons purchase more calorically dense, high-fat foods and hoard these items for longer periods of time relative to lean or satiated persons [8-11]. In turn, elucidating the mechanisms mediating ingestive behaviors as a whole represents a novel approach for the development of obesity reversal or prevention options.

To investigate the central nuclei regulating appetitive (i.e. food foraging and hoarding) and consummatory (i.e. food intake) ingestive behaviors necessitates an animal model that naturally hoards food. Siberian hamsters (Phodopus sungorus), like humans, are natural and prodigious food hoarders [12], and we have previously shown that energetic challenges (e.g. food deprivation and ghrelin) robustly increase this behavior [12-14]. We have developed a unique experimental approach to test the central and peripheral factors regulating ingestive behaviors by which animals earn food through wheel running in a top “foraging” cage, and store

this food for future meals in a bottom "hoarding" cage [15]. With this experimental set up, we have begun to elucidate the complex neuroendocrine network mediating these appetitive and consummatory ingestive behaviors (for review see [6]).

The stomach-derived orexigenic hormone ghrelin is of particular interest in the context of ingestive behaviors due to its preprandial rise and postprandial decrease [16-18]. Exogenous ghrelin treatment, mimicking an energy deplete state, markedly increases ingestive behaviors in humans and laboratory rodents including Siberian hamsters [19-22]. We have recently shown that third ventricular or intraperitoneal exogenous ghrelin treatment acutely increases food intake and food foraging (~2-4 h), and drives chronic (~5-7 days) food hoarding increases, both of which are blocked by central ghrelin receptor antagonism [23]. The ghrelin receptor (growth hormone secretagogue receptor 1a [GHSR]) is broadly distributed in the brain [24, 25], including on hypothalamic arcuate nucleus (Arc) neurons that coexpress agouti-related protein (AgRP), neuropeptide Y (NPY), and gamma-aminobutyric acid (GABA)- termed AgRP neurons as AgRP is spatially limited to the Arc [25, 26]. The Arc contains receptors for numerous circulating endocrine signals (e.g. ghrelin and leptin), and exogenous ghrelin treatment robustly increases AgRP/NPY expression [27, 28]. A critical role of these neurons in regulating energy homeostasis is further supported by the finding that ablation of these neurons in adult mice results in profound hypophagia [29]. In addition, AgRP neurons regulate ingestive behaviors through temporally discrete mechanisms. Pharmacogenetic or optogenetic AgRP neuron activation drives rapid, NPY/GABA-dependent food intake, and delayed, but prolonged, AgRP-dependent food intake in mice [30]. Although AgRP and NPY are sufficient to mediate food intake through distinct temporal mechanisms, it remains unclear if these neuropeptides regulate acute and chronic food foraging and food hoarding through similar mechanisms. To this end, we

recently demonstrated that central NPY administration markedly increases food foraging, food hoarding, and food intake in Siberian hamsters, but this effect is transient and gone by 24 h post-injection [31]. ICV blockade of the NPY Y1 receptor completely blocks fasting- and ghrelin-induced food foraging and food intake, but has comparatively little effect on food hoarding, suggesting either other NPY receptors or neurochemical systems mediate this behavior [32]. In support of an NPY-independent mechanism regulating multi-day food hoarding following energetic challenges, we found that central AgRP robustly increases both acute and chronic (through 7 days) food hoarding to a much greater extent than food foraging or food intake in Siberian hamsters [33]. These findings collectively suggest the presence of separate neurochemical mechanisms regulating appetitive and consummatory behaviors following energetic challenges, and that this differential neuropeptide regulation of ingestive behaviors occurs through temporally discrete mechanisms such that acute changes in consummatory behavior are not intrinsically followed by changes in appetitive behaviors. We therefore tested whether AgRP discretely regulates food deprivation- or ghrelin-induced appetitive and consummatory ingestive behavior, including food intake, foraging, and hoarding.

To test the necessity of AgRP in regulating food deprivation- and ghrelin-induced increases in ingestive behaviors necessitates a novel approach that specifically targets AgRP. The development of DICER small interfering RNA (DsiRNA) duplexes and other antisense oligonucleotides has facilitated in vivo, targeted mRNA knockdown in non-genetically engineered animals including humans (for review see [34]). AgRP-DsiRNA mediated gene knockdown circumvents the inherent confounds of germ-line knockout models or non-specific receptor antagonism, and affords the ability to directly test the endogenous function of AgRP in a natural animal model of food hoarding. Here, we tested the role of AgRP in the regulation of

ingestive behaviors by giving chronic AgRP-DsiRNA injections throughout energetic challenges in Siberian hamsters housed in our foraging and hoarding system. In addition, we have used a protocol modified from our previous studies, which enables us to more accurately examine the effects of AgRP knockdown on ingestive behaviors at discrete time points.

## 3.3 Materials and Methods

### *3.3.1 Animals*

Adult male Siberian hamsters aged ~2 months and weighing 30-40 g were obtained from our breeding colony as previously described [35]. Hamsters were sexed and group housed from birth in a summer-like photoperiod (16:8-h light-dark cycle, light offset at 1900) with *ad libitum* access to food (formula 5001, Purina, St. Louis, MO) and water. Room temperature was maintained at 21.0 ± 2°C. All procedures were approved by the Georgia State University Institutional Animal Care and Use Committee and were in compliance with the Public Health Service and United States Department of Agriculture guidelines

### *3.3.2 RNAi-mediated gene knockdown*

To specifically knockdown Arc AgRP, we chose a DICER small interfering RNA (DsiRNA) directed against AgRP (MMC.RNAI.N007427.12.1; Integrated DNA Technologies [AgRP-DsiRNA]) and a control scrambled RNA (DsiRNA; NC1; Integrated DNA Technologies [scRNA]) directed against no known mRNA sequence. scRNA and AgRP-DsiRNA were initially reconstituted in sterile $dH_2O$, aliquoted, and frozen at -80°C to prevent RNA degradation. For hydrodynamic injections, scRNA (0.4µg/g body mass [BM]) and AgRP-DsiRNA (0.4µg/g BM) were diluted in sterile saline and rapidly injected intraperitoneally (i.p.) as previously described [36-38].

### *3.3.3 Blood brain barrier permeability and central effects of DsiRNA-mediated AgRP knockdown*

Blood brain barrier permeability was tested using peripheral sodium fluorescein injections (10%, 5ml/kg, i.p.; Sigma-Aldrich). Following a single i.p. injection, animals were returned to their home cage for 30 min and then killed by an overdose of Fatal Plus (300 mg/kg, i.p.; Vortech Pharmaceuticals). Animals were transcardially perfused with 10 ml ice cold 0.1 M PBS followed by 30 ml ice cold 4.0% paraformaldehyde in 0.1 M PBS. Brains were then extracted and transferred to 4.0% paraformaldehyde in 0.1 M PBS overnight and then 18.0% sucrose at 4°C. Brains were subsequently sectioned with a cryostat at 20 µm and the Arc immediately visualized with fluorescent microscopy.

To test the efficacy of AgRP-DsiRNA-mediated gene knockdown, we chose a 48 h food deprivation challenge as this energetic challenge typically causes a marked increase of AgRP and NPY expression in Siberian hamsters [39, 40]. Preliminary experiments indicated daily AgRP-DsiRNA (0.4µg/g BM i.p.) injections most effectively blocked AgRP mRNA expression (data not shown), so we adopted this approach for all subsequent experiments [**Fig. 1A**]. In one cohort of hamsters used for *in situ* hybridization, animals were food deprived for 48 h and given either scRNA (0.4µg/g BM i.p.) or AgRP-DsiRNA (0.4µg/g BM i.p.) daily at 0900 (two total injections at t=0 and t + 24 h). Animals were killed by an overdose of Fatal Plus 48 h after food removal (i.e. 24 h after the last injection), and then transcardially perfused with 75 ml of heparinized 0.9% NaCl in RNase free 0.01% diethylpyrocarbonate (DEPC)-treated $dH_2O$ followed by 150 ml 4.0% paraformaldehyde in 0.1 M PBS in sterile filtered $dH_2O$. Brains were subsequently removed, post fixed in sterile 4.0% paraformaldehyde in 0.1 M PBS overnight, and then transferred to sterile 0.01% DEPC-treated 18.0% sucrose at 4°C. Brains were sectioned with a

cryostat at 20 µm in series across 3 slides to cover the entirety of the Arc, and then frozen at -80°C to reduce mRNA degradation.

In a separate cohort of hamsters used for quantitative PCR (qPCR) analysis, animals were either food deprived or allowed *ad libitum* access to food. Food deprived and *ad libitum* fed animals were given either scrambled RNA (scRNA) or AgRP-DsiRNA (0.4µg/g BM i.p.) injections daily at 0900 across 48 h (two total injections at t=0 and t + 24 h). Animals were killed by rapid decapitation 24 h later (i.e. t + 48 h), the brain extracted, and 1 mm sagittal sections taken from both sides of the midline. The hypothalamus was identified and cut rostrally at the optic chiasm, caudally at the mammillary bodies, and a ~0.5 mm dorsal cut made to isolate the Arc which was immediately flash frozen in liquid nitrogen. Frozen hypothalamic tissue was stored at -80°C until processing to reduce mRNA degradation. Importantly, qPCR analysis was repeated in three separate cohorts of animals to ensure consistent results and a robust physiological effect of the AgRP-DsiRNA.

### *3.3.4 Fluorescent in situ hybridization for AgRP and NPY mRNA*

We used double-fluorescent *in situ* hybridization to analyze both AgRP and NPY expression following a 48 h food deprivation challenge and treatment with either scRNA or AgRP-DsiRNA as previously described [40, 41]. In brief, single-stranded antisense mRNA fragments against rat AgRP (a generous gift from Dr. Kevin Grove) and hamster NPY (provided by S. Chua, Columbia University, New York, NY) were reverse transcribed from plasmid DNA and labeled with digoxigenin (DIG RNA Labeling Mix; Roche Applied Sciences) or FITC (FITC RNA Labeling Mix; Roche Applied Sciences). A rat antisense AgRP riboprobe was used as previously described [42] because of its consistently robust, specific staining. Frozen slides containing the mounted sections were removed from -80°C ~20 min before use to reach room

temperature. Slides were submerged in 2x SSC, acetylated with 0.1 M triethanolamine/0.25% acetic anhydride solution in 0.1% DEPC-treated $dH_2O$, and then fixed the tissues with a 1:1 acetone/methanol mixture. We next added 150 µl prehybridization buffer, coverslipped the slides, and left the sections at room temperature for 30 min. Coverslips were then removed and tissues hybridized with antisense riboprobes (150 ng/slide) for AgRP and NPY in a humid chamber for 16-20 h at 58°C. Slides were subsequently removed from humid chambers and submerged in an RNase A/ 2x SSC solution (20µg/ml) at 37°C to degrade unbound RNA. Sections were washed in decreasing 2x SSC concentrations to 0.5x, quenched for endogenous peroxidase activity with 1.0% $H_2O_2$, and permeabilized with 0.5% Tween 20 in 0.1 M Tris-HCL. Sections were then blocked in 10% normal sheep serum (NshS) and 5.0% casein in 0.1 M tris-buffered saline (TBS) for 30 min. We next incubated the sections with sheep anti-digoxigenin FAB fragments (1:250; Roche Applied Sciences) in 10.0% NShS and 5.0% casein in 0.1 M TBS for 2 h at room temperature and amplified the signal with tyramide signal amplification (TSA; 1:200; TSA Plus Cyanine 3 Kit; PerkinElmer Lifer and Analytical Sciences). To amplify and reveal the second (FITC) riboprobe, we used a second peroxidase quenching step with 3% $H_2O_2$ in 0.1 M TBS, blocked the sections for 30 min in 10% NShS and 5.0% casein, and then incubated the sections for 2 h at room temperature with anti-FITC FAB fragments (1:250; Roche Applied Sciences) that were subsequently amplified via TSA (1:200; TSA Plus Fluorescein; PerkinElmer Life and Analytical Sciences). Slides were coverslipped with Prolong antifade fluorescent medium (Invitrogen) and stored at room temperature, shielded from light, until image capture.

### *3.3.5 Fluorescent quantification*

Fluorescent labeling in the Arc was quantified with experimenters blind to treatment conditions. A mouse brain atlas (Paxinos and Franklin [43]) was used as it most closely matches the Siberian hamster brain and no Siberian hamster brain atlas exists. Total cells expressing NPY and AgRP were counted across the Arc in each animal and then averaged for each treatment group. Relative fluorescent intensity (RFI) was measured for each mRNA probe for all animals as previously described [40, 44]. In brief, background was normalized for all sections and NIH ImageJ software was used to capture and measure fluorescent intensity of a defined Arc region. Intensity measurements of either AgRP or NPY were then averaged across all animals for each treatment group.

### *3.3.6 Quantitative PCR analysis*

RNA from frozen hypothalamic tissue was extracted using TRIzol Reagent (Thermo Fisher) and subsequently reverse transcribed into cDNA with a High-Capacity cDNA Reverse Transcription Kit (Thermo Fisher) according to the manufacturer's instructions. AgRP and NPY gene expression was measured using TaqMan Gene Expression Master Mix (Thermo Fisher) and a 7500-Fast RT-PCR machine (Applied Biosystems). As Siberian hamster TaqMan primers and probes are not commercially available, custom primer/probe sets were generated (Applied Biosystems) based on previously described Siberian hamster AgRP and NPY sequences [45]. AgRP primers/probe- forward primer: AGGCCCTGCTGCAGAAG, reverse primer: GACTCGCGATTCTGTGGATCTAG, reporter probe: ACCTCCGCCAACGCT; NPY primers/probe- forward primer: CTCCGCTGGTGCATCCT, reverse primer: GTGCTGGCTGAGGGATACC, reporter probe: AAGCCTGACAATCCTG. Mouse glyceraldehyde-3-phosphate dehydrogenase (GAPDH) (Applied Biosystems) was used as an

endogenous control as its expression was consistent across all animals and treatments (A.T. and T.J.B. unpublished observations).

### *3.3.7 Foraging and hoarding apparatus*

At the start of the experiment, animals were transferred to the foraging/hoarding room and singly housed in polypropylene cages (27.8 X 17.5 X 13.0 cm) with Alpha-dri bedding (Specialty Papers, Kalamazoo, MI) and a single cotton Nestlet (Ancare, Belmore, NY). Animals were allowed *ad libitum* access to the experimental diet (purified 75-mg Dustless Precision Pellets, Bio-Serve, Frenchtown, NJ) and water, and given two weeks to acclimate to the new light cycle (16:8-h light-dark cycle, light offset at 1200). Following acclimation to the new photoperiod, animals were transferred to our foraging and hoarding apparatus, modified from Perrigio and Bronson [46], as previously described [15]. In brief, animals were given unrestrained access to a top "foraging" cage (456 mm long × 234 mm wide × 200 mm high) equipped with a running wheel, pellet dispenser, and water bottle, and a bottom "hoarding" cage (290 mm long × 180 mm wide × 130 mm high) containing Alpha-Dri bedding and one cotton nestlet. The foraging and hoarding cages were connected by convoluted polyvinylchloride tubing (38.1 mm inner diameter, ~1.5 m long) with bends and runs to facilitate movement between the two cages. Animals were allowed a two-week training period to the foraging and hoarding apparatus before experimental manipulation. During the first two days of this training period, animals were given free access to food pellets and were able to earn an additional pellet by completing 10 wheel revolutions. Following this two-day period, free access to food was removed and all food had to be earned through wheel running (1 pellet/10 wheel revolutions), during which time wheel revolutions, pellets earned, food intake, and food hoarding were measured daily.

### *3.3.8 Measurement of food foraging, food hoarding, and food intake experimental protocol*

For all behavioral experiments, food foraging, food hoarding, and food intake was assessed daily at 0900. Food foraging was defined as the number of wheel revolutions divided by 10, as 10 revolutions were required for each pellet delivery. Food hoarding was defined as the number of pellets present in the bottom hoarding cage in addition to pellets removed from the cheek pouches of hamsters. Food intake was defined as [the number of pellets earned – (number of pellets remaining in the top cage that were not hoarded + number of pellets hoarded)]. All food pellets were weighed on an electronic scale set to "parts" measurement with one 75 mg food pellet= 1, and fractions of pellets calculated as well.

#### *3.3.8.1 Experiment 1: Does AgRP-DsiRNA block food deprivation-induced increases in appetitive behaviors?*

At the end of the training period, animals were divided into two groups counterbalanced for BM, food foraging, food hoarding, and food intake: 1) scRNA (0.4µg/g BM i.p.); 2) AgRP-DsiRNA (0.4µg/g BM i.p.). At the start of the food deprivation challenge, animals were transferred to a new hoarding cage, provided water, and blocked in this cage to prevent access to the top foraging cage for 48 h. At the conclusion of the 48 h food deprivation, animals were unblocked from the hoarding cage at lights off (1200) and allowed access to the foraging cage. scRNA or AgRP-DsiRNA injections were given daily (at 0900) throughout the food deprivation, and then daily at the same time as data collection (0900) throughout the duration of the experiment for a total of 8 injections (i.e. 2 days of food deprivation and 6 total days of post-fast refeeding behavioral data collection) [**Fig. 1B**].

#### *3.3.8.2 Experiment 2: Does AgRP-DsiRNA block Ghrelin-induced increases in appetitive behaviors?*

Following the training period in a separate cohort of hamsters, animals were divided into four groups counterbalanced for BM, food foraging, food hoarding, and food intake: 1) i.p. saline + scRNA (0.4µg/g BM i.p.); 2) i.p. ghrelin (30 µg/kg BM i.p.) + scRNA (0.4µg/g BM i.p.); 3) i.p. ghrelin (30 µg/kg BM i.p.) + AgRP-DsiRNA (0.4µg/g BM i.p.); 4) i.p. saline + AgRP-DsiRNA (0.4µg/g BM i.p.). To ensure adequate AgRP knockdown, animals received either scRNA or AgRP-DsiRNA injections (at 0900) for two days prior to ghrelin injection. On experimental test day, food was removed from the top foraging cage and animals were placed into a new, clean hoarding cage immediately following AgRP-DsiRNA injections. Animals were blocked in this cage at 0900 to prevent wheel running, food intake, or food hoarding prior to ghrelin injection at lights off at 1200 as previously described [22, 23]. Immediately after lights off, animals were injected with either saline or ghrelin and cages were unblocked to allow for access to the top cage. On subsequent days, animals were given either scRNA or AgRP-DsiRNA injections at the same time as data collection for the duration of the experiment (0900). Hence, animals received a total of 9 injections throughout the experiment (i.e. 2 days prior to ghrelin injection, the morning of ghrelin injection, and 6 days of post-ghrelin behavioral data collection) [**Fig. 1C**].

### *3.3.9 Body composition measurements*

Body composition measurements for *experiment 1* and *experiment 2* hamsters were taken using our Minispec LF90 TD-NMR analyzer (Bruker Optics). For all measurements, animals were briefly removed from their home cage, placed in the body composition analyzer, and then immediately returned to their home cage. Body composition measurements were taken for all

animals prior to the start of *experiment 1* and *experiment 2*, and then again at the conclusion of the experiments.

### *3.3.10 Statistical analysis*

All data are expressed as mean ± S.E. Relative AgRP and NPY gene expression as measured by quantitative PCR were normalized to GAPDH. For behavioral experiments, data for each animal on experiment day(s) (i.e., number of pellets earned, consumed, or hoarded) were compared with the average data across the three days prior to the experiment start (i.e. baseline values) for the same animal. For a subset of statistical analyses where percent baseline (% baseline) was used, % baseline for each animal on experimental day(s) was calculated as given by the formula [(animal X on experimental day(s)/animal X baseline)*100] and compared with that animals normalized baseline value as given by the formula [(animal X baseline/average for all animals in the group)*100]. Data were analyzed by a Student's t-test, Mann-Whitney U test, or a one-way or two-way ANOVA followed by Duncan's Multiple-Comparison post-hoc analysis where appropriate. For all experiments, differences among groups was considered statistically significant at $P<0.05$ and trending toward significance at $P<0.1$.

## 3.4 Results

### *3.4.1 AgRP-DsiRNA blocks food deprivation-induced Arc AgRP expression*

i.p. sodium fluorescein injections revealed extensive neuronal labeling within the Arc, but not in nearby hypothalamic nuclei including the ventromedial hypothalamus (VMH) or dorsomedial hypothalamus (DMH) [**Fig. 3.2A**], indicating that peripherally administered drugs are sufficient to reach Arc neurons. We therefore sought to test whether i.p. administered AgRP-DsiRNA was sufficient to block AgRP, but not NPY, expression following an energetic challenge that typically causes marked increases in AgRP and NPY expression in Siberian

hamsters [40]. We initially used *in situ* hybridization against AgRP and NPY mRNA to visualize mRNA expression following a 48 h fast, and measured relative fluorescent intensity and neuronal number as markers for AgRP and NPY activation [**Fig. 3.1A**]. We observed extensive AgRP and NPY mRNA expression in scrambled RNA (scRNA) treated animals [**Fig. 3.2, B-D**], but a marked decrease in AgRP, but not NPY, mRNA expression in AgRP-DsiRNA treated animals [**Fig. 3.2, E-G**]. Relative fluorescent intensity quantification revealed AgRP-DsiRNA significantly decreased AgRP mRNA expression by approximately 50% [$P<0.05$; **Fig. 3.2H**], but had no effect on NPY mRNA Expression [**Fig. 3.2I**]. In addition, the number of AgRP-positive neurons was significantly decreased in AgRP-DsiRNA treated animals compared with scRNA treatment [$P<0.05$; **Fig. 3.2J**], but there was no effect on NPY-positive neurons [**Fig. 3.2J**].

To confirm our *in situ* data, and to further validate the efficacy of AgRP-DsiRNA, we repeated the 48 h food deprivation challenge in a separate cohort of animals and measured AgRP and NPY mRNA expression with quantitative PCR (qPCR). AgRP-DsiRNA significantly decreased AgRP mRNA expression in *ad libitum* fed animals compared with scRNA treated animals [$P<0.05$; **Fig. 3.3A**]. Moreover, 48 h food deprivation significantly increased AgRP mRNA expression in scRNA treated animals, but this effect was abrogated by AgRP-DsiRNA treatment [$P<0.05$; **Fig. 3.3A**]. By contrast to AgRP mRNA expression, AgRP-DsiRNA treatment had no effect on NPY mRNA expression in either *ad libitum* fed animals or 48 h food deprived animals compared with control scRNA treated animals [**Fig. 3.3B**].

### *3.4.2 AgRP-DsiRNA attenuates food deprivation-induced food hoarding*

After confirming the efficacy of AgRP-DsiRNA, we tested whether AgRP knockdown affects food foraging, food intake, or food hoarding following a food deprivation challenge [**Fig.**

**3.1B**]. Upon refeeding after a 48 h fast, the number of pellets earned was significantly decreased in both scRNA and AgRP-DsiRNA treated animals relative to baseline, and this marked decrease in foraging effort failed to return to baseline levels throughout the experiment [*P<0.05;* **Fig. 3.4A**]. In addition, a trend of increased pellets earned (foraging) was observed in AgRP-DsiRNA treated animals compared with scRNA treatment at day 1 [*P<0.1;* **Fig. 3.4A**]. However, we observed no difference in foraging effort between treatment groups at days 2-6 post-refeeding. Food intake was significantly decreased at day 1 and day 2 post-refeeding for both scRNA and AgRP-DsiRNA treated animals relative to baseline [*P<0.05;* **Fig. 3.4B**], but AgRP-DsiRNA had no effect on pellets consumed compared with scRNA treatment at any time point examined [**Fig. 3.4B**]. By contrast, food hoarding was markedly increased relative to baseline for both AgRP-DsiRNA and scRNA treated animals on days 1 and 2 post-refeeding [*P<0.05;* **Fig. 3.4C**], but AgRP knockdown blocked this relative increase at day 4. Moreover, AgRP-DsiRNA significantly decreased food hoarding at days 1 and 4 post-refeeding compared with scRNA treated animals [*P<0.05*; **Fig. 3.4C**], and a trend of decreased food hoarding was observed at day 5 post-refeeding [*P=0.1*; **Fig. 3.4C**].

Because we previously found central AgRP increases food hoarding across multiple days [33], we combined the total number of pellets earned, consumed, or hoarded across days 2-3 and 4-6 post-refeeding (**Fig. 3.4D-F**) to identify changes in behavioral trends that may not otherwise be apparent when discretely examining each day as previously described [40]. Of note, we omitted day 1 from our analysis of combined days 2-3 as the data at this time point were markedly different from ensuing time points and tended to skew the data on these days. Despite the trend of decreased food foraging at day 1 post-refeeding [*P<0.1*; **Fig. 3.4D**], we found no difference in foraging effort on days 2-3 or 4-6 [**Fig. 3.4D**]. In addition, AgRP-DsiRNA

treatment had no effect on food intake on either day 1 post-refeeding, or on combined days 2-3 or 4-6 [**Fig. 3.4E**]. By contrast to food foraging and food intake, AgRP-DsiRNA treatment significantly decreased pellets hoarded at day 1 post refeeding [*P<0.05*; **Fig. 3.4F**], and a trend of decreased pellets hoarded was observed on combined days 4-6 compared with scRNA treated animals [*P=0.054*; **Fig. 3.4F**].

We next converted raw food foraging, food intake, and food hoarding values into percentage of baseline (% baseline) (**Fig. 3.4G-I**) to compare the effects of AgRP-DsiRNA on ingestive behaviors in an energy deplete state with an *ad lib*-fed condition. Food deprivation markedly decreased food foraging in both AgRP-DsiRNA and scRNA treated animals compared with baseline on day 1 post-refeeding and for combined days 2-3 and 4-6, and never returned above ~80% baseline levels [*P<0.05*; **Fig. 3.4G**]. AgRP-DsiRNA treatment tended to increase pellets earned on day 1 post-refeeding compared with control animals [*P<0.1*; **Fig. 4G**], which reached statistical significance on combined days 2-3 [*P<0.05*; **Fig. 3.4G**]. Food deprivation significantly decreased food intake relative to baseline in both AgRP-DsiRNA and scRNA treated animals on day 1 and combined days 2-3 post-refeeding [*P<0.05*; **Fig. 3.4H**], with the food intake returned to baseline values on combined days 4-6 post-refeeding [**Fig. 3.4H**]. However, no difference in food intake was observed between treatments at any time point examined. By contrast to the marked decrease in food foraging and food intake, food deprivation robustly increased food hoarding relative to baseline at day 1 post-refeeding, and remained increased over baseline on days 2-3 and 4-6 post-refeeding in scRNA treated hamsters [*P<0.05*; **Fig. 3.4I**]. AgRP-DsiRNA treatment significantly decreased food hoarding by ~50% on day 1 post-refeeding compared with control animals [*P<0.05*; **Fig. 3.4I**], and attenuated this increase on days 4-6 [*P<0.05*; **Fig. 3.4I**].

48 h food deprivation resulted in a profound ~20% decrease in body mass in both scRNA and AgRP-DsiRNA treated animals, and this change in body mass remained significantly decreased relative to baseline in both groups for the duration of the experiment [*P<0.05*; **Fig. 3.5A**]. Moreover, food deprivation significantly decreased % fat mass and increased % lean mass relative to baseline for both AgRP-DsiRNA and scRNA treated animals [*P<0.05*; **Fig. 3.5B** and **3.5C**], but we found no differences in % fat mass or % lean mass at any time point between these groups (**Fig. 3.5B** and **3.5C**).

### *3.4.3 AgRP-DsiRNA attenuates ghrelin-induced food hoarding*

Because food deprivation markedly increases circulating ghrelin, we next tested whether AgRP mRNA knockdown is sufficient to block ghrelin-induced ingestive behaviors [**Fig. 3.1C**]. AgRP-DsiRNA treatment had no effect on pellets earned, consumed, or hoarded prior to the exogenous ghrelin treatment when compared with baseline values [**Fig. 3.6A-C**]. However, we found a significant decrease in foraging effort for all groups on day 1 following exogenous ghrelin [*P <0.05*; **Fig. 3.6A]**, an effect likely stemming from the novelty of the experimental procedure as ghrelin injections occurred at lights off (1200) on the preceding day and pre-ghrelin scRNA or AgRP-DsiRNA injections (at 0900) had no effect on behavior arguing against a possible pain response. Subsequent to this initial decrease in food foraging, we found no differences in food foraging for the remainder of the experiment nor food intake at any time point examined for all groups following exogenous ghrelin [**Fig. 3.6A** and **3.6B**]. By contrast, systemic ghrelin significantly increased food hoarding compared with control saline + scRNA treated animals at day 1 post-injection [*P<0.05;* **Fig. 3.6C**], and AgRP-DsiRNA treatment attenuated this increase. We found no subsequent differences in the number of pellets hoarded among any group on days 2-6 post-injection [**Fig. 3.6C**].

We next combined the raw pellets foraged for, consumed, or hoarded on days 1-3 and 4-6 (**Fig. 3.6D-F**) and then converted these values into a percent change from baseline (**Fig. 6G-I**) to identify any cumulative effects of exogenous ghrelin or AgRP-DsiRNA on behavior. We found no difference between any group in the absolute number of pellets earned [**Fig. 3.6D**], consumed [**Fig. 3.6E**], or hoarded [**Fig. 3.6F**] on either combined days 1-3 or 4-6. By contrast, we found a significant decrease in pellets earned relative to baseline for all groups on days 1-3 post injection [**Fig. 3.6G**], most likely stemming from the novelty of the procedure. Although exogenous ghrelin had no effect on food foraging in combined days 1-3, we found a significant increase compared with scRNA treated animals on days 4-6, and this effect was attenuated with AgRP-DsiRNA treatment [$P<0.05$; **Fig. 3.6G**]. In line with our food deprivation data, exogenous ghrelin significantly decreased food intake during combined days 1-3 relative to baseline in ghrelin + scRNA, but this effect was absent in AgRP-DsiRNA treated animals [$P<0.05$; **Fig. 3.6H**]. Moreover, saline + AgRP-DsiRNA treatment significantly increased pellets consumed compared with saline + scRNA and ghrelin + scRNA treatment on combined days 1-3 and 4-6 [$P<0.05$; **Fig. 3.6H**]. Ghrelin + AgRP-DsiRNA treatment also significantly increased pellets consumed compared with ghrelin + scRNA treatment on combined days 1-3 [$P<0.05$; **Fig. 3.6H**]. As expected, exogenous ghrelin robustly and significantly increased food hoarding relative to baseline on days 1-3 post-injection compared with all other groups [$P<0.05$; **Fig. 3.6I**]. Of note, we found no change in food hoarding in AgRP-DsiRNA treated animals compared with baseline or scRNA control animals, indicating AgRP knockdown specifically abrogated ghrelin-induced hoarding behavior. No subsequent change in food hoarding was observed in any group on combined days 4-6 post-injection [**Fig. 3.6I**].

Concurrent with our behavior experiment, we measured body mass and body composition to uncover any effects of AgRP-DsiRNA on body mass, % fat mass, or % lean mass across time. We found no difference in body mass change across time, or in % fat mass or % lean mass at either baseline or at the conclusion of the experiment [**Fig. 3.7A-C**].

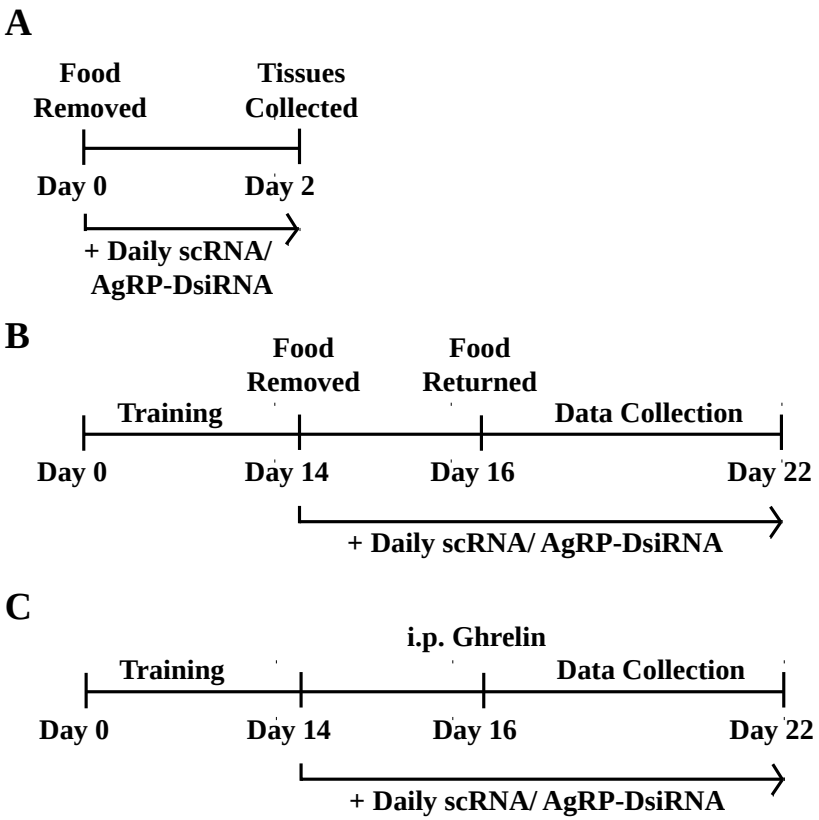


**Fig. 3.1** Experimental timeline.
Experimental timeline for AgRP-DsiRNA (0.4µg/g BM i.p.) in situ hybridization and quantitative PCR efficacy tests (A). Experimental timelines for training, AgRP-DsiRNA (0.4µg/g BM i.p.) or scRNA (0.4µg/g BM i.p.) treatment, and data collection for behavioral Experiment 1 (B) or behavioral Experiment 2 (C).

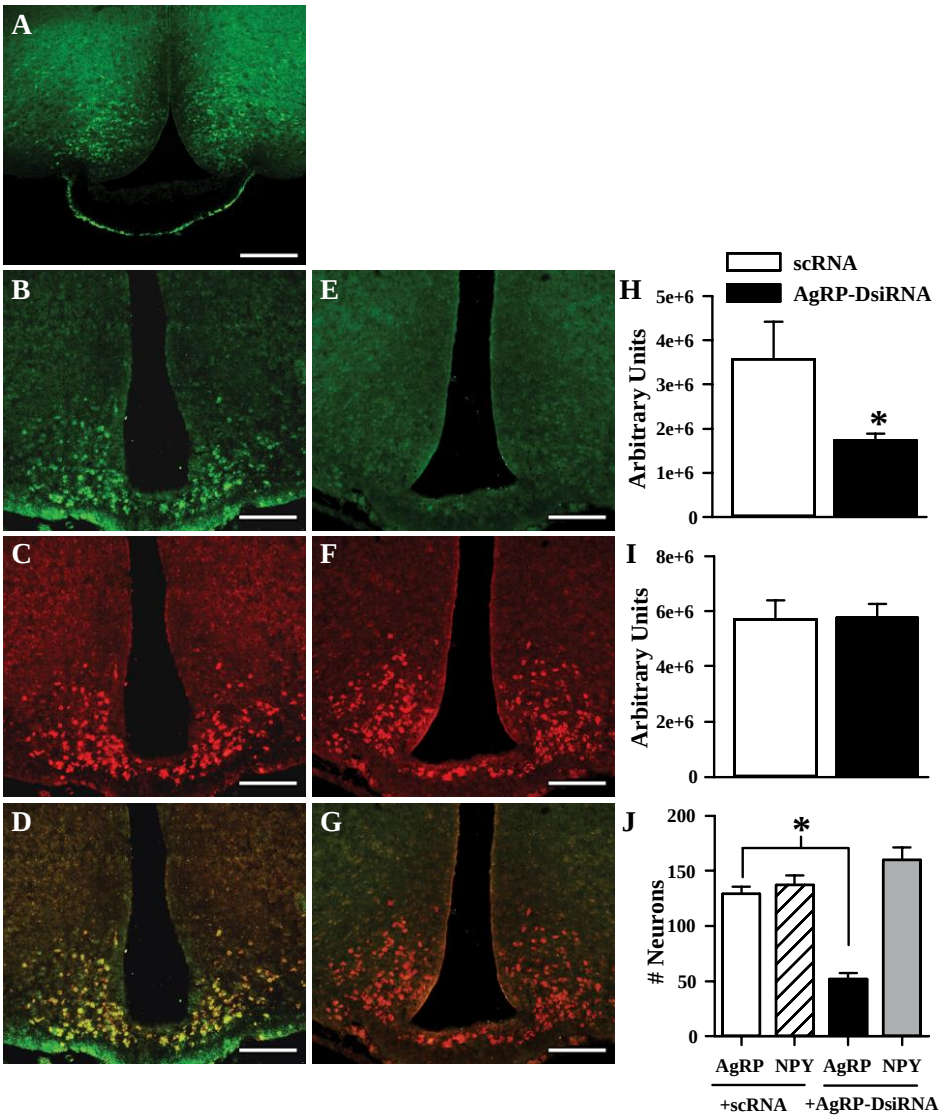


**Fig. 3.2** AgRP-DsiRNA selectively blocks AgRP expression.
Representative image of arcuate nucleus neuronal labeling following sodium fluorescein injections (10%, 5ml/kg, i.p) (A). Representative double-fluorescent in situ hybridization images for AgRP (green), NPY (red), and merged sections in scRNA (0.4µg/g BM i.p.) (B-D) and AgRP-DsiRNA (0.4µg/g BM i.p.) treated (E-G) animals. Relative fluorescent intensity (RFI) measurements for AgRP (H) and NPY (I) (n=4-5 per group). Average number of arcuate nucleus AgRP-positive and NPY-positive neurons in AgRP-DsiRNA and scRNA treated animals (J) (n=4-5 per group). Scale bar in A-G= 100 µm. Data reported as mean ± S.E.M. *P<0.05 vs. scRNA treatment.

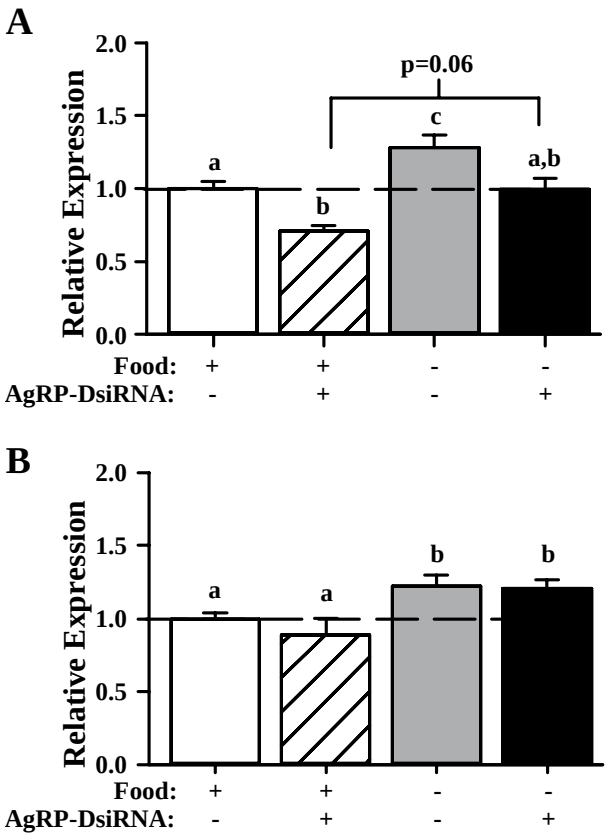


**Fig. 3.3** AgRP-DsiRNA blocks food deprivation-induced AgRP increases. Relative arcuate nucleus *AgRP* (*A*) and *NPY* (*B*) mRNA expression as measured by qPCR in *ad libitum* fed and food deprived animals receiving either scRNA (0.4µg/g BM i.p.) or AgRP-DsiRNA (0.4µg/g BM i.p.) (n=8-15 per group). Data are averages across three experimental cohorts. Data reported as mean ± S.E.M. Values that do not share a common superscript are significantly different at $P<0.05$.

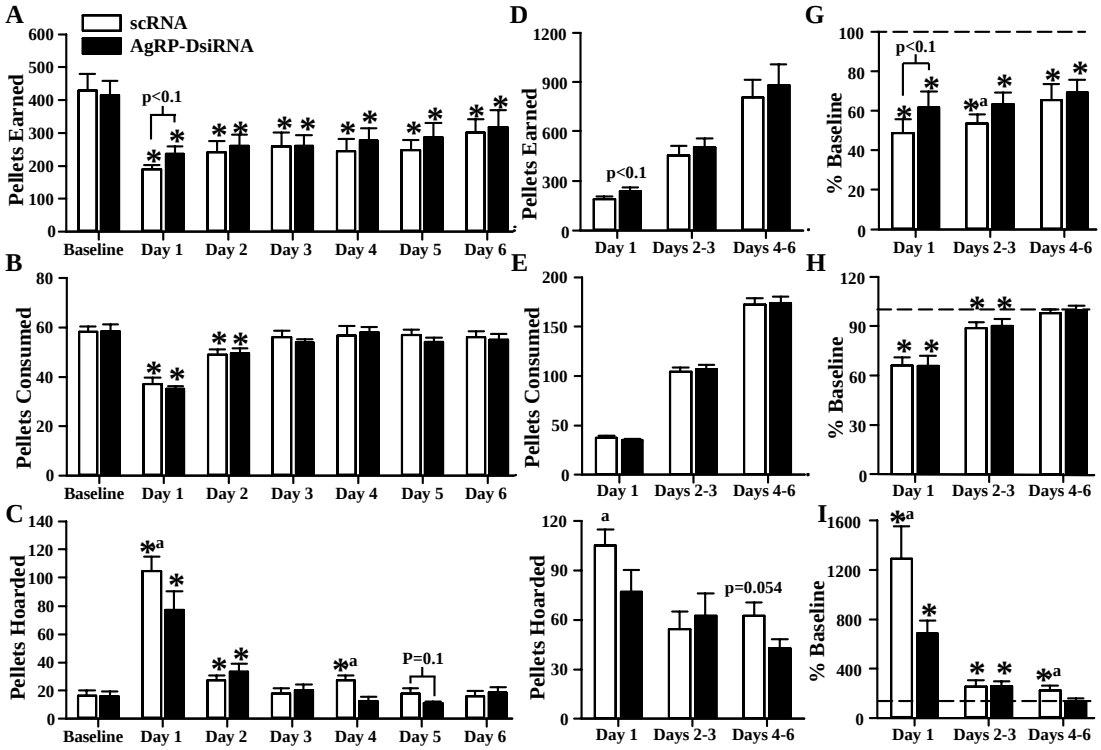


**Fig. 3.4** AgRP knockdown attenuates food deprivation-induced food hoarding. Average number of pellets earned (*A*), consumed (*B*), and hoarded (*C*) prior to food removal (baseline) and upon refeeding after a 48 h food deprivation challenge in scRNA (0.4µg/g BM i.p.) and AgRP-DsiRNA (0.4µg/g BM i.p.) treated animals. Day 1 and combined days 2-3 and 4-6 number of pellets earned (*D*), consumed (*E*), and hoarded (*F*) following refeeding. Percent baseline converted pellets earned (*G*), pellets consumed (*H*), and pellets hoarded (*I*) for day 1 and combined days 2-3 and 4-6. n= 19-20 per group. (*A*-*C*), baseline values were calculated as the 3 day pellet average prior to experimental start time. (*G*-*I*), baseline (i.e. 100%) was calculated for each animal using the formula [(3 day animal baseline average/ average of all animals in the group)*100] when comparing day 1, [((3 day animal baseline average*2)/ average of all animals in the group)*100] when comparing days 2-3, or [((3 day animal baseline average*3)/ average of all animals in the group)*100] when comparing days 4-6. Data reported as mean ± S.E.M. [a]*P*<0.05 vs. AgRP-DsiRNA treated animals; **P*<0.05 vs. baseline.

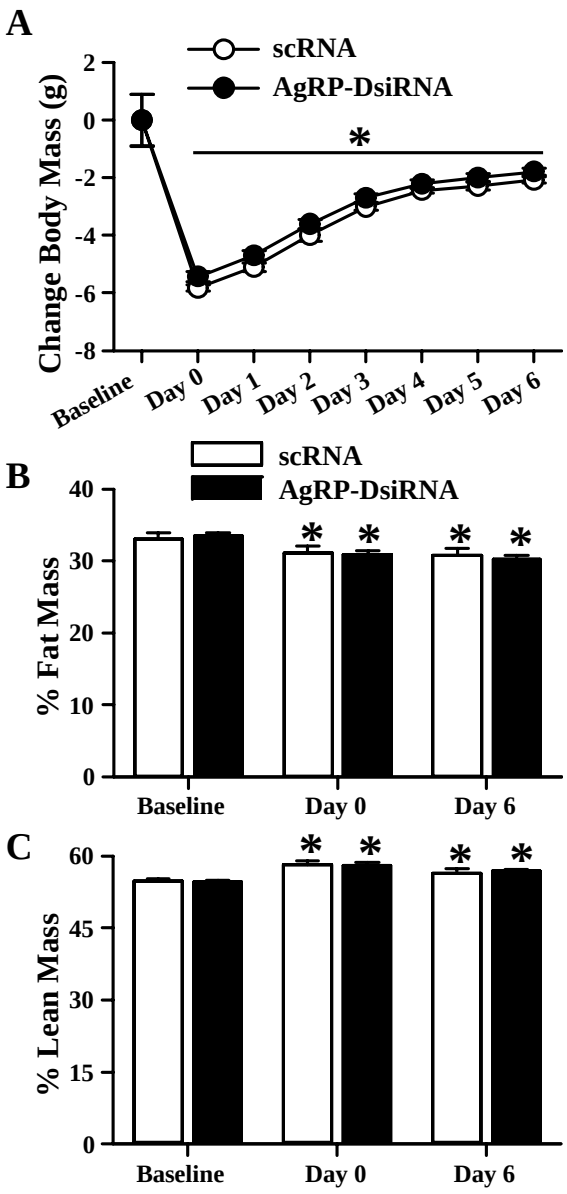


**Fig. 3.5** AgRP knockdown has no effect on body mass, fat mass, or lean mass following food deprivation.
Baseline, food returned (Day 0), and daily body mass change measurements in food-deprived scRNA (0.4µg/g BM i.p.) and AgRP-DsiRNA (0.4µg/g BM i.p.) treated animals (*A*). Baseline, food returned (Day 0), and final fat mass (Day 6) (*B*) and percent lean mass (*C*) body composition measurements for scRNA and AgRP-DsiRNA treated animals. n= 19-20 per group for all measurements. Data reported as mean ± S.E.M. **P*<0.05 vs. baseline.

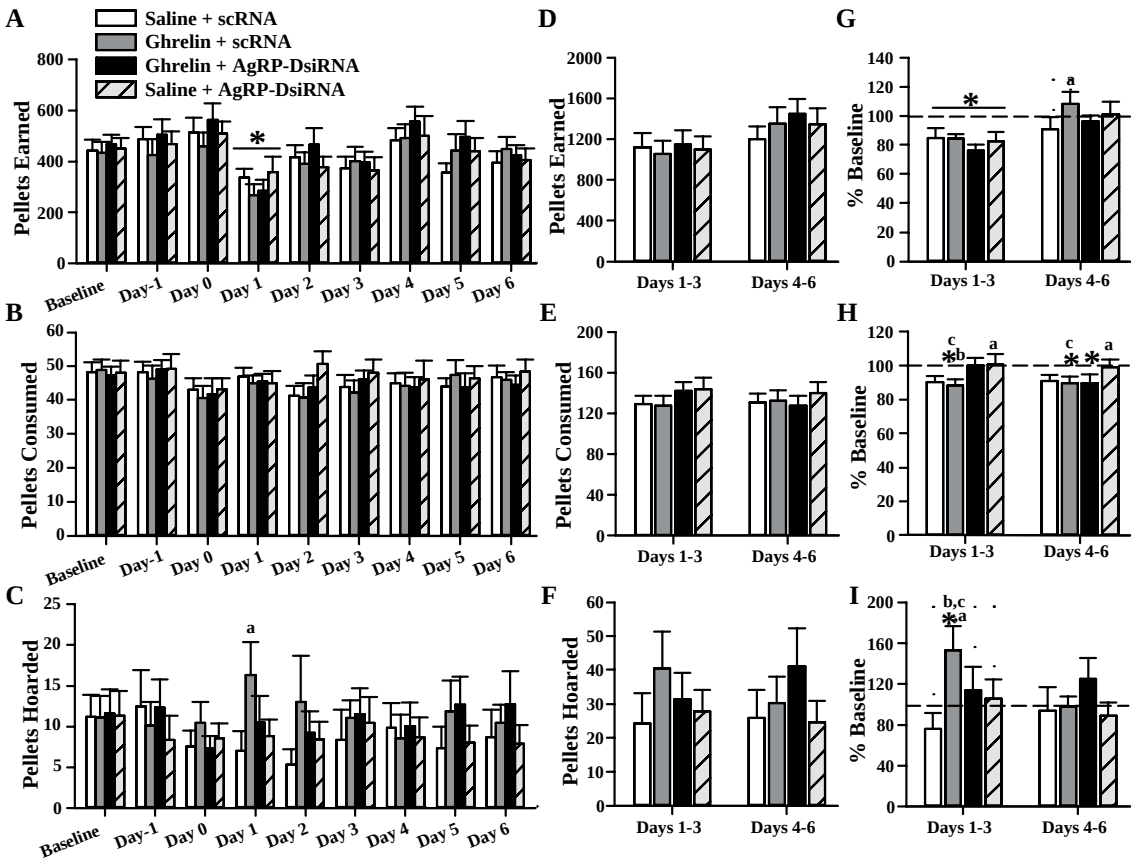


**Fig. 3.6** AgRP knockdown blocks ghrelin-induced food hoarding.
Number of pellets earned (*A*), consumed (*B*), and hoarded (*C*) prior to injections (baseline) and in response to saline + scRNA (0.4µg/g BM i.p.), ghrelin (30µg/kg i.p.) + scRNA (0.4µg/g BM i.p.), ghrelin (30µg/kg i.p.) + AgRP-DsiRNA (0.4µg/g BM i.p.), or saline + AgRP-DsiRNA (0.4µg/g BM i.p.). Combined number of pellets earned (*D*), consumed (*E*), and hoarded (*F*) on days 1-3 and 4-6. Percent baseline converted pellets earned (*G*), consumed (*H*), and hoarded (*I*) on combined days 1-3 and 4-6. n=15 per group. (*A-C*), baseline values were calculated as the 3 day pellet average prior to experimental start time. (*G-I*), baseline (i.e. 100%) was calculated for each animal using the formula [((3 day animal baseline average*3)/ average of all animals in the group)*100]. Data reported as mean ± S.E.M. [a]*P*<0.05 vs. saline + scRNA treatment; [b]*P*<0.05 vs. ghrelin + AgRP-DsiRNA treatment; [c]*P*<0.05 vs. saline + AgRP-DsiRNA treatment; **P*<0.05 vs. baseline.

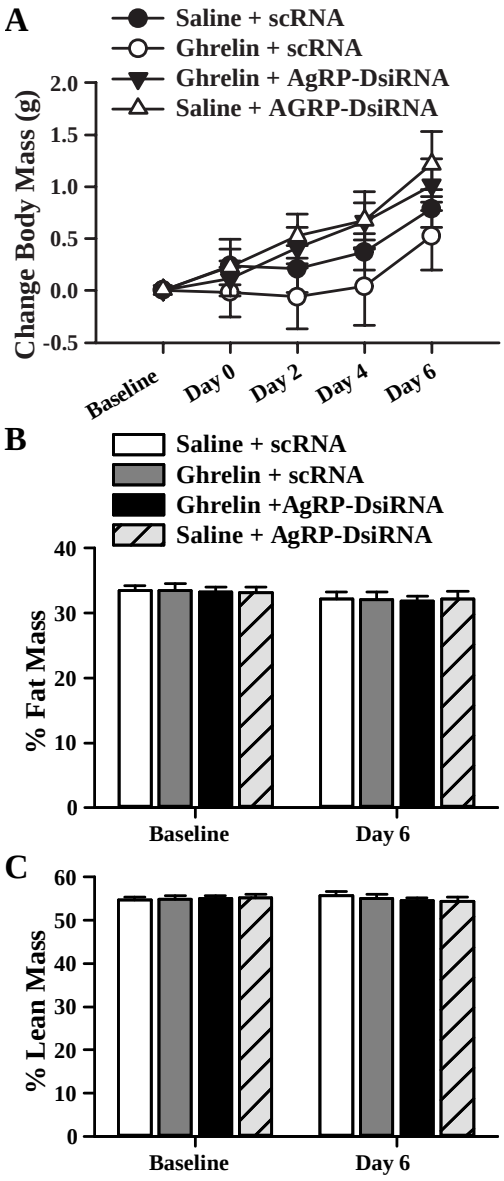


**Fig. 3.7** AgRP knockdown has no effect on ghrelin-induced changes in body mass, fat mass, or lean mass.
Body mass change measurements in scRNA (0.4µg/g BM i.p.) or AgRP-DsiRNA (0.4µg/g BM i.p.) treated animals at baseline and following exogenous ghrelin (30µg/kg i.p.) or saline treatment (at Day 0) (*A*). Baseline and final percent fat mass (*B*) and percent lean mass (*C*) body composition measurements for all animals and groups. n= 15 per group for all measurements. Data reported as mean ± S.E.M.

## 3.5 Discussion

Given the multitude of pharmacological studies by us and others implicating discrete functional and temporal roles of AgRP and NPY in regulating ingestive behaviors [30, 31, 33], we tested here for the first time if AgRP knockdown affects food hoarding following energetic challenges. We initially confirmed that peripherally administered substances, and thus antisense oligos, are sufficient to reach the Arc and, in turn, circumvents the need for central cannulations and drug delivery. By employing a novel AgRP-DsiRNA, we were able to attenuate food deprivation-induced increases in AgRP mRNA expression and decrease basal AgRP expression in ad libitum fed hamsters without affecting NPY mRNA expression. We chose to test the efficacy of AgRP-DsiRNA using a 48 h food deprivation challenge as this represents a natural energetic challenge that markedly upregulates AgRP and NPY expression [40, 47, 48]. Importantly, we confirmed the efficacy of AgRP-DsiRNA-mediated gene knockdown with two complementary techniques (in situ hybridization and qPCR), repeated across multiple experimental cohorts, and found a comparable ~40-50% knockdown with both approaches. Although antisense oligo stability in vivo may be increased with the use of transfection agents [49], the sufficiency of saline diluted oligos demonstrated here and by others [38] circumvents possible toxicity affecting behavior (for review see [34]). In addition, modified oligo duplexes (i.e. DsiRNAs) have an elimination half-life of approximately ~0.8 h compared with ~1.5 h for conjugated duplexes [50]; however, we overcame this temporal limitation by giving a relatively high dose of AgRP-DsiRNA (0.4µg/g BM) daily to efficiently block AgRP expression. Our experimental approach employed here has several advantages and broad implications for future work. Of note, DsiRNA facilitates targeted gene knockdown without surgery, virally mediated gene delivery, or genome modification, and is in turn clinically relevant for humans. Indeed,

there are currently at least 20 antisense drugs in development and one currently approved (Vitravene) for humans [34, 51]. Moreover, this approach can be rapidly adapted to any animal species and mRNA sequence with minimal side effects, and therefore avoids the inherent limitations of generating knockout or knockin animal models.

Our findings here that AgRP knockdown attenuates food deprivation- and ghrelin-induced increases in food hoarding is complementary to our recent pharmacological data demonstrating central AgRP drives food hoarding largely independent of food foraging or food intake [33]. AgRP-DsiRNA attenuated short-term (days 1-3) food hoarding following food deprivation and exogenous ghrelin, and prolonged (combined days 4-6) food deprivation-induced hoarding. This is of particular importance and clinical relevance as studies suggest food deprivation increases food hoarding but not food intake in humans [8-11]. Although AgRP knockdown attenuated food deprivation-induced increases in food hoarding on days 4-6 relative to baseline, we found no difference between AgRP-DsiRNA and scRNA treatment on days 2-3 post-refeeding. To this end, the profound energy deficit following a food deprivation challenge markedly upregulates AgRP and NPY expression, and although AgRP-DsiRNA significantly decreases AgRP mRNA, we speculate that remaining AgRP mRNA due to an incomplete knockdown is sufficient to drive the acute increase in food hoarding relative to baseline. Our findings that AgRP-DsiRNA treatment had no effect on basal hoarding levels compared with controls (i.e. saline + scRNA) prior to exogenous ghrelin or on any subsequent day for the duration of the experiment would support this and suggests food hoarding increases are dependent on AgRP upregulation. We cannot, however, rule out the possibility that NPY signaling is sufficient to regulate food hoarding on days 2-3 post-refeeding or basal food hoarding in the absence of AgRP. In addition, we did not examine other Arc neuron populations

that AgRP antagonizes, including neurons expressing the anorectic peptide pro-opiomelanocortin (POMC) [27, 52]. It is therefore possible an increase in POMC due to inhibition release, or compensatory decrease due to an absence of AgRP antagonism, is involved in our observed phenotype. However, as POMC neurons are also inhibited by NPY [53], which was left unchanged during AgRP knockdown, we speculate that POMC neurons are not involved in AgRP-DsiRNA-mediated hoarding blockade.

Under the baseline condition where food was abundantly available, we observed the significantly large "surplus" pellets left on top of the foraging apparatus. This was possibly due to their constant effort to forage enough pellets in order to prevent any possible food deficiency; whereas under energetic challenges (eg, food deprivation), they forage less, hoard more, and waste less to conserve energy, and to achieve the same purpose, to avoid future food deficiency. Under the latter condition, the marked food deprivation-induced increase in food hoarding was coupled with significantly decreased food intake and food foraging compared with baseline in both scRNA and AgRP-DsiRNA treated animals. Although food intake returned to baseline by day 3 or combined days 4-6 post-refeeding, food foraging remained depressed for the duration of the experiment in both groups. Of note, this decrease in food foraging and food intake was coupled with a marked decrease in body mass and % fat mass, and would lend support to our previous findings that lipectomized hamsters markedly increase food hoarding and decrease foraging across 12 weeks [54]. We speculate this decrease in food foraging is an evolutionary adaption to conserve energy in response to the profound energetic challenge of food deprivation and resulting depletion of energy stores. Food deprivation markedly increases AgRP expression, which conveys a negative valence signal [55], causing the avoidance of situations associated with painful experiences (hunger). Animals compensate for decreased energy supply, in part, by

decreasing energy expenditure (i.e. wheel running) [56], and once food becomes available, food hoarding is markedly increased as a mechanism to avoid future energetic challenges and negative valence signals. As the number of pellets earned is decreased, and pellets hoarded increased, there is a resulting decrease in pellets consumed and surplus pellets. Hence, animals decrease wheel running/foraging effort (thereby conserving energy), hoard more, and waste less in an effort to regain body mass and avoid future energetic challenges. Our data would support this idea as there is a marked decrease in surplus pellets following refeeding (~50 pellets) compared with baseline (~320 pellets). Moreover, the number of pellets hoarded is several orders of magnitude greater than baseline at day 1, and this corresponds with the greatest decrease in food intake and pellet surplus. On days 2-3 and 4-6, food intake begins to return to baseline and there is a concurrent decrease in food hoarding. As we found a significant difference in foraging effort between AgRP-DsiRNA and scRNA treated animals, we speculate that AgRP knockdown attenuates the negative valence signals conveyed by AgRP neurons and this translates, at least initially, to a relative increase in food foraging and decrease in food hoarding. The marked decrease in body mass and food foraging through day 6 post-refeeding strongly suggests the profound energy deficit following fasting is compensated for through increased food hoarding and decreased food foraging.

Although we found here a marked increase in food hoarding following exogenous ghrelin at combined days 1-3, this was coupled with a notable absence, and in fact significant decrease, in food foraging and food intake in contrast to our previous findings [22, 23]. We posit that these seemingly contrasting results are primarily due to differences in experimental design. We have previously used a within subject design when measuring the effects of ghrelin on ingestive behaviors at hourly time points, and converted data to % control (i.e. relative to vehicle) rather

than a between subject design in this study in which data are expressed as raw values or % baseline. In turn, stress associated with the novelty of the injection procedure is abrogated with a within subject, but readily apparent in a between subject design or when compared with % baseline (in which animals are not manipulated). Moreover, and perhaps most significantly, ghrelin-induced increases in food foraging and food intake are comparatively small relative to hoarding and are gone by ~4 h post- injection [22, 23]. In turn, the experimental design here in which we examine daily changes in ingestive behaviors following energetic challenges does not allow for the temporal resolution necessary to identify changes in food foraging or food intake following exogenous ghrelin treatment. We therefore speculate significant increases in hoarding are apparent with daily measurements, but increases in food foraging and food intake necessitate greater temporal resolution (e.g. hourly measurements). As such, we are as of now unable to definitely state that AgRP knockdown has no effect on acute food foraging or food intake following energetic challenges.

### 3.6 Conclusions

In summary, our results collectively indicate a critical role of AgRP signaling in regulating food hoarding following energetic challenges. To this end, AgRP neurons project, in discrete populations, to a distributed network of forebrain and hindbrain nuclei [57]; however, future work investigating AgRP efferent nuclei is necessary to fully elucidate the exact mechanism of AgRP-mediated food hoarding. Coupled with our previous findings that central AgRP selectively drives food hoarding, our finding here showing that AgRP knockdown attenuates ghrelin- and food deprivation-induced increases in food hoarding strongly suggests downstream AgRP signaling underlies this important behavior. Moreover, as NPY drives acute increases in ingestive behaviors [31], we hypothesize that energetic challenges increase

appetitive and consummatory feeding behaviors through temporally distinct mechanisms. AgRP neurons function, at least in part, to negate energy deficits (i.e. following food deprivation) through short-term, NPY-mediated food intake and prevent future challenges through AgRP-mediated food hoarding.

### 3.7 Acknowledgements

This research was supported by NIH R01DK035254 to T.J.B. and B.X., NIH R01DK107544 to B.X., and a Georgia State University pre-doctoral dissertation grant to M.A.T.

### 3.8 Disclosures

The authors have nothing to disclose, financial or otherwise.

### 3.9 References

[1] Calle, E. E., Rodriguez, C., Walker-Thurmond, K., Thun, M. J. Overweight, obesity, and mortality from cancer in a prospectively studied cohort of U.S. adults. N.Engl.J Med. 2003,348:1625-38.

[2] Goldstein, L. B., Bushnell, C. D., Adams, R. J., Appel, L. J., Braun, L. T., Chaturvedi, S., et al. Guidelines for the primary prevention of stroke: a guideline for healthcare professionals from the American Heart Association/American Stroke Association. Stroke. 2011,42:517-84.

[3] Harvey, A. E., Lashinger, L. M., Hursting, S. D. The growing challenge of obesity and cancer: an inflammatory issue. Ann.N.Y.Acad.Sci. 2011,1229:45-52.

[4] Vague, J., Vague, P., Tramoni, M., Vialettes, B., Mercier, P. Obesity and diabetes. Acta Diabetol.Lat. 1980,17:87-99.

[5] Zalesin, K. C., Franklin, B. A., Miller, W. M., Peterson, E. D., McCullough, P. A. Impact of obesity on cardiovascular disease. Med.Clin.North Am. 2011,95:919-37.

[6] Bartness, T. J., Keen-Rhinehart, E., Dailey, M. J., Teubner, B. J. Neural and hormonal control of food hoarding. Am.J Physiol. 2011,301:R641-R55.

[7] Craig, W. Appetites and aversions as constituents of instincts. Biol.Bull. 1918,34:91-107.

[8] Beneke, W. M., Davis, C. H. Relationship of hunger, use of a shopping list and obesity to food purchases. Int.J.Obes. 1985,9:391-9.

[9] Dodd, D. K., Stalling, R. B., Bedell, J. Grocery purchases as a function of obesity and assumed food deprivation. Int.J Obes. 1977,1:43-7.

[10] Mela, D. J., Aaron, J. I., Gatenby, S. J. Relationships of consumer characteristics and food deprivation to food purchasing behavior. Physiol Behav. 1996,60:1331-5.

[11] Ransley, J. K., Donnelly, J. K., Botham, H., Khara, T. N., Greenwood, D. C., Cade, J. E. Use of supermarket receipts to estimate energy and fat content of food purchased by lean and overweight families. Appetite. 2003,41:141-8.

[12] Bartness, T. J., Clein, M. R. Effects of food deprivation and restriction, and metabolic blockers on food hoarding in Siberian hamsters. Am.J.Physiol. 1994,266:R1111-R7.

[13] Wood, A. D., Bartness, T. J. Food deprivation-induced increases in hoarding by Siberian hamsters are not photoperiod-dependent. Physiol Behav. 1996,60:1137-45.

[14] Bartness, T. J. Food hoarding is increased by pregnancy, lactation and food deprivation in Siberian hamsters. Am.J.Physiol. 1997,272:R118-R25.

[15] Day, D. E., Bartness, T. J. Effects of foraging effort on body fat and food hoarding by Siberian hamsters. J.Exp.Zool. 2001,289:162-71.

[16] Date, Y., Kojima, M., Hosoda, H., Sawaguchi, A., Mondal, M. S., Suganuma, T., et al. Ghrelin, a novel growth hormone-releasing acylated peptide, is synthesized in a distinct endocrine cell type in the gastrointestinal tracts of rats and humans. Endocrinology. 2000,141:4255-61.

[17] Ariyasu, H., Takaya, K., Tagami, T., Ogawa, Y., Hosoda, K., Akamizu, T., et al. Stomach is a major source of circulating ghrelin, and feeding state determines plasma ghrelin-like immunoreactivity levels in humans. J.Clin.Endocrinol.Metab. 2001,86:4753-8.

[18] Cummings, D. E., Purnell, J. Q., Frayo, R. S., Schmidova, K., Wisse, B. E., Weigle, D. S. A preprandial rise in plasma ghrelin levels suggests a role in meal initiation in humans. Diabetes. 2001,50:1714-9.

[19] Tschop, M., Smiley, D. L., Heiman, M. L. Ghrelin induces adiposity in rodents. Nature. 2000,407:908-13.

[20] Wren, A. M., Small, C. J., Ward, H. L., Murphy, K. G., Dakin, C. L., Taheri, S., et al. The novel hypothalamic peptide ghrelin stimulates food intake and growth hormone secretion. Endocrinology. 2000,141:4325-8.

[21] Wren, A. M., Seal, L. J., Cohen, M. A., Brynes, A. E., Frost, G. S., Murphy, K. G., et al. Ghrelin enhances appetite and increases food intake in humans. J.Clin.Endocrinol.Metab. 2001,86:5992.

[22] Keen-Rhinehart, E., Bartness, T. J. Peripheral ghrelin injections stimulate food intake, foraging and food hoarding in Siberian hamsters. Am.J.Physiol. 2005,288:R716-R22.

[23] Thomas, M. A., Ryu, V., Bartness, T. J. Central ghrelin increases food foraging/hoarding that is blocked by GHSR antagonism and attenuates hypothalamic paraventricular nucleus neuronal activation. Am J Physiol Regul Integr Comp Physiol. 2015:ajpregu 00216 2015.

[24] Faulconbridge, L. F., Cummings, D. E., Kaplan, J. M., Grill, H. J. Hyperphagic effects of brainstem ghrelin administration. Diabetes. 2003,52:2260-5.

[25] Zigman, J. M., Jones, J. E., Lee, C. E., Saper, C. B., Elmquist, J. K. Expression of ghrelin receptor mRNA in the rat and the mouse brain. J.Comp Neurol. 2006,494:528-48.

[26] Wang, Q., Liu, C., Uchida, A., Chuang, J. C., Walker, A., Liu, T., et al. Arcuate AgRP neurons mediate orexigenic and glucoregulatory actions of ghrelin. Mol.Metab. 2014,3:64-72.

[27] Cone, R. D., Cowley, M. A., Butler, A. A., Fan, W., Marks, D. L., Low, M. J. The arcuate nucleus as a conduit for diverse signals relevant to energy homeostasis. Int.J Obes.Relat Metab Disord. 2001,25 Suppl 5:S63-S7.

[28] Chen, H. Y., Trumbauer, M. E., Chen, A. S., Weingarth, D. T., Adams, J. R., Frazier, E. G., et al. Orexigenic action of peripheral ghrelin is mediated by neuropeptide Y and agouti-related protein. Endocrinology. 2004,145:2607-12.

[29] Gropp, E., Shanabrough, M., Borok, E., Xu, A. W., Janoschek, R., Buch, T., et al. Agouti-related peptide-expressing neurons are mandatory for feeding. Nat.Neurosci. 2005,8:1289-91.

[30] Krashes, M. J., Shah, B. P., Koda, S., Lowell, B. B. Rapid versus delayed stimulation of feeding by the endogenously released AgRP neuron mediators GABA, NPY, and AgRP. Cell Metab. 2013,18:588-95.

[31] Day, D. E., Keen-Rhinehart, E., Bartness, T. J. Role of NPY and its receptor subtypes in foraging, food hoarding, and food intake by Siberian hamsters. Am.J Physiol Regul.Integr.Comp Physiol. 2005,289:R29-R36.

[32] Keen-Rhinehart, E., Bartness, T. J. NPY Y1 receptor is involved in ghrelin- and fasting-induced increases in foraging, food hoarding, and food intake. Am.J Physiol Regul.Integr.Comp Physiol. 2007,292:R1728-R37.

[33] Day, D. E., Bartness, T. J. Agouti-related protein increases food hoarding, but not food intake by Siberian hamsters. Am.J.Physiol. 2004,286:R38-R45.

[34] Behlke, M. A. Progress towards in vivo use of siRNAs. Mol Ther. 2006,13:644-70.

[35] Bowers, R. R., Festuccia, W. T. L., Song, C. K., Shi, H., Migliorini, R. H., Bartness, T. J. Sympathetic innervation of white adipose tissue and its regulation of fat cell number. Am.J.Physiol. 2004,286:R1167-R75.

[36] Hamar, P., Song, E., Kokeny, G., Chen, A., Ouyang, N., Lieberman, J. Small interfering RNA targeting Fas protects mice against renal ischemia-reperfusion injury. Proc Natl Acad Sci U S A. 2004,101:14883-8.

[37] Suda, T., Liu, D. Hydrodynamic gene delivery: its principles and applications. Mol Ther. 2007,15:2063-9.

[38] Ocker, M., Neureiter, D., Lueders, M., Zopf, S., Ganslmayer, M., Hahn, E. G., et al. Variants of bcl-2 specific siRNA for silencing antiapoptotic bcl-2 in pancreatic cancer. Gut. 2005,54:1298-308.

[39] Mercer, J. G., Moar, K. M., Ross, A. W., Morgan, P. J. Regulation of leptin receptor, POMC and AGRP gene expression by photoperiod and food deprivation in the hypothalamic arcuate nucleus of the male Siberian hamster (Phodopus sungorus). Appetite. 2000,34:109-11.

[40] Garretson, J. T., Teubner, B. J., Grove, K. L., Vazdarjanova, A., Ryu, V., Bartness, T. J. Peroxisome proliferator-activated receptor gamma controls ingestive behavior, agouti-related protein, and neuropeptide Y mRNA in the arcuate hypothalamus. J Neurosci. 2015,35:4571-81.

[41] Vazdarjanova, A., McNaughton, B. L., Barnes, C. A., Worley, P. F., Guzowski, J. F. Experience-dependent coincident expression of the effector immediate-early genes arc and Homer 1a in hippocampal and neocortical neuronal networks. J.Neurosci. 2002,22:10067-71.

[42] Garretson, J. T., Teubner, B. J., Ryu, V., Bartness, T. J. Role of Peroxisome Proliferator-activated Receptor ã in Appetite Control. The Obesity Society. 2013.

[43] Paxinos, G., Franklin, K. B. J. The Mouse Brain in Stereotaxic Coordinates. 2nd ed. New York: Academic Press; 2007.

[44] van der Laan, S., Lachize, S. B., Schouten, T. G., Vreugdenhil, E., de Kloet, E. R., Meijer, O. C. Neuroanatomical distribution and colocalisation of nuclear receptor corepressor (N-CoR) and silencing mediator of retinoid and thyroid receptors (SMRT) in rat brain. Brain Res. 2005,1059:113-21.

[45] Mercer, J. G., Moar, K. M., Ross, A. W., Hoggard, N., Morgan, P. J. Photoperiod regulates arcuate nucleus POMC, AGRP, and leptin receptor mRNA in Siberian hamster hypothalamus. Am.J.Physiol. 2000,278:R271-R81.

[46] Perrigo, G., Bronson, F. H. Foraging effort, food intake, fat deposition, and puberty in female mice. Biology of Reproduction. 1983,29:455-63.

[47] Harrold, J. A., Williams, G., Widdowson, P. S. Changes in hypothalamic agouti-related protein (AGRP), but not alpha- MSH or pro-opiomelanocortin concentrations in dietary-obese and food- restricted rats. Biochemical and Biophysical Research Communications. 1999,258:574-7.

[48] Bi, S., Robinson, B. M., Moran, T. H. Acute food deprivation and chronic food restriction differentially affect hypothalamic NPY mRNA expression. Am.J.Physiol Regul.Integr.Comp Physiol. 2003,285:R1030-R6.

[49] Soutschek, J., Akinc, A., Bramlage, B., Charisse, K., Constien, R., Donoghue, M., et al. Therapeutic silencing of an endogenous gene by systemic administration of modified siRNAs. Nature. 2004,432:173-8.

[50] Morrissey, D. V., Lockridge, J. A., Shaw, L., Blanchard, K., Jensen, K., Breen, W., et al. Potent and persistent in vivo anti-HBV activity of chemically modified siRNAs. Nat Biotechnol. 2005,23:1002-7.

[51] Crooke, S. T. Progress in antisense technology. Annual review of medicine. 2004,55:61-95.

[52] Dhillo, W. S., Small, C. J., Stanley, S. A., Jethwa, P. H., Seal, L. J., Murphy, K. G., et al. Hypothalamic interactions between neuropeptide y, agouti-related protein, cocaine- and amphetamine-regulated transcript and alpha-melanocyte-stimulating hormone in vitro in male rats. J.Neuroendocrinol. 2002,14:725-30.

[53] Garcia de, Y. E., Li, S., Fournier, A., St-Pierre, S., Pelletier, G. Regulation of proopiomelanocortin gene expression by neuropeptide Y in the rat arcuate nucleus. Brain Res. 1995,674:112-6.

[54] Dailey, M. E., Bartness, T. J. Fat pad-specific effects of lipectomy on foraging, food hoarding, and food intake. Am.J.Physiol Regul.Integr.Comp Physiol. 2008,294:R321-R8.

[55] Betley, J. N., Xu, S., Cao, Z. F., Gong, R., Magnus, C. J., Yu, Y., et al. Neurons for hunger and thirst transmit a negative-valence teaching signal. Nature. 2015,521:180-5.

[56] Luz, J., Griggio, M. A., Natrieli, R. M., Aumond, M. D. Energy balance of rats subjected to continuous and intermittent food restriction. Braz.J Med.Biol.Res. 1995,28:1019-23.

[57] Betley, J. N., Cao, Z. F., Ritola, K. D., Sternson, S. M. Parallel, redundant circuit organization for homeostatic control of feeding behavior. Cell. 2013,155:1337-50.

# 4 GHRELIN ACTIVATES PERIPHERAL SENSORY NEURONS TO REGULATE METABOLIC HOMEOSTASIS INDEPENDENT OF FOOD INTAKE

## 4.1 Abstract

Obesity is a major health and economic burden with approximately 35% of United States citizens classified as either overweight or obese, and medical spending for treating obesity and its comorbidities exceeds $200 billion annually. The stomach-derived orexigenic hormone ghrelin is a key mediator of energy homeostasis and adiposity in humans due to its regulation of food intake, gut motility, energy expenditure, nutrient partitioning, glycemia, and body temperature. The ghrelin receptor, growth hormone secretagogue receptor 1a (GHSR), is widely expressed in the brain and on gastrointestinal vagal sensory neurons, and neuronal GHSR knockout results in a profoundly beneficial metabolic profile and diet-induced obesity (DIO) resistance. Moreover, *ghsr* knockout mice have impaired metabolic regulation during energetic challenges, and *ghsr* restoration in the brain does not fully restore ghrelin's effects suggesting peripheral ghrelin signaling is critical for metabolic control. In the current study, we demonstrate that in addition to the well characterized vagal GHSRs, gastrointestinal sensory neurons emanating from spinal dorsal root ganglia (DRG) robustly express GHSRs that are activated by energetic challenges indicating a novel mechanism mediating ghrelin's effects on energy homeostasis. Sensory neuron GHSR deletion attenuates DIO through increased energy expenditure and sympathetic outflow to BAT and WAT, and this upregulated sympathetic outflow results in a marked increase in cold tolerance and adipose tissue browning capacity. Hence, these findings demonstrate a novel ghrelin signaling pathway critical for maintaining energy homeostasis and provides another point of attack for behavioral and/or pharmacological interventions to combat obesity.

## 4.2 Introduction

The number of overweight and obese persons worldwide has continually risen across the last four decades with the current number of affected persons estimated 1.9 billion [1]. Prolonged energy intake that exceeds energy expenditure can result in obesity and markedly increase the risk for secondary health consequences including type 2 diabetes, cardiovascular disease, and cancer [2-4]. As such, there has been considerable effort placed on uncovering the mechanisms regulating energy homeostasis. Neuroendocrine systems that mediate this homeostasis are broadly distributed in the brain and periphery and form a complex, interconnected framework governing energy intake and expenditure, adipose tissue metabolism, and ingestive behaviors [5-7]. Both central and peripheral endocrine signaling is sufficient to regulate metabolism (for review see [5]), yet the mechanisms through which these pathways function independently or in parallel is largely unstudied. To this end, gastric sensory neurons that detect nutrients or distension express endocrine receptors [8], and these afferents are sufficient to regulate adipose tissue metabolism [9]. Moreover, these sensory neurons can form short or long feedback loops within the spinal cord and hindbrain respectively [9-11], and this central-peripheral crosstalk is critical for maintaining metabolic homeostasis. As the number of obese persons worldwide continues to increase, a comprehensive study investigating the peripheral mechanisms controlling ingestive behaviors and energy homeostasis may provide more accessible pharmacological interventions as these receptors are independent of the brain and blood brain barrier.

Ghrelin is a 28-amino acid peptide hormone secreted from the stomach [12]. Circulating ghrelin levels rise pre-prandially (i.e. during fasting) and decrease post-prandially, and the rise and fall of ghrelin concentrations is suggested as contributor to normal energy homeostasis and

overall metabolic health [13, 14]. In both humans and rodents, activation of the ghrelin receptor, growth hormone secretagogue receptor 1a (GHSR) [15], markedly increases adiposity through increased food intake [16, 17], decreased energy expenditure, and reduced fatty acid utilization [18, 19]. Moreover, exogenous ghrelin decreases core body temperature [20], attenuates brown adipose tissue (BAT) thermogenesis [20], and reduces insulin secretion resulting in hyperglycemia [21, 22]. GHSRs are widely expressed in the brain and on peripheral neurons including gastric vagal afferents [23, 24], and GHSR deletion or blockade prevents diet-induced obesity (DIO), ghrelin-induced ingestive behaviors [17, 25, 26], and significantly increases energy expenditure [27], thermogenic capacity [27], and insulin sensitivity [28]. However, *ghsr* restoration in the brain does not fully restore ghrelin's effects suggesting peripheral ghrelin signaling is critical for metabolic control [29]. Integration of peripheral sensory information in the brain is mandatory for maintaining energy homeostasis [30-32], and dysregulated sensory neuron function and ghrelin signaling is well documented in the obese [33-35]. In lean humans and rodents, activation of gastric stretch or nutrient receptors promotes satiety [36-38], and their activity is directly enhanced by anorectic gut hormones and inhibited by ghrelin [5, 39]. In addition, activation of intestinal nutrient receptors increases BAT thermogenesis [9], a key mediator of whole body energy expenditure and adiposity [40], indicating an important link between gastrointestinal stimuli, sensory neuron activation, ghrelin signaling, and metabolic control. Initial studies suggested ghrelin-mediated energy expenditure regulation, thermogenesis, gut motility, and glycemic control is dependent on intact gastric vagal afferents [41-43]. However, non-vagal sensory neurons innervate the gut at all levels [44], and vagotomized animals have normal adaptation to cold challenges and gastric responses to an exogenous ghrelin challenge suggesting non-vagal GHSR-containing sensory neurons are sufficient to mediate

these responses [45-48]. Total sensory neuron ablation following capsaicin treatment impairs adipose tissue metabolism, cold-induced thermogenic responses, and, at the very least, ghrelin's gastric effects indicating DRG sensory neurons are mandatory for metabolic control [49-51].

To interrogate the role of peripheral ghrelin signaling in regulating metabolic homeostasis, we used a GHSR-IRES-tauGFP mouse [52] and found robust GHSR expression on DRG sensory neurons that are activated by energetic challenges including food deprivation and cold exposure. We next characterized the necessity of this peripheral ghrelin signaling pathway in regulating metabolic homeostasis by generating a novel, sensory neuron specific GHSR knockout mouse, and found these mice had a marked increase in energy expenditure and adipose thermogenic gene expression that resulted in diet-induced obesity resistance and improved cold tolerance despite no changes in food intake. This peripheral ghrelin signaling pathway functions in parallel to previously defined central feeding circuits and indicates a novel mechanism through which sensory neuron ghrelin signaling regulates adipose tissue metabolism and whole-body energy homeostasis. Hence, this discrete sensory neuron pathway may provide a novel therapeutic avenue to prevent or reverse obesity.

## 4.3 Materials and Methods

### *4.3.1 Animals*

Adult *Ghsr*-IRES-tauGFP mice were obtained from the Jackson Laboratory (Stock No: 019908). To generate a sensory neuron specific Ghsr knockout model, we crossed our existing *Advillin-Cre* mouse line [53, 54] with $Ghsr^{f/f}$ mice [27] (mouse lines were kindly provided by Drs. Fan Wang from Duke University and Yuxiang Sun at Texas A&M University respectively) to generate $Advillin\text{-}Cre^{+/-}$;$Ghsr^{f/f}$ mice (henceforth referred to as AGKO). Male AGKO or f/f littermate mice were fed either a standard chow diet (catalog no.: 5001; LabDiet; Purina, St.

Louis, MO) or high fat diet (HFD) consisting of 60% calories from fat (catalog no. 12492; Research Diets, New Brunswick, NJ). Body mass measurements were taken weekly for the duration of the experiment. Animals were maintained at ~23°C with 12-hour light/dark cycles (0700-1900 light). All procedures were approved by the Georgia State University Institutional Animal Care and Use Committee and were in compliance with the Public Health Service and United States Department of Agriculture guidelines.

### *4.3.2 **Physiology Measurements***

Glucose and insulin tolerance tests were performed on male AGKO or f/f littermate mice after 12 weeks on either Chow or high-fat diet (HFD) as we observed the greatest difference in body mass during this time. For glucose tolerance tests, animals were fasted for 16 hours overnight. Baseline glucose measurements were obtained from a tail nick using a OneTouch Ultra Blood Glucose Meter and glucose test strips (LifeScan, Inc., Milpitas, CA). Following the initial measurement, mice were intraperitoneally injected with a 20% dextrose solution (1g/kg body mass), and subsequent blood glucose measurements were performed at 15, 30, 60, 90, and 120 minutes after the glucose injection. For the insulin tolerance test (ITT), mice were fasted for 4 hours prior to the start of the procedure, and baseline blood glucose was measured from a small tail nick. Mice were then intraperitoneally injected with 1.0 U/kg insulin (Humulin R; Eli Lilly, Indianapolis, IN), and blood glucose was measured at the same time points used for the GTT. Energy expenditure, oxygen consumption, carbon dioxide production, respiratory exchange ratio, and physical activity data were collected for male AGKO or f/f littermate mice using a TSE PhenoMaster metabolic chamber system (TSE Systems, Chesterfield, MO) after 12 weeks on Chow or HFD. Animals were allowed a 48-hour acclimation period prior to the start of data collection and then returned to their home cage at the end of the experiment.

### 4.3.3 *Body Composition Measurements*

Body composition measurements were taken for HFD-fed male AGKO or f/f littermate mice using our Minispec LF90 TD-NMR analyzer (Bruker Optics). For all measurements, animals were briefly removed from their home cage, placed in the body composition analyzer, and then immediately returned to their home cage. Body composition measurements were taken for all animals prior to the start of HFD feeding, after 8 weeks of HFD feeding, and then again at the conclusion of the experiment.

### *4.3.4 Tissue Collection*

At the end of each experiment, mice were euthanized using carbon dioxide inhalation. Blood serum was collected and stored at −80°C until analysis. Animals were then perfused with ice cold 0.1M PBS and fat pads (brown (iBAT), epididymal (eWAT), and inguinal (iWAT)), liver, brain, and DRGs (L5-T5 levels) dissected and flash frozen in liquid nitrogen. For brain microdissection, the brain was placed on an ice cold cutting block and 1 mm sagittal sections taken from both sides of the midline. The arcuate hypothalamus, paraventricular hypothalamus, ventromedial hypothalamus, and ventral tegmental area were then microdissected according to a mouse brain atlas (Paxinos and Franklin [55]) and flash frozen in liquid nitrogen. A sample of each fat pad and liver was taken prior to freezing and placed in formalin for later histological analysis. In a separate set of *Ghsr-GFP* mice used for immunohistochemical analysis, animals were euthanized by carbon dioxide inhalation and then transcardially perfused with 75 ml 0.9% heparinized saline followed by 150 ml 4.0% paraformaldehyde in 0.1 M PBS in sterile filtered dH2O. DRGs (L5-T5 levels) were subsequently removed and dehydrated in an 18% sucrose solution until immunohistochemical analysis.

### *4.3.5 Fast Blue Injections*

1% Fast Blue in sterile $dH_2O$ (17740-1, Polysciences, Warrington, PA) was used as a fluorescent retrograde neuronal tracer to identify gastrointestinal-projecting sensory neurons. In brief, animals were deeply anesthetized with 1-2% isoflurane, and a small incision was made on the ventral midline to expose the peritoneal cavity and discrete gut regions (i.e. stomach and small and large intestine). A series of 0.5-1 µl injections were given across 4 loci along greater curvature of the stomach or across 8 evenly spaced loci along the small or large intestine through a 26-gauge needle and syringe. The peritoneal cavity was then closed with sterile dissolvable sutures and the skin incision closed with sterile wound clips. Animals were given 7 days to recover and allow for retrograde Fast Blue transport before euthanization and tissue extraction as described above.

### *4.3.6 Histological Analysis*

For DRG GFP immunohistochemical quantification in our *Ghsr-GFP* mice injected with Fast Blue (see above), DRGs (L5-T5 levels) were removed from the sucrose solution and sliced in a cryostat at 25 µm. DRG sections were taken in series across three slides (SuperFrost Plus slides (Thermo Fisher Scientific); 8 sections/slide total) to prevent a single neuron being present multiple times on the same slide as previously described [30, 53]. For immunohistochemical staining, in brief, slides were washed 3X15 min in sterile 0.1M PBS on a rotator. DRG sections were blocked with 5% normal horse serum containing 0.3% Triton X-100 in 0.1M PBS for 1 h. Slides were then incubated overnight at room temperature with rabbit anti-cFOS (1:500; sc-52, Santa Cruz Biotechnology, Santa Cruz, CA) and chicken anti-GFP (1:400; GFP2020, AvesLabs, Tigard, OR) antibodies in 0.1M PBS with 0.3% Triton X-100 and 10% normal horse serum. Next, slides were washed 3X 15 min in 0.1M PBS and then incubated at 4°C for 24 h with

donkey anti-chicken-488 (1:1000; 703-545-155, Jackson Immunoresearch, West Grove, PA) and donkey anti-rabbit-CY3 (1:400; 711-165-152, Jackson Immunoresearch, West Grove, PA) in 0.1M PBS. Slides were then washed 3 X 15 min with 0.1M PBS and coverslipped with Prolong antifade fluorescent medium (Invitrogen). Images were captured using an Olympus DP73 photomicroscope and CellSens software (Olympus, Waltham, MA). For GFP, cFOS, and Fast Blue quantification, total cell numbers were estimated by counting the number of fluorescently positive neurons on a single section and then multiplying this number by 8 as each slide contains 8 sections as previously described [32].

For adipose tissue immunohistochemical analysis, samples were removed from formalin, dehydrated through a series of increasing isopropanol washes, and embedded in paraffin blocks. iBAT, iWAT, and eWAT were sliced at 5 µm on a rotating microtome and mounted on SuperFrost Plus slides (Thermo Fisher Scientific). Slides were deparaffinized and hydrated by washing in p-xylenes followed by a series of decreasing ethanol washes. Sections were next incubated in DAKO antigen retrieval solution (DAKO, S1699) and heated in a microwave for 14 minutes total. Rabbit anti-UCP1 antibody (ab10983, Abcam) 1:150 was applied to all sections and then incubated overnight at 4°C. Slides were then washed 4 X 30s in a tris buffer solution and the secondary biotinylated mouse adsorbed donkey anti-rabbit antibody (Jackson ImmunoResearch, 711-065-152) applied to all sections and incubated for 30 min. at room temperature. Slides were washed 4 X 30s in tris buffer and then incubated in an ABC solution (Vector Labs, PK-6100) for 30 min. at room temperature. Sections were then washed 2 X 30s in 1M tris-HCl solution and then incubated in a DAB reaction solution (Vector Labs, SK-4100) for 5-15 min. Slides were washed in dH2O for 5 min. and then dehydrated through graded alcohol washes followed by a final p-xylene wash. Slides were then coverslipped with permount (Fisher,

SP15-100), allowed to dry, and imaged with an Olympus DP73 photomicroscope and CellSens software (Olympus, Waltham, MA).

For hematoxylin and eosin adipose tissue histology, samples were removed from formalin, dehydrated through a series of increasing isopropanol washes, and embedded in paraffin blocks. iBAT, iWAT, and eWAT were sliced at 5 µm on a rotating microtome and mounted on SuperFrost Plus slides (Thermo Fisher Scientific). Tissue morphology was visually analyzed using hematoxylin and eosin staining (Sigma-Aldrich). Adipose histology images were captured using an Olympus DP73 photomicroscope and CellSens software (Olympus, Waltham, MA).

### *4.3.7 In Vitro DRG Culture*

Adult *Ghsr-GFP* mice were euthanized by carbon dioxide inhalation, and DRGs (L5-T5 levels) immediately removed and placed in ice cold 0.1M PBS with 20mM HEPES. This solution was then replaced with 1mg/ml collagenase 1 (Worthington Biochemical Corporation CLS-1) in 0.1M PBS and 20mM HEPES for 60-90 min at 37°C followed by 0.05% Trypsin-EDTA (Sigma T9201) solution in 0.1M PBS and 20mM HEPES for 7 min at 37°C. DRGs were then washed 2X with 1ml complete neurobasal media (Fisher 10888022) with 1X B-27 (Fisher 17504044) and 200µM L-glutamine (Fisher 25030149). Next, 600µl complete neurobasal media was added and the DRGs triturated 30X. Dissociated neurons were filtered through a 100µm cell strainer into a new microcentrifuge tube and then washed 2X with 500µl complete neurobasal media. Neurons were then centrifuged for 5 min at 200g, the supernatant removed and replaced with 1ml complete neurobasal media, triturated 3X, and then seeded onto Poly-D-Lysine and Laminin coated coverslips. Cultured neurons were transferred to a 37°C + 0.5% $CO_2$ incubator until use.

### *4.3.8 Calcium Imaging and Electrophysiology*

For calcium imaging, coverslips containing cultured DRG neurons were transferred to a new 3.5mm dish containing 5µM Fura-2 AM (MilliporeSigma 344905) in complete neurobasal media and placed in a 37°C + 0.5% CO2 incubator for 30 min. Neurons were then washed 3X with an extracellular recording solution composed of 152mM NaCl, 2.8mM KCl, 10mM HEPES, 2mM CaCl2, and 10mM glucose and placed in a 37°C for 20-30 min to allow for intracellular deesterification. Neuronal recording was performed using a Polychrome V monochromator (TILL Photonics). In brief, GFP-positive neurons were identified under a microscope and baseline calcium currents were measured for 5-10 min. Next, either 100nM ghrelin (Bachem 4033076) or vehicle (extracellular recording solution) was administered and changes in calcium currents measured for 30-60 min. At the end of each recording, 60mM KCL was given as a positive control for neuronal viability, and only neurons that were depolarized by KCl were used for analysis.

For electrophysiological recordings, DRG neurons were extracted from *Ghsr-GFP* mice and dissociated as described above. Dissociated neurons were plated into 35 mm plastic dishes coated with poly-D-lysine and used for recording 3-5 days after plating. GFP-labeled DRG neurons were visualized using a GFP-filtered excitation and emission fluorescent light under an inverted microscope. Patch-clamp recordings were performed using a Multiclamp 700B amplifier, Digidata 1440A interphase, and pClamp 10 software (Molecular Devices, Union City, CA) under voltage-clamp and current clamp modes. The external solution (pH 7.3) consisted of 152 mM NaCl, 2.8 mM KCL, 10 mM HEPES, 2 mM CaCl2, and 10 mM glucose. The intracellular solution (pH 7.3) consisted of 130 mM K-gluconate, 10 mM HELES, 0.6 mM EGTA, 0.3 mM K-ATP, 0.3 mM Na-GTP, and 10 mM phosphocreatine.

### *4.3.9 Quantitative Gene and Protein Analysis*

RNA from frozen tissues was extracted using TRIzol Reagent (Thermo Fisher) according to the manufacturer's instructions. Gene expression was measured using a 7500-Fast RT-PCR machine (Applied Biosystems), ABI Universal PCR Master Mix (Applied Biosystems, Foster City, CA), and primer and probe sets purchased from Applied BioSystems. Relative gene expression was determined using the ΔΔCt method with cyclophilin as an internal control [56]. The following genes were assayed:

Acyl-CoA Oxidase 1 (*Acox1*); β3 Adrenergic Receptor (*β3AR*); Carnitine Palmitoyltransferase 1B (*Cpt1b*); Cell Death-Inducing DFFA-Like Effector A (*Cidea*); Cyclooxygenase 1 (*Cox1*); ELOVL Fatty Acid Elongase 3 (*Elovl3*); Growth Hormone Secretagogue Receptor 1a (*Ghsr*); Iodothyronine Deiodinase 2 (*Dio2*); Peroxisome Proliferator Activated Receptor Alpha (*Ppar-α*); Peroxisome Proliferator Activated Receptor Gamma (*Ppar-γ*); PPARG Coactivator 1 Beta (*Pgc-1β*); PR domain containing 16 (*Prdm16*); Uncoupling Protein 1 (*Ucp-1*); Uncoupling Protein 3 (*Ucp-3*).

For Western blot analysis, proteins were extracted using a radioimmunoprecipitation assay buffer with protease inhibitor cocktails (Sigma-Aldrich, St. Louis, MO) and a handheld homogenizer. Protein concentration was quantified with a DC Protein Assay (BioRad, Hercules, CA), and protein samples were denatured at 37°C for 30 minutes. 20 to 30 µg protein was loaded onto a 4% to 15% gradient polyacrylamide gel (Criterion TGX; BioRad, Hercules, CA) and then transferred to a polyvinylidene difluoride membrane. We immunoblotted the membranes by blocking with 5% nonfat milk and followed by antibodies against uncoupling protein 1 (1:500) (catalog no. 23841; Abcam, Cambridge, MA), tyrosine hydroxylase (1:1000)

(catalog no. AB152; Millipore Sigma, Burlington, MA), pHSL (1:1000) (catalog no. 4126; Cell Signaling, Danvers, MA), or α-tubulin (1:500) (catalog no. ABCENT4777; Advanced Biochemicals, Lawrenceville, GA) overnight at 4°C. Next, samples were incubated in an Alexa Fluor goat anti-rabbit 680 secondary antibody (catalog no. A21109; Thermo Fisher Scientific, Waltham, MA) at 1:5000 concentration for 3 hours. Bands were visualized and quantified using an Odyssey Fc Imaging System (Li-Cor, Lincoln, NE) with background subtracted. All membranes were immunoblotted with and normalized to α-tubulin antibody at 1:500 dilution (catalog no. 2144S; Cell Signaling).

### *4.3.10 Cold Exposure*

2 weeks prior to the start of cold exposure, 10-week-old AGKO and f/f littermate mice were implanted with temperature transponders (IPTT-300, BMDS, Seaford, DE). In brief, animals were deeply anesthetized with 1-2% isoflurane and a small incision made along the ventral midline to expose the peritoneal cavity. Sterile temperature transponders were inserted into the peritoneal cavity, the incision closed with sterile dissolvable sutures, and the skin incision closed with sterile wound clips. Following transponder implantation, animals were singly housed in shoebox cages with only corn cob bedding for recovery. At the start of the experiment, baseline body temperature measurements were taken for all animals before being placed in a 10°C cooler for 7 days. Core body temperature measurements were taken for all mice every hour for the first 8 hours of the study, and then every 2 hours through 24 h. Measurements were taken every 2 hours from 0700 to 1900 for the remaining 6 days. At the end of the experiment, animals were removed from the cooler, immediately euthanized, and tissues extracted as described above. In a separate set of *Ghsr-GFP* mice used for immunohistochemical analysis, mice were placed in the 10°C cooler for 7 days exactly as

described above, but without implantation of temperature transponders or core body temperature measurements taken.

### *4.3.11 Food Intake Studies*

For ghrelin-induced food intake measurements, single housed ad libitum Chow-fed or HFD-fed AGKO and f/f littermate mice were given a 0.5 mg/kg subcutaneous ghrelin challenge (4033076, Bachem, Torrance, CA) at 0800. Food intake was measured at 30, 60, 90, and 120 min post-injection. For food deprivation-induced food intake, single housed Chow-fed or HFD-fed AGKO and f/f littermate mice were food deprived for 16 hours. At 0800, food was returned, and food intake measured at 30, 60, 90, and 120 min post-refeeding.

### *4.3.12 Statistical Analysis*

All data were expressed as mean ± S.E. Relative expression for all genes measured by quantitative PCR were normalized to cyclophilin. For calcium imaging experiments, $\Delta F/F\%$ was calculated by first taking the average baseline fluorescence across the initial 5-10 min. of the study. Next, % change in fluorescence was calculated at each timepoint using the formula [[(TimepointX-baseline)/baseline] * 100]. Experimental data were analyzed by a Student's t-test, paired t-test, or a two-way or three-way Repeated Measures ANOVA followed by Duncan's Multiple-Comparison post-hoc analysis where appropriate. For all experiments, differences among groups was considered statistically significant at $P<0.05$ and trending toward significance at $P\leq0.1$.

## 4.4 Results

### *4.4.1 GHSRs are expressed in vagal and DRG neurons that project to the gastrointestinal system*

We first sought to identify organs innervated by GHSR-containing sensory neurons using the neuronal tracer Fast Blue. Because ghrelin is predominantly produced in the stomach, we hypothesized that gastrointestinal sensory neurons would express GHSRs. Indeed, we found that stomach, small intestine, and large intestine sensory neurons largely originate in the vagus nerve, but significant DRG innervation exists between T12 and T5 ganglia for all areas [**Fig. 4.1 A**]. GFP immunohistochemistry revealed strong, consistent labeling in the nodose ganglia and across all DRG levels in our *Ghsr*-IRES-tauGFP mice (data not shown), but because Fast Blue most strongly labeled T12-T5 ganglia we chose to focus our efforts on these levels [**Fig. 4.1 B**]. Extensive GFP and Fast Blue double labeled neurons were present in these ganglia [**Fig. 4.1 C-E**]. We found significant GFP and Fast Blue colocalization in vagal and DRG neurons that project to the stomach [**Fig. 4.1 F**] or small intestine [**Fig. 4.1 G**] with between 10%-40% GFP neurons co-labeled with Fast Blue and between 20%-60% Fast Blue neurons co-labeled with GFP. By contrast, we found significantly less Fast Blue and GFP colocalization in large intestine projecting sensory neurons and therefore focused our efforts on the stomach and small intestine (data not shown). Although the presence of GFP indicates GHSR expression in DRGs and the nodose ganglia, we confirmed these GHSRs were responsive to ghrelin using in vitro DRG cultures and a combination of electrophysiology and calcium imaging. Using dissociated DRG neurons from *Ghsr*-IRES-tauGFP mice, we found that 100 nmol ghrelin increased the neurons membrane potential and resulted in spontaneous action potentials [**Fig. 4.1 H**]. Moreover, patch clamp studies found that 100 nmol ghrelin, but not vehicle, significantly

decreased neuron hyperpolarization [**Fig. 4.1 I-J**]. We next used in vitro calcium imaging to confirm our electrophysiology results on Ghsr-IRES-tauGFP mouse DRG neurons. 100 nmol ghrelin markedly increased calcium efflux from GFP-positive DRG neurons, but this effect was absent in GFP-negative neurons given 100 nmol ghrelin and in GFP-positive and GFP-negative neurons receiving vehicle [**Fig. 4.1 K-L**].

### *4.4.2 Sensory neuron GHSRs are activated by energetic challenges*

After we identified the anatomical distribution of sensory neuron-containing GHSRs and their response to ghrelin in vitro, we next tested whether these neurons are activated by energetic challenges. We chose overnight food deprivation and acute (24 h) cold exposure challenges as these elicit a robust increase in circulating ghrelin [13, 57]. We found that both fasting and cold exposure significantly increased Arc GHSR expression, but only cold exposure significantly increased DRG GHSR expression [**Fig. 4.2 A, E**]. By contrast, neither fasting nor cold exposure significantly affected the total number of GFP-positive DRG or vagal sensory neurons [**Fig. 4.2 B, F**]. We next examined whether food deprivation or cold exposure activated DRG and vagal GHSR-positive neurons in vivo using triple labeling for GFP, Fast Blue, and the neuronal activity marker cFos [58]. We found that both food deprivation and cold exposure significantly increased stomach [**Fig. 4.2 C, G**] and small intestine [**Fig. 4.2 D, H**] projecting GHSR sensory neuron activity, and that these energetic challenges robustly induced cFos immunoreactivity allowing for triple immunofluorescence labeling [**Fig. 4.2 I-L**].

### *4.4.3 Sensory neuron GHSR knockout does not affect chow-fed mice*

We next examined the endogenous role of sensory neuron GHSR signaling in regulating energy homeostasis by generating a novel, sensory neuron GHSR knockout mouse model. To

accomplish this, we crossed our sensory neuron-specific *advillin-cre* driver mouse line with the recently generated *ghsr*$^{f/f}$ mouse [27, 53]. The resultant offspring (henceforth referred to as AGKO) had normal hypothalamic GHSR expression, but an approximately 90% decrease in DRG GHSR expression indicating GHSR deletion is specific to peripheral sensory neurons [**Fig. 4.3 A**]. Chow-fed AGKO mice had no difference in body mass [**Fig. 4.3 B, D**] nor in interscapular brown adipose tissue (iBAT), epididymal adipose tissue (eWAT), inguinal adipose tissue (iWAT), or liver mass compared with f/f littermates [**Fig. 4.3 C, E-G**]. As GHSRs are necessary for exogenous ghrelin-induced food intake, we next tested whether AGKO mice respond to a peripheral ghrelin challenge (0.5 mg/kg body mass) and whether these mice have a normal feeding response following an overnight fast. In line with previous work indicating central GHSRs are sufficient to regulate food intake [16, 29], we found that both an exogenous ghrelin challenge and an overnight fast comparably increased food intake in AGKO and f/f control mice [**Fig. 4.3 H-I**]. Moreover, we found no difference in 24 h food intake between AGKO and f/f littermates [**Fig. 4.3 G**]. Because *ghrelin* and *ghsr* knockout mice have improved glucose disposal and insulin sensitivity, we next tested glucose and insulin tolerance in our AGKO mice. We found that chow-fed AGKO and f/f littermate mice had no difference in glucoregulation following a glucose tolerance test [**Fig. 4.3 K**], overnight fasting [**Fig. 4.3 L**], insulin tolerance test [**Fig. 4.3 M**], or in *ad lib* fed plasma insulin concentrations [**Fig. 4.3 N**].

### *4.4.4 Chow-fed AGKO mice have increased energy expenditure and adipose thermogenic gene expression*

To characterize the metabolic phenotype of our AGKO mice, we used indirect calorimetry measurements in our metabolic cage system. We found that AGKO and f/f control mice had slightly elevated energy expenditure at several time points throughout the experiment

[**Fig. 4.4 A**], although we found no significant difference in area under the curve [**Fig. 4.4 B**]. We found several instances of AGKO mice having higher respiratory quotient measurements indicating a preferential use of carbohydrates [**Fig. 4.4 C**], but no difference between AGKO and f/f mice during either daytime or nighttime as measured by area under the curve [**Fig. 4.4 D**]. To identify the mechanism driving this increased energy expenditure, we examined thermogenic gene expression in adipose tissue as previous studies demonstrated *ghsr* knockout mice have significantly increased thermogenic capacity [27]. We found that AGKO mice had markedly increased thermogenic and β3-adrenergic receptor gene expression in iBAT, eWAT, and iWAT compared with f/f controls suggesting increased adipose tissue thermogenesis underlies the elevated energy expenditure in AGKO mice [**Fig. 4.4 E-G**]. Moreover, AGKO mice had significantly increased UCP-1 protein content in iBAT, a trend of increased UCP1 in eWAT, and significantly increased TH proteins in eWAT and iWAT compared with f/f control mice compared with [**Fig. 4.4 H-J**].

To confirm our gene and protein expression results, we analyzed AGKO and f/f adipose tissues using hematoxylin and eosin (H&E) staining and UCP-1 immunohistochemistry (IHC). Compared with f/f H&E and UCP-1IHC stained iBAT [**Fig. 4.5 A, C**], AGKO iBAT was notably darker and had a greater density of UCP-1 staining [**Fig. 4.5 B, D**]. H&E stained eWAT was comparable in f/f [**Fig. 4.5 E**] and AGKO [**Fig. 4.5 F**], yet AGKO mice had significantly more UCP-1 staining compared with f/f mice [**Fig. 4.5 G, H**]. iWAT histological analysis revealed a marked difference between H&E stained f/f [**Fig. 4.5 I**] and AGKO [**Fig. 4.5 J**] mice such that AGKO iWAT was significantly more BAT-like. Indeed, UCP-1 IHC revealed markedly more staining in AGKO iWAT compared with f/f iWAT [**Fig. 4.5 K, L**].

### *4.4.5 Diet-induced obesity is attenuated in AGKO mice*

The significant increase in energy expenditure and thermogenic capacity led us to hypothesize that AGKO mice would resist the development of diet induced obesity. We found that a HFD consisting of 60% calories from fat markedly increased body mass and overall fat mass in f/f control mice, but this effect was attenuated in AGKO mice [**Fig. 4.6 A-B, D**]. Tissue analysis revealed a significant decrease in liver and iWAT mass and a trend for decreased iBAT mass [**Fig. 4.6 C, E-H**]. We next tested the food intake response to an exogenous ghrelin (0.5mg/kg body mass) or overnight fasting challenge, and found that, like chow-fed mice, HFD-fed AGKO and f/f control mice had comparable food intake following both ghrelin and fasting [**Fig. 4.6 I-J**]. In addition, AGKO and f/f mice have comparable 24 h food intake suggesting sensory neuron GHSR knockout does not affect food intake on HFD [**Fig. 4.6 K**]. As obese can lead to Type 2 Diabetes development in humans and mice, we tested the glucoregulatory ability in HFD-fed AGKO and f/f mice. We found that sensory neuron GHSR deletion significantly improved glucose disposal during a glucose tolerance test and decreased fasting glucose [**Fig. 4.6 L-M**]. In addition, AGKO mice had a trend of decreased circulating glucose 15 min. after an insulin challenge [**Fig. 4.6 N**] and decreased *ad lib* fed plasma insulin concentrations [**Fig. 4.6 O**] suggesting these mice are more insulin sensitive compared with f/f controls.

### *4.4.6 HFD-fed AGKO mice have increased energy expenditure and thermogenic gene expression*

We hypothesized that the DIO resistance in AGKO mice was due to increased energy expenditure as we found chow-fed mice had increased energy expenditure and thermogenic capacity [**Fig. 4.4** and **Fig. 4.5**]. Indeed, HFD-fed AKO mice had significantly increased energy expenditure during both daytime and nighttime compared with f/f control mice [**Fig. 4.7 A-B**].

In addition, AGKO mice had significantly decreased respiratory quotient during nighttime hours indicating a preferential utilization of fatty acids as fuel [**Fig. 4.7 C-D**]. In contrast, there was no difference in the activity levels between fl/fl and AGKO mice (data not shown). We next examined adipose tissue gene expression with a focus on thermogenic genes as these were upregulated in chow-fed animals. We found a significant increase in numerous thermogenic and browning genes in iBAT [**Fig. 4.7 E**], eWAT [**Fig. 4.7 F**], and iWAT [**Fig. 4.7 G**] when compared with f/f control mice suggesting the increased energy expenditure is due to upregulated thermogenic pathways in adipose tissue. Moreover, we found significantly higher UCP1, TH, and a trend of increased pHSL protein content in AGKO iBAT compared with f/f animals [**Fig. 4.7 H**]. We observed a trend of increased TH protein in AGKO eWAT and significantly higher pHSL protein in AGKO iWAT compared with f/f control mice [**Fig. 4.7 I-J**].

We next performed H&E staining and UCP-1 IHC in fat tissues to confirm our gene and protein expression data. We found that f/f mice had significantly larger adipocyte cell size in iBAT compared with AGKO mice [**Fig. 4.8 A, B**], and significantly less iBAT UCP-1 staining when compared with AGKO mice [**Fig. 4.8 C, D**]. Moreover, compared with f/f mice, we found a marked reduction in adipocyte size in AGKO eWAT [**Fig. 4.8 E, F**], iWAT [**Fig. 4.8 I, J**], and significantly decreased liver lipid deposits [**Fig. 4.8 G, H**].

### *4.4.7 AGKO mice are markedly more cold tolerant*

The marked increase in adipose tissue thermogenic genes would suggest AGKO mice have a greater capacity to maintain body temperature during a cold challenge. Hence, we next tested the thermoregulatory ability in AGKO and f/f mice during an acute (1 day) 4°C or chronic (10 day) 10°C cold challenge. We found that AGKO mice had significantly increased baseline

body temperature and were able to more rapidly normalize their temperature compared with f/f control mice in response to an acute 4°C cold challenge [**Fig. 4.9 A**]. In addition, AGKO mice had significantly increased core body temperature at several time points during a 7 day 10°C challenge and as measured by area under the curve [**Fig. 4.9 B-C**]. We next examined adipose thermogenic gene expression in these mice and found that a 1 day 4°C cold challenged AGKO mice had significantly increased thermogenesis and browning genes in iBAT, eWAT, and iWAT [**Fig. 4.9 D-F**]. Similarly, we found a 7 day 10°C challenged AGKO mice had significantly upregulated thermogenic genes in iBAT, eWAT, and iWAT [**Fig. 4.9 G-I**].

We further examined adipose depots from 1 day and 7 day cold exposed animals using H&E and UCP-1 IHC analysis. H&E staining was comparable for 1 day cold exposed f/f and AGKO iBAT and eWAT [**Fig. 4.10 A, B** and **E, F**], although AGKO mice had significantly increased UCP-1 IHC staining in iBAT [**Fig. 4.10 C, D**] and eWAT [**Fig. 4.10 G, H**]. H&E stained iWAT in AGKO mice had a more BAT-like morphology compared with f/f mice [**Fig. 4.10 I, J**], and iWAT UCP-1 IHC revealed markedly more staining for AGKO mice compared with f/f mice [**Fig. 4.10 K, L**]. Our analysis of adipose tissues from 7 day cold exposed animals complemented 1 day tissue analysis. Compared with f/f mice, 7 day cold exposed AGKO mice had significantly darker H&E stained iBAT [**Fig. 4.10 M, N**], eWAT [**Fig. 4.10 Q, R**], and iWAT [**Fig. 4.10 U, V**]. Moreover, we found a marked increase in UCP-1 IHC staining in AGKO iBAT [**Fig. 4.10 O, P**], eWAT [**Fig. 4.10 S, T**], and iWAT [**Fig. 4.10 W, X**] as compared with f/f mice.

We next sought to further study whether increased BAT thermogenesis and WAT beiging in AGKO mice during cold exposure was due to increased sympathetic activity by measuring TH

protein levels using Western Blot analysis. We found 1 day cold exposure significantly increased AGKO TH protein in iBAT [**Fig. 4.11 A**] and iWAT [**Fig. 4.11 C**], but not in eWAT [**Fig. 4.11 B**]. In addition, 7 day cold exposed AGKO mice also had a trend of increased TH protein in iBAT [**Fig. 4.11 D**], eWAT [**Fig. 4.11 E**], and iWAT [**Fig. 4.11 F**]. Interestingly, we also found a significant increase in iWAT pHSL in 7 day cold exposed AGKO mice [**Fig. 4.11 F**].

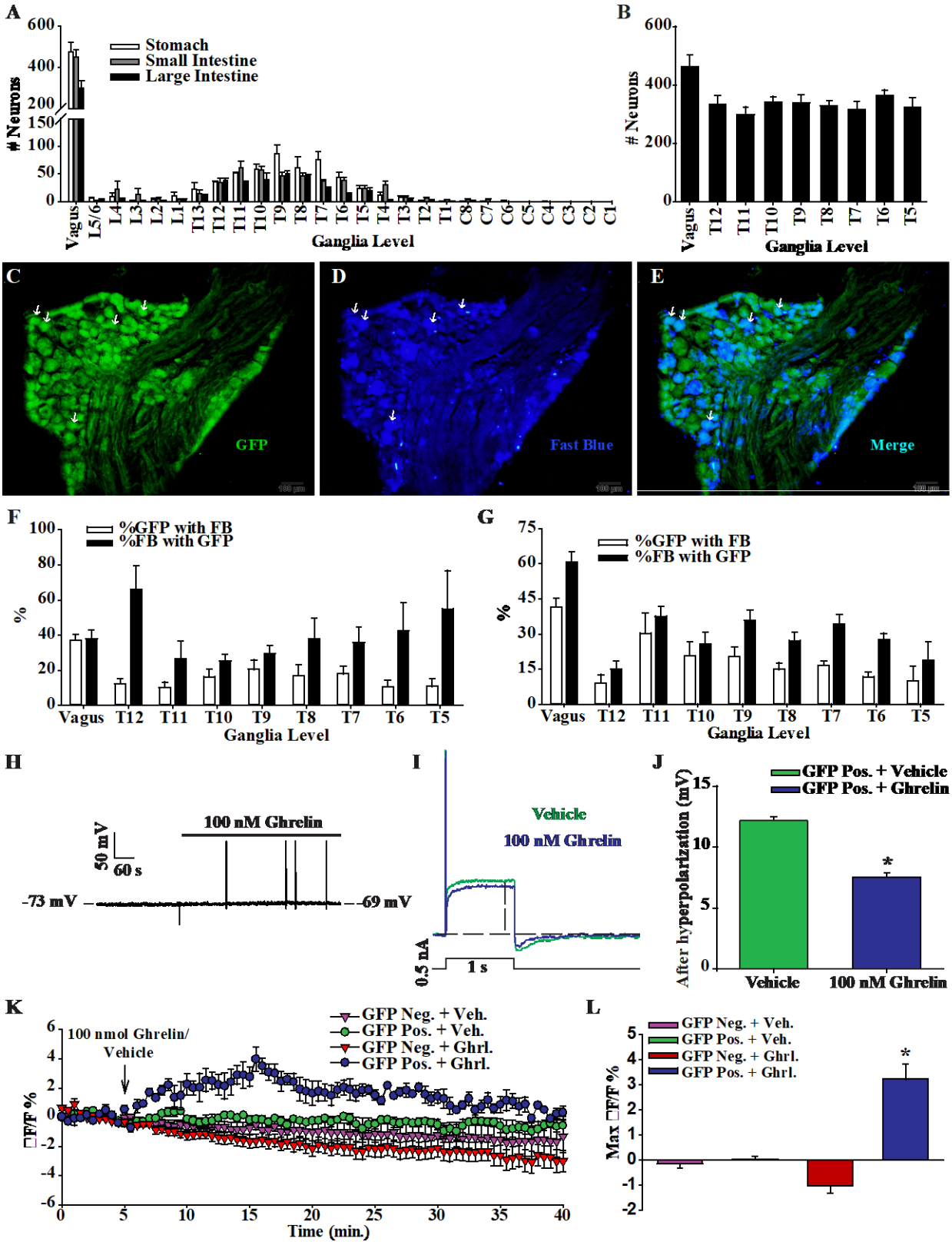
A
# Neurons
Stomach
Small Intestine
Large Intestine
Vagus L5/6 L4 L3 L2 L1 T13 T12 T11 T10 T9 T8 T7 T6 T5 T4 T3 T2 T1 C8 C7 C6 C5 C4 C3 C2 C1
Ganglia Level
B
# Neurons
Vagus T12 T11 T10 T9 T8 T7 T6 T5
Ganglia Level
C
GFP
D
Fast Blue
E
Merge
F
%GFP with FB
%FB with GFP
%
Vagus T12 T11 T10 T9 T8 T7 T6 T5
Ganglia Level
G
%GFP with FB
%FB with GFP
%
Vagus T12 T11 T10 T9 T8 T7 T6 T5
Ganglia Level
H
100 nM Ghrelin
50 mV
60 s
-73 mV
-69 mV
I
Vehicle
100 nM Ghrelin
0.5 nA
1 s
J
GFP Pos. + Vehicle
GFP Pos. + Ghrelin
After hyperpolarization (mV)
*
Vehicle
100 nM Ghrelin
K
100 nmol Ghrelin/
Vehicle
GFP Neg. + Veh.
GFP Pos. + Veh.
GFP Neg. + Ghrl.
GFP Pos. + Ghrl.
□F/F %
Time (min.)
L
GFP Neg. + Veh.
GFP Pos. + Veh.
GFP Neg. + Ghrl.
GFP Pos. + Ghrl.
Max □F/F %
*

**Fig. 4.1** GHSR-positive neurons emanate from DRGs.
Average number of stomach, small intestine, or large intestine injected Fast Blue positive neurons in the vagus and L5/6-C1 DRG levels (A) (n=8). Average number of GFP-positive neurons in the vagus and T12-T5 DRG levels (B) (n=8). Representative fluorescent image of T10 level DRG stained for GFP (C) and Fast Blue (D), and superimposed images showing colocalization of staining (E). Average number of GFP-positive neurons labeled with Fast Blue and number of Fast Blue-positive neurons expressing GFP that project to the stomach (F) or small intestine (G) (n=4-6 per group). Representative electrophysiology recording from GFP-positive DRG neurons given 100 nmol ghrelin (H). Representative patch clamp recording from GFP-positive DRG neuron given either vehicle (green trace) or 100 nmol ghrelin (blue trace) (I). Quantification from all GFP-positive DRG patch clamp experiments (J) (n=6 neurons). Average intracellular calcium change for GFP-positive and GFP-negative DRG neurons given either 100 nmol ghrelin (Ghrl.) or vehicle (Veh.) (K), and the maximum change in fluorescence (L) (n=5-12 neurons per group). White arrows in C-E denote GFP and Fast Blue double labeled neurons. Data reported as mean ± S.E.M. *P<0.5 vs. baseline.

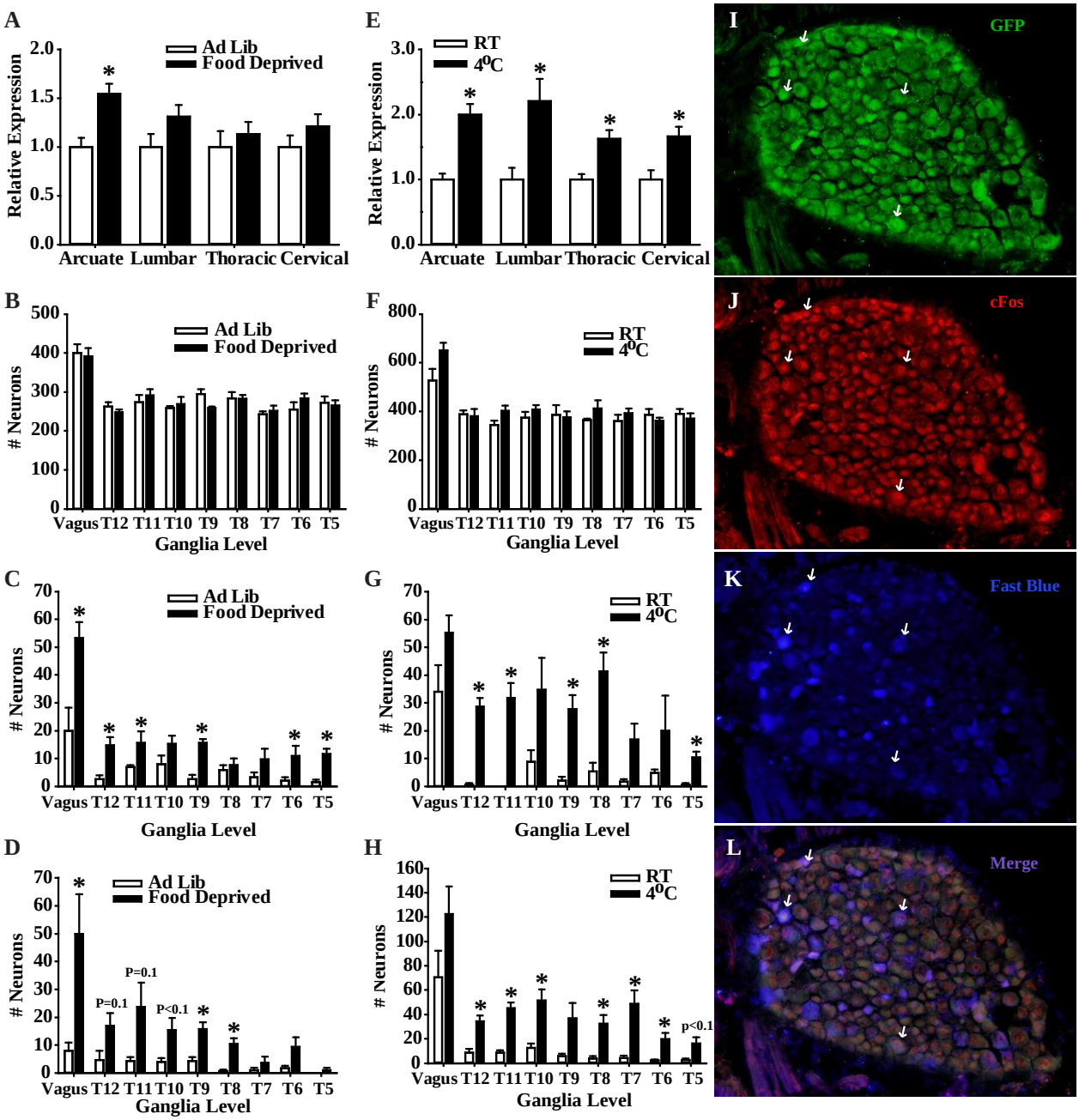


**Fig. 4.2** GHSR-positive sensory neurons are activated by energetic challenges. Relative GHSR expression in the arcuate nucleus, lumbar DRGs, Thoracic DRGs, or Cervical DRGs following 12h food deprivation (A) or 24h cold exposure challenge (E) (n=4 per group). Average number of GHSR-positive neurons in the vagus and T12-T5 DRG levels following 12h food deprivation (B) or 24h cold exposure challenge (F) (n=4-6 per group). Number of triple labeled (GFP, cFos, and Fast Blue) neurons projecting to the stomach (C) or small intestine (D) following a 12h food deprivation challenge (n=4-5 per group). Number of triple labeled (GFP,

cFos, and Fast Blue) neurons projecting to the stomach (G) or small intestine (H) following a 24h cold exposure challenge (n=4-5 per group). Representative T7 DRG level fluorescent immunostaining for GFP (I), cFOS (J), Fast Blue (K), and superimposed labeling showing colocalization (L). White arrows in I-L denote GFP, cFos, and Fast Blue triple labeled neurons. Data reported as mean ± S.E.M. *P<0.5 vs. *ad libitum* fed or room temperature control animals.

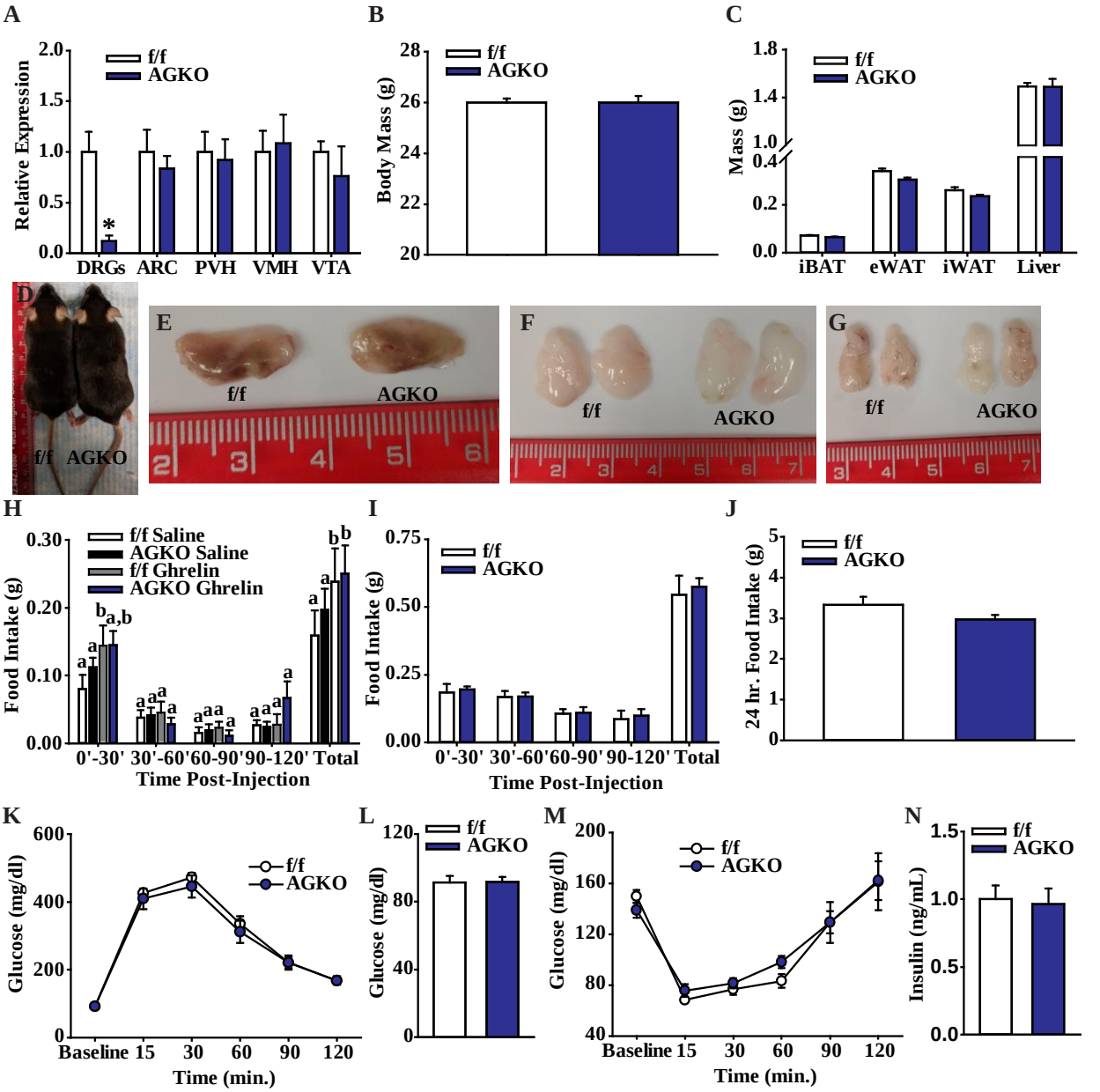


**Fig. 4.3** Sensory neuron specific GHSR knockout has no effect on chow-fed mice. Relative GHSR expression in DRGs, arcuate nucleus (ARC), paraventricular hypothalamus (PVH), ventromedial hypothalamus (VMH), and ventral tegmental area (VTA) in AGKO and WT mice (A) (n=4-6 per group). Body mass (B) and tissue mass (C) for AGKO and WT mice chow-fed for 12 weeks (n=7-8 per group). Food intake measurements for AGKO and WT mice following a saline or ghrelin challenge (0.5mg/kg body mass S.C.) (D), or an overnight fast (E) (n=8-9 per group). 24-hour food intake measurements for AGKO and WT mice (F) (n=8-9 per group). Glucose tolerance test (1.5mg/kg body mass) (G), fasting blood glucose (H), insulin tolerance test (1U/kg body mass) (I), and *ad lib* fed plasma insulin concentrations (N) for AGKO and WT mice (n=8 per group). Data reported as mean ± S.E.M. *P<0.5 vs. WT control animals.

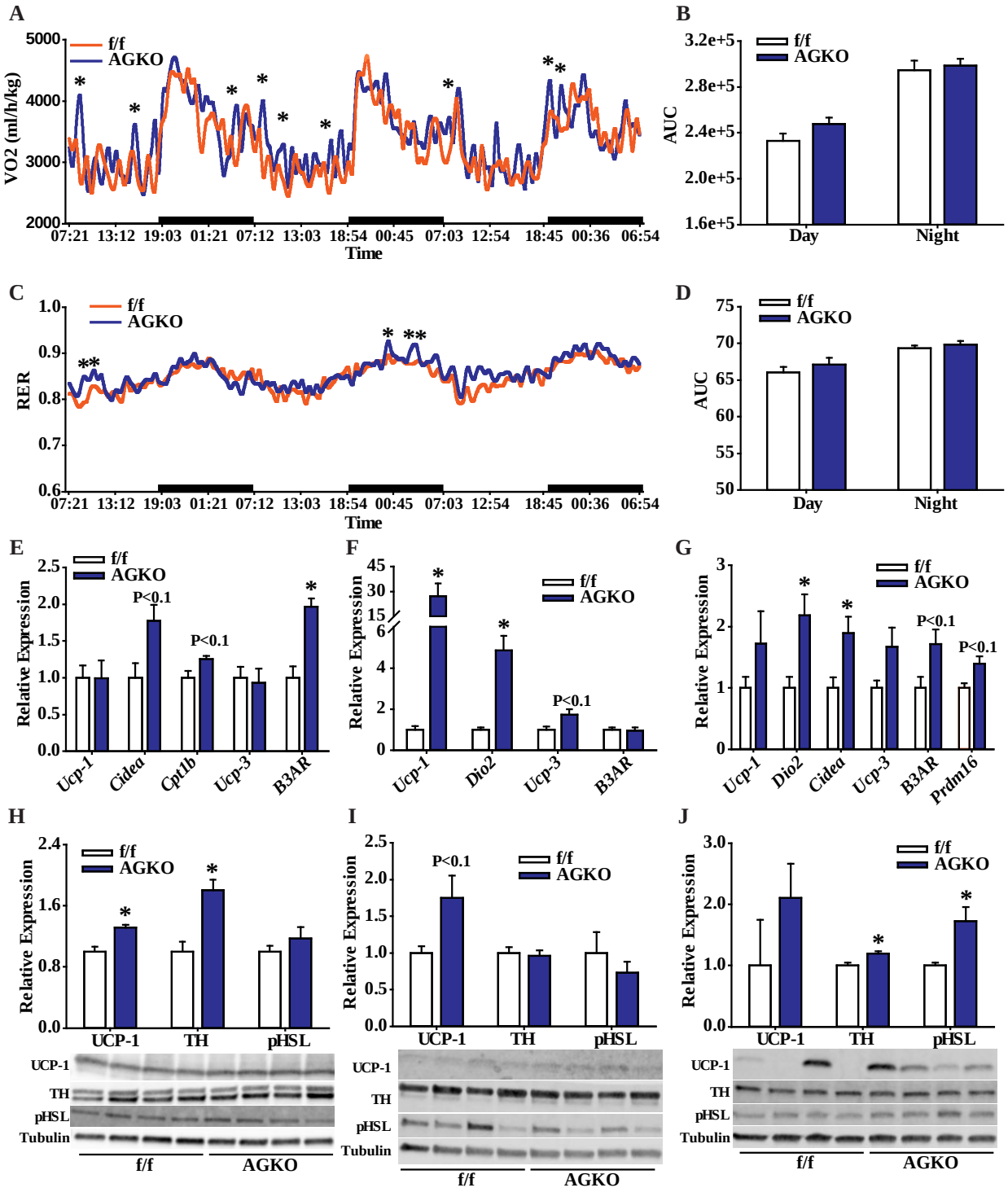


**Fig. 4.4** Chow-fed AGKO mice have upregulated thermogenic genes and proteins. Average daily energy expenditure for AGKO and WT mice (A) and day/night area under the curve values (B) (n=7 per group). Average daily respiratory quotient for AGKO and WT mice (C) and day/night area under the curve values (D) (n=7 per group). Relative expression of thermogenic genes in iBAT (E), eWAT (F), and iWAT (G) for AGKO and WT mice (n=8 per group). Relative thermogenic protein content in iBAT (H), eWAT (I), and iWAT (J) for AGKO and WT mice (n=4 per group). Data reported as mean ± S.E.M. *P<0.5 vs. WT control animals.

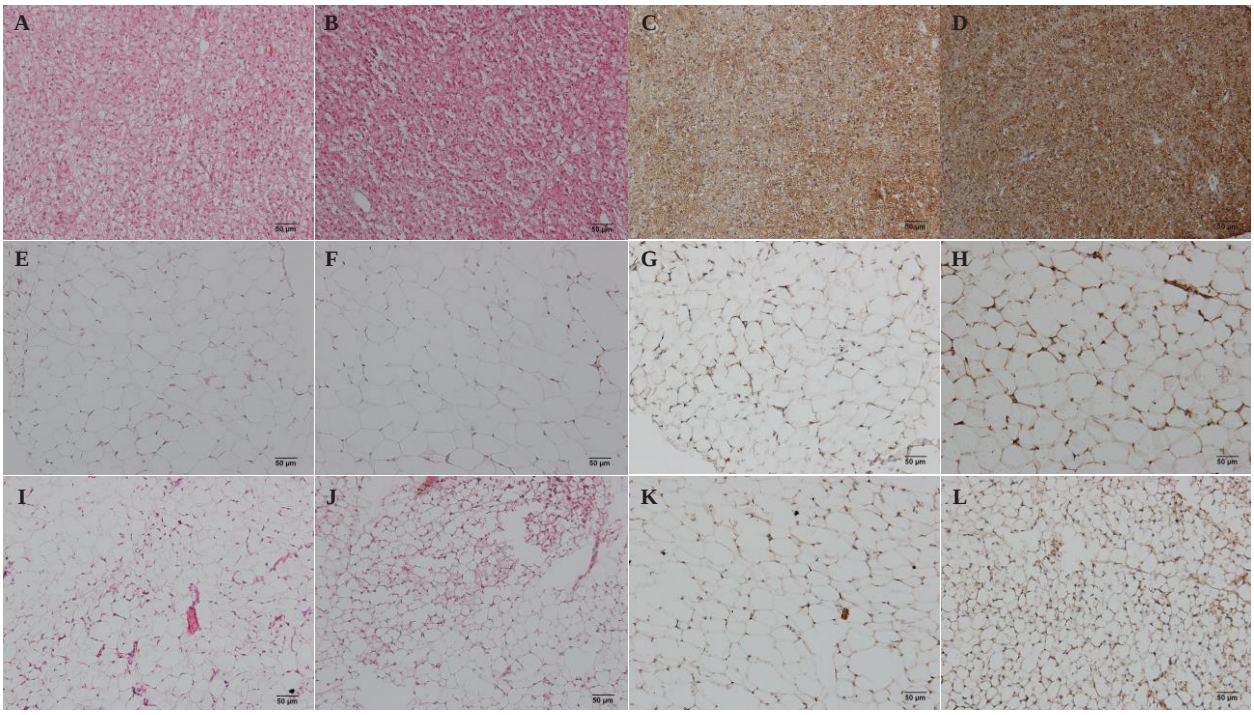


**Fig. 4.5**. 12 wk. chow-fed H&E and UCP-1 IHC adipose tissue histology. Representative images of H&E stained iBAT from f/f (A) and AGKO mice (B), and representative UCP-1 IHC iBAT images from f/f (C) and AGKO mice (D). Representative images of H&E stained eWAT from f/f (E) and AGKO mice (F), and representative UCP-1 IHC eWAT images from f/f (G) and AGKO mice (H). Representative images of H&E stained iWAT from f/f (I) and AGKO mice (J), and representative UCP-1 IHC iWAT images from f/f (K) and AGKO mice (L).

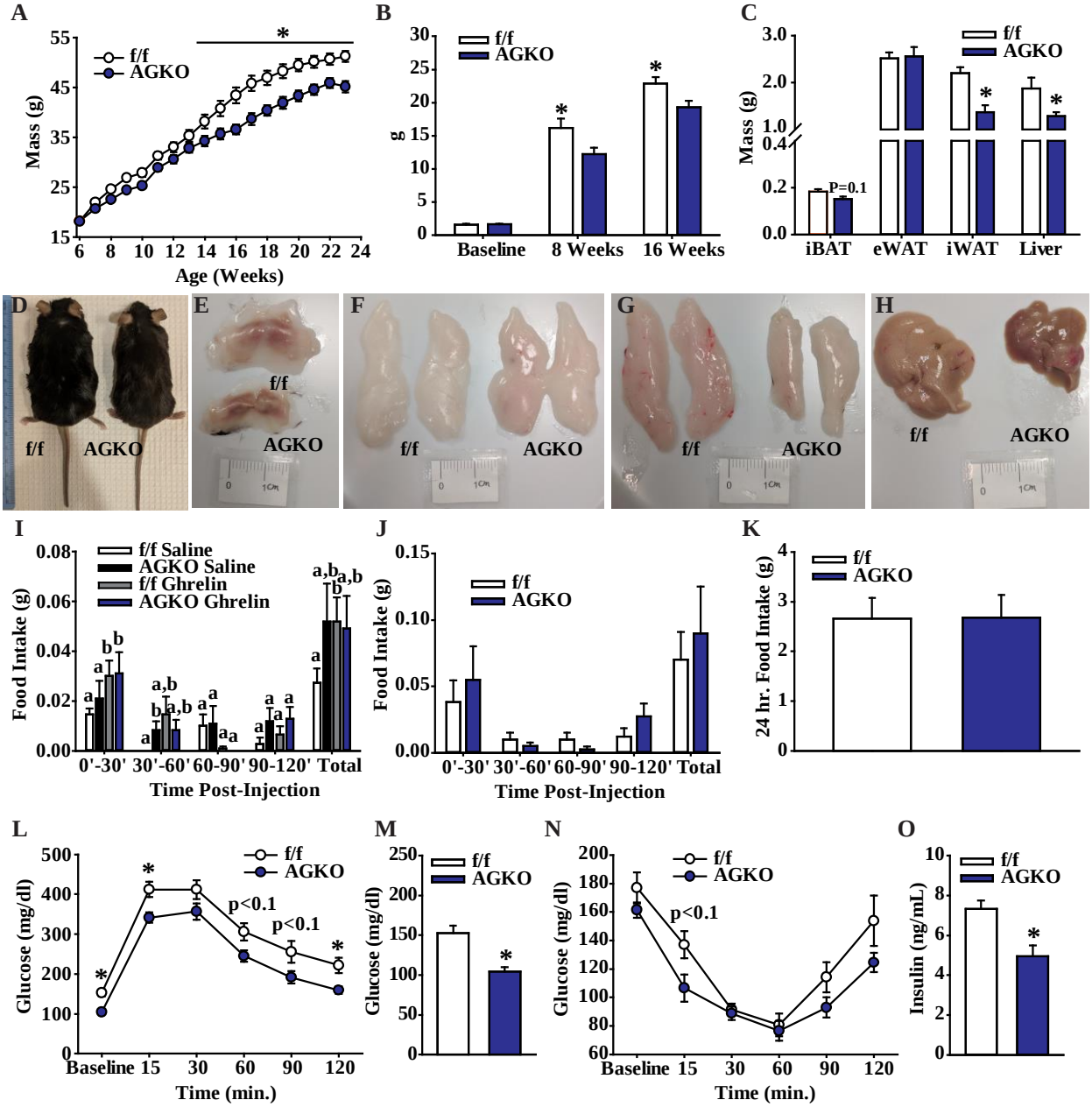


**Fig. 4.6** Sensory neuron GHSR knockout attenuates diet induced obesity.
Weekly body mass measurements for AGKO and WT mice (A) (n=15-17 per group). Baseline, 8 week, and 16 week fat mass for AGKO and WT mice (B) (n=15-17 per group). Tissue weights following 12 week high-fat-diet feeding for AGKO and WT mice (C) (n=8 per group). Representative images of AGKO and WT mice (D), iBAT (E), eWAT (F), iWAT (G), and the liver (H). Food intake measurements for high-fat-diet fed AGKO and WT mice following a saline or ghrelin challenge (0.5mg/kg body mass) (I), or an overnight fast (J) (n=8 per group). 24-hour food intake measurements for high-fat-diet fed AGKO and WT mice (K) (n=9 per group). Glucose tolerance test (1.5mg/kg body mass) (L), fasting blood glucose (M), insulin tolerance test (1U/kg body mass) (N), and *ad lib* fed plasma insulin concentrations (O) for high-fat-diet fed AGKO and WT mice (n=8 per group). Data reported as mean ± S.E.M. *P<0.5 vs. WT control animals.

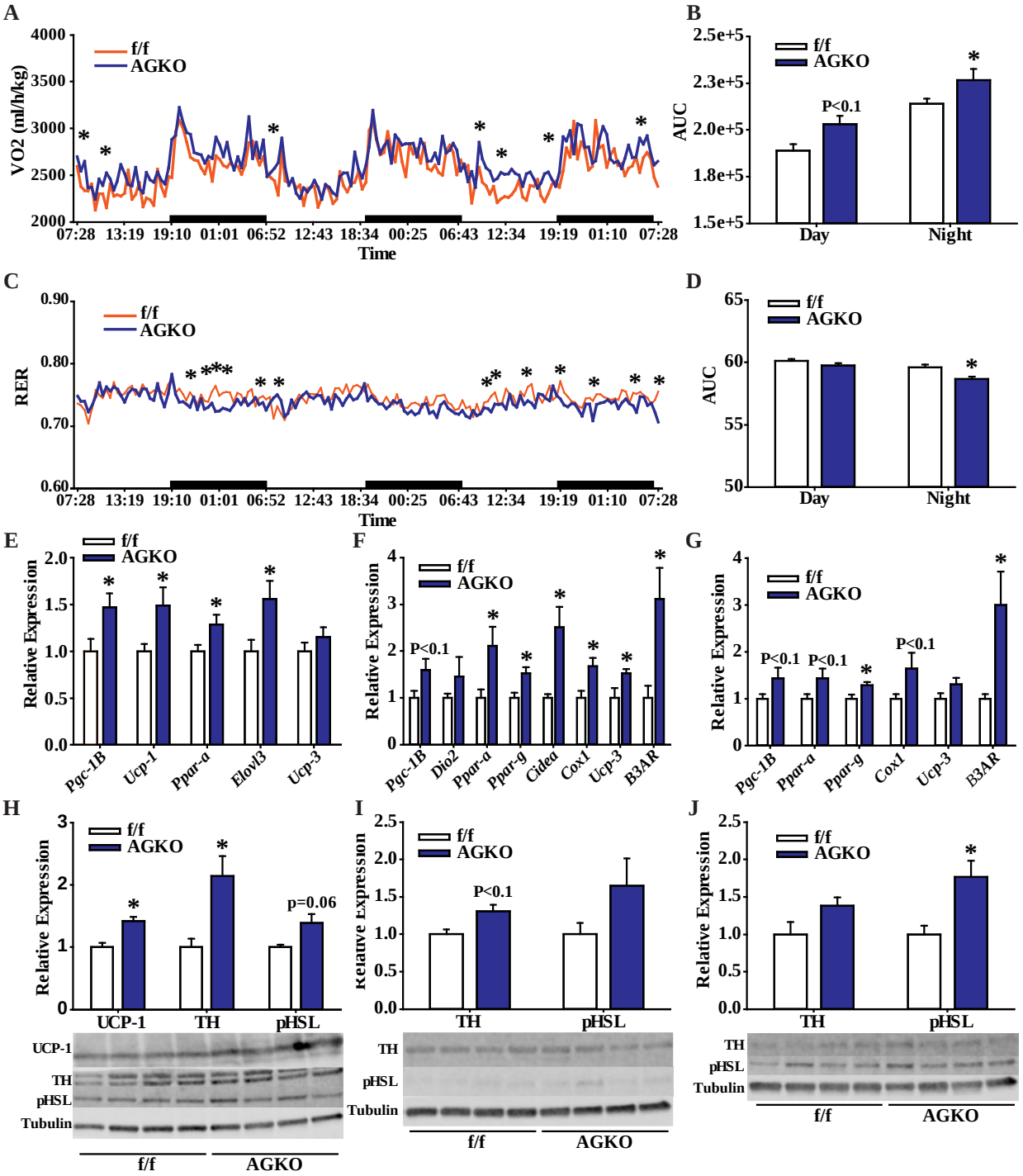


**Fig. 4.7** Sensory neuron GHSR knockout mice have increased energy expenditure and thermogenic capacity on high-fat-diet.

Average daily energy expenditure for high-fat-diet fed AGKO and WT mice (A) and day/night area under the curve values (B) (n=7 per group). Average daily respiratory quotient for high-fat-diet fed AGKO and WT mice (C) and day/night area under the curve values (D) (n=7 per group). Relative expression of thermogenic genes in iBAT (E), eWAT (F), and iWAT (G) for high-fat-

diet fed AGKO and WT mice (n=8 per group). Relative thermogenic protein content in iBAT (H), eWAT (I), and iWAT (J) for AGKO and WT mice (n=4 per group). Data reported as mean ± S.E.M. *P<0.5 vs. WT control animals.

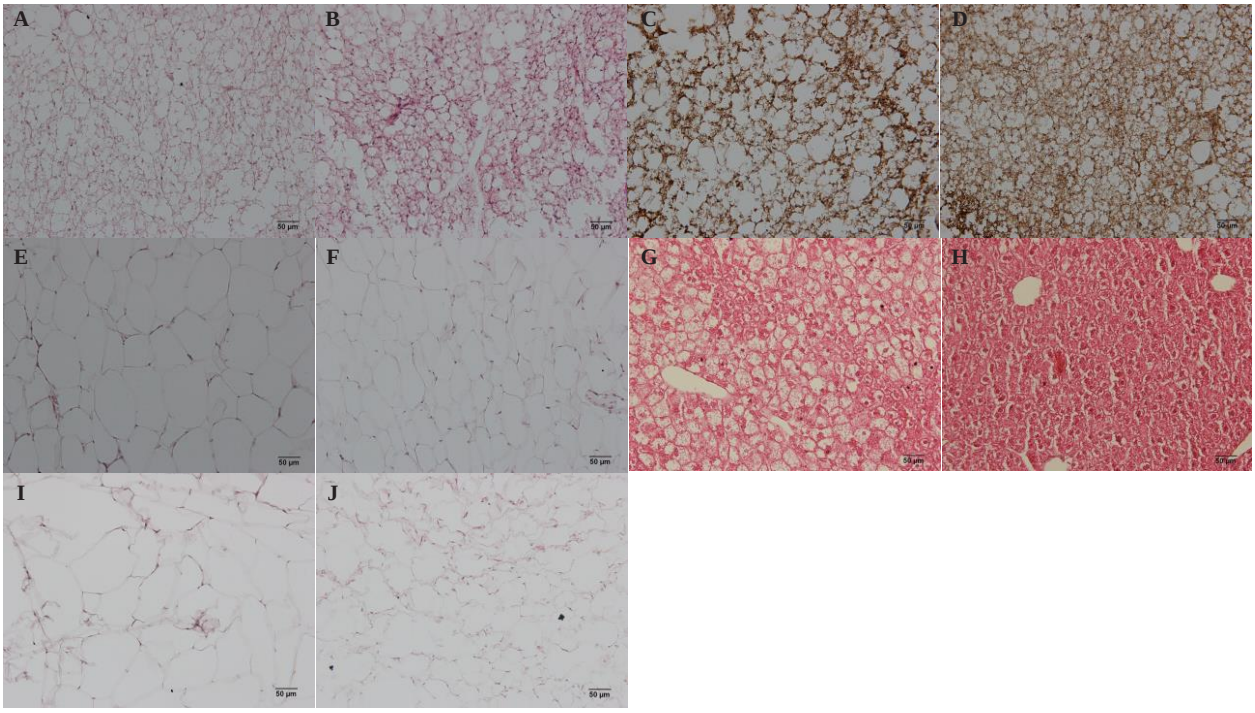


**Fig. 4.8**. 12 wk. HFD-fed H&E and UCP-1 IHC histological analysis. Representative images of H&E stained iBAT from f/f (A) and AGKO mice (B), and representative UCP-1 IHC iBAT images from f/f (C) and AGKO mice (D). Representative images of H&E stained eWAT from f/f (E) and AGKO mice (F), and H&E stained liver from f/f (G) and AGKO mice (H). H&E stained iWAT from f/f (I) and AGKO mice (J).

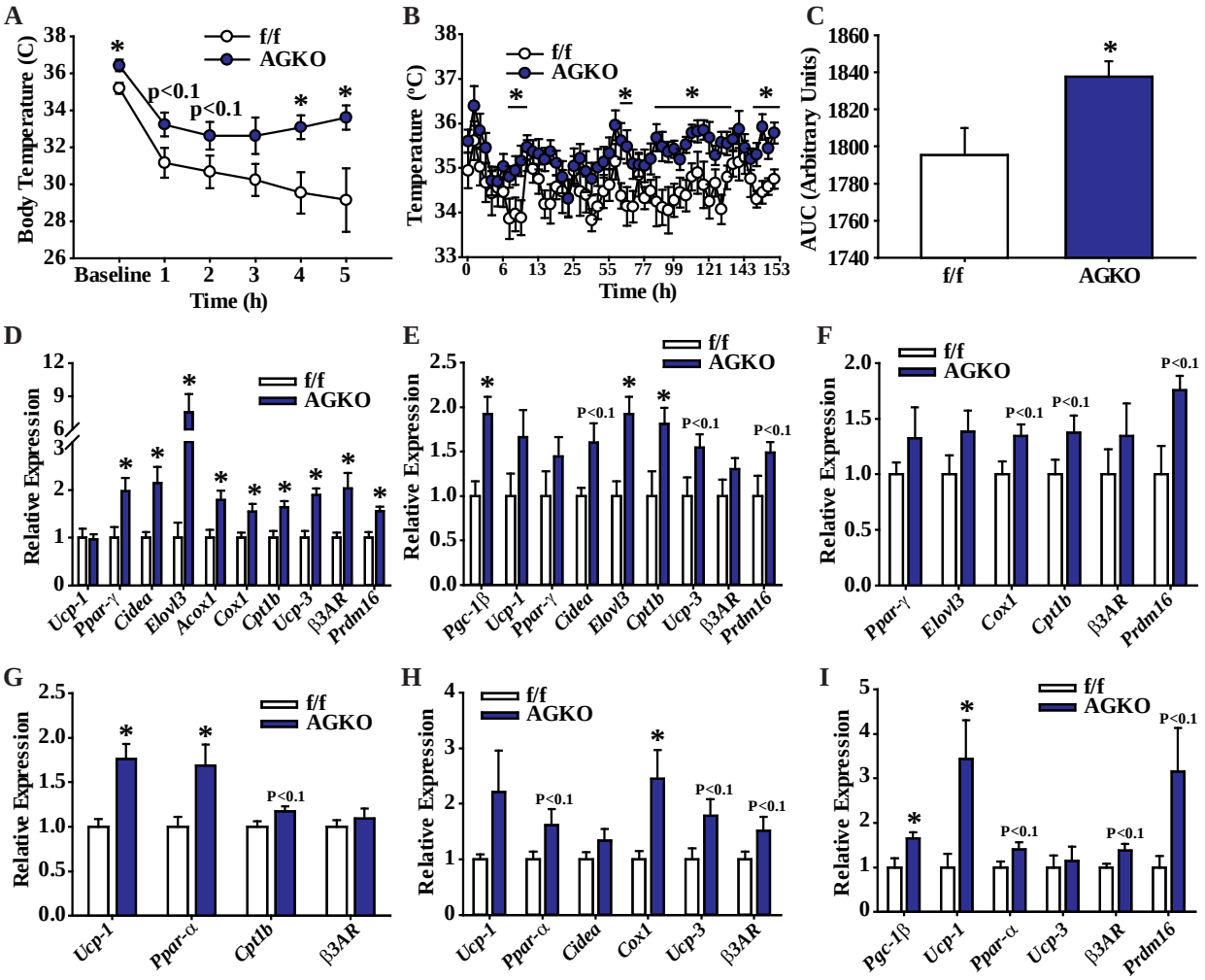


**Fig. 4.9** Sensory neuron GHSR knockout mice have increased cold tolerance.
Body temperature measurements in AGKO and WT mice following an acute 4°C cold challenge (A) (n=5-7 per group). Body temperature measurements in AGKO and WT mice following a 7 day 10°C cold challenge (B) and area under the curve values (C) (n=10 per group). Relative expression of thermogenic genes in iBAT (D), eWAT (E), and iWAT (F) for acute 4°C cold challenged AGKO and WT mice (n=5-7 per group). Relative expression of thermogenic genes in iBAT (G), eWAT (H), and iWAT (I) for 7 day 10°C cold challenged AGKO and WT mice (n=10 per group). Data reported as mean ± S.E.M. *P<0.5 vs. WT littermate control animals.

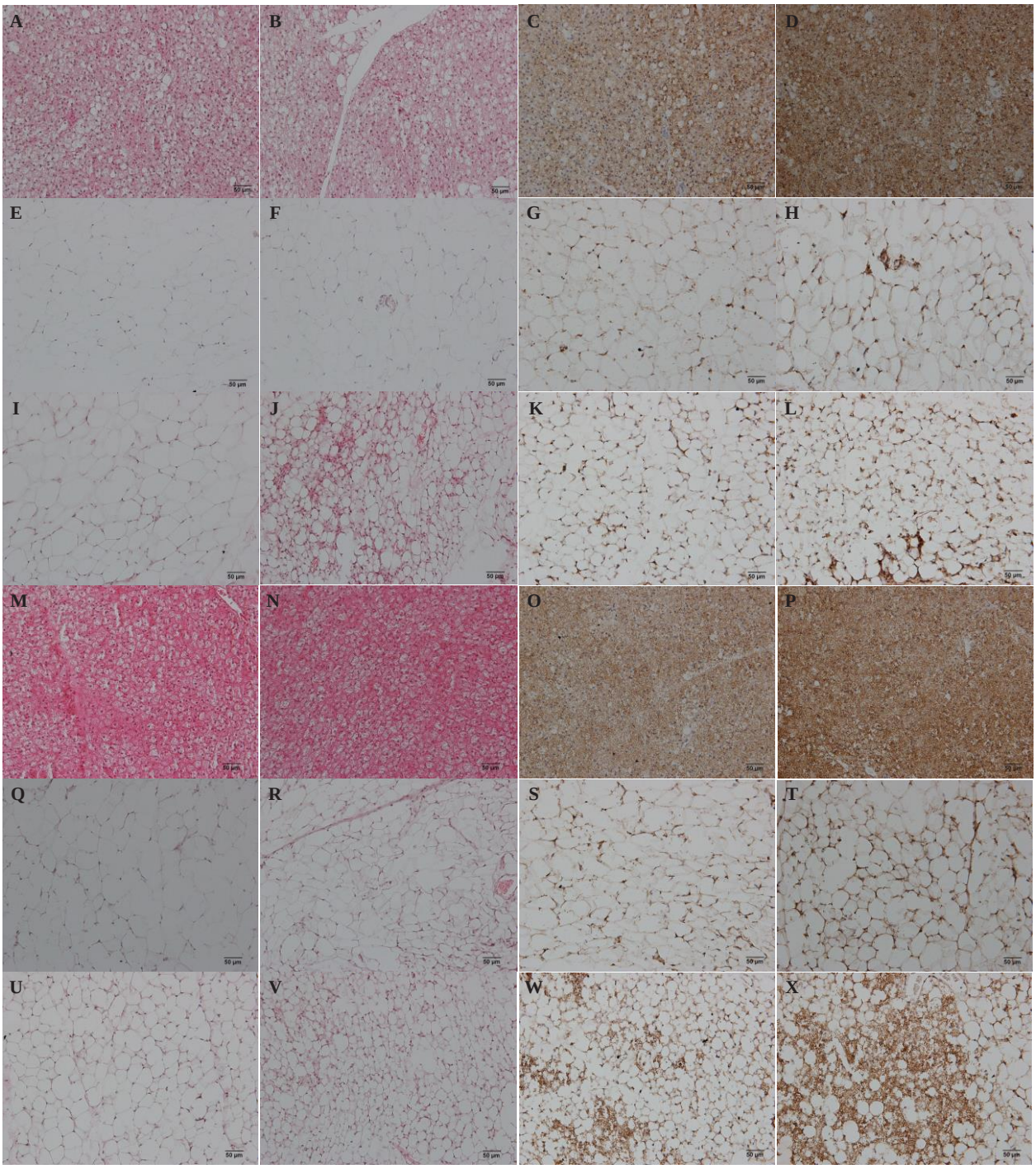


**Fig. 4.10.** 1 day and 7 day cold exposure H&E and UCP-1 IHC adipose tissue histology. Representative images of 1 day cold exposed H&E stained iBAT from f/f (A) and AGKO mice (B), and representative UCP-1 IHC iBAT images from 1 day cold exposed f/f (C) and AGKO mice (D). Representative images of H&E stained eWAT from 1 day cold exposed f/f (E) and AGKO mice (F), and representative UCP-1 IHC eWAT images from 1 day cold exposed f/f (G) and AGKO mice (H). Representative images of H&E stained iWAT from 1 day cold exposed f/f (I) and AGKO mice (J), and representative UCP-1 IHC iWAT images from 1 day cold

exposed f/f (K) and AGKO mice (L). Representative images of 7 day cold exposed H&E stained iBAT from f/f (A) and AGKO mice (B), and representative UCP-1 IHC iBAT images from 7 day cold exposed f/f (C) and AGKO mice (D). Representative images of H&E stained eWAT from 7 day cold exposed f/f (E) and AGKO mice (F), and representative UCP-1 IHC eWAT images from 7 day cold exposed f/f (G) and AGKO mice (H). Representative images of H&E stained iWAT from 7 day cold exposed f/f (I) and AGKO mice (J), and representative UCP-1 IHC iWAT images from 7 day cold exposed f/f (K) and AGKO mice (L).

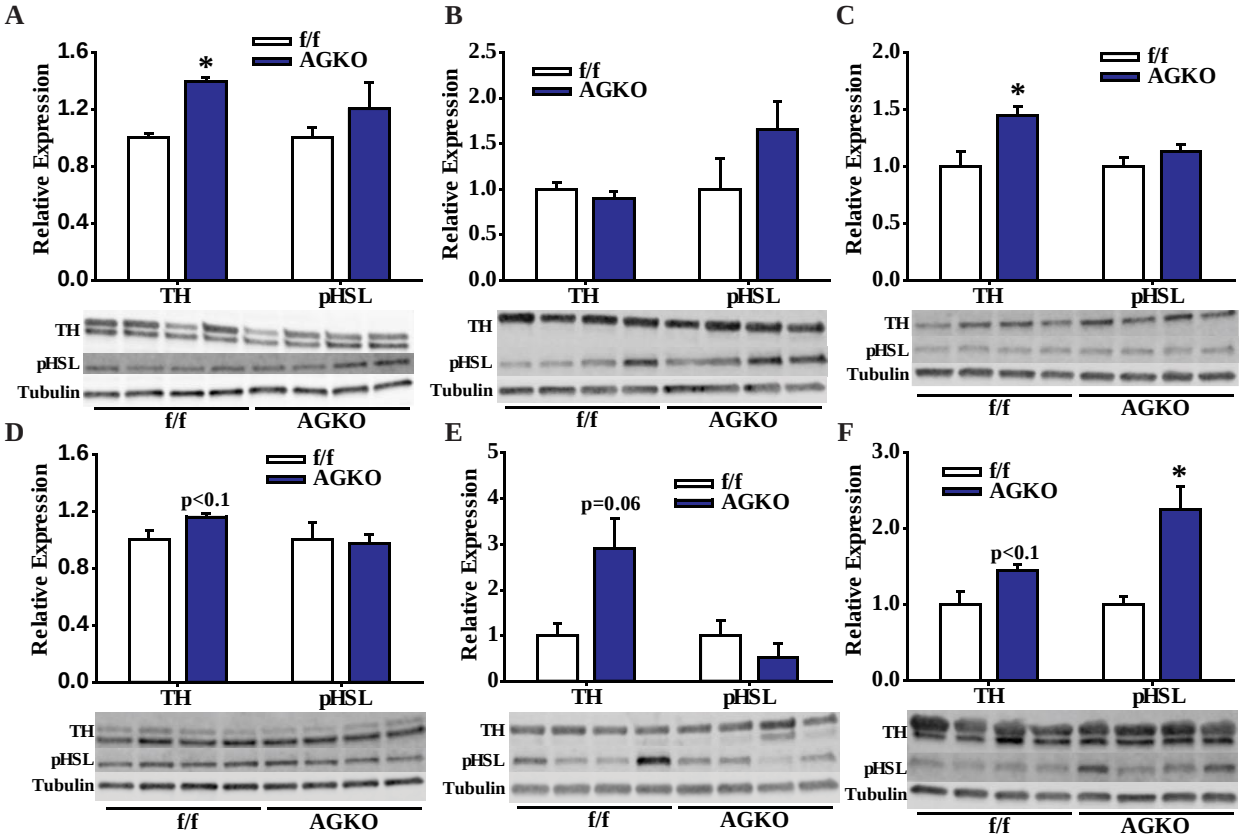


**Fig. 4.11** 1 day and 7 day adipose tissue western blot analysis.
Relative thermogenic protein content in iBAT (A), eWAT (B), and iWAT (C) for acute 4°C cold challenged AGKO and WT mice (n=5-7 per group). Relative thermogenic protein content in iBAT (D), eWAT (E), and iWAT (F) for 7 day 10°C cold challenged AGKO and WT mice (n=4 per group).

## 4.5 Discussion

In the current study, we have identified a novel ghrelin signaling mechanism through which peripheral sensory neurons mediate energy expenditure and adipose tissue metabolism independent of central GHSRs. While central GHSR signaling has been extensively studied, the

mechanisms through which ghrelin activates peripheral sensory neurons has received considerably less attention. We have identified here broad GHSR expression on DRGs that respond to ghrelin both in vitro and in vivo, and confirm previous reports demonstrating the presence of ghrelin responsive sensory neurons in the nodose ganglia. Many of these GHSR expressing DRG neurons project to the stomach and are activated by both food deprivation and cold exposure. Interrogating the physiological role of these neurons in the context of metabolic homeostasis necessitated the generation of a novel, sensory neuron specific GHSR knockout mouse. We crossed our sensory neuron specific *advillin-cre* mouse driver line with the newly developed $ghsr^{f/f}$ mouse to generate AGKO mice. These mice have increased energy expenditure, thermogenic capacity, and attenuated HFD-induced obesity. Collectively, our results demonstrate a novel mechanism through which ghrelin regulates whole body energy homeostasis.

Given the multitude of studies demonstrating ghrelin's role in obesity development and pathological conditions such as Prader-Willi Syndrome [25, 59-61], it is unsurprising ghrelin has emerged as an important regulator of metabolic homeostasis. Within the brain, GHSRs are expressed across the neuroaxis including on agouti-related protein/neuropeptide Y expressing neurons (AgRP neurons) in the hypothalamic arcuate nucleus (Arc) [16, 23]. Discrete AgRP neuron activation is sufficient to rapidly drive food intake [62], and ablation of these neurons in adults results in profound hypophagia [63, 64]. AgRP neurons can mediate ghrelin's orexigenic effects independent of other central nuclei or peripheral GHSR activation [65], and these neurons have been extensively studied in the context of ghrelin signaling and obesity development. However, GHSRs are also expressed on the vagus nerve and in numerous hindbrain nuclei involved in metabolic control including the dorsal motor vagus (DMV) and nucleus tractus

solitarius (NTS), and fourth ventricular ghrelin infusion is sufficient to drive food intake independent of forebrain nuclei [66-68]. The DMV and NTS receive significant peripheral sensory information from the vagus nerve and DRGs, and these nuclei are critical for modulating sympathetic outflow [69-72]. Vagal GHSRs were initially hypothesized to be necessary and sufficient to ghrelin signaling [41], yet subsequent studies in vagotomized animals found no change in, at the very least, ghrelin-induced food intake [73]. Our finding here that GHSRs are also expressed in DRGs, and that total sensory neuron GHSR deletion (i.e. on both vagal and DRGs) imparts a beneficial metabolic phenotype, suggests a possible DRG-involved compensatory mechanism that is sufficient to mediate ghrelin's peripheral effects independent of the vagus. Indeed, Dass et al. found that exogenous ghrelin elicits prokinetic activity in rat and human gastric preparations and hypothesized these effects are mediated by both vagal and enteric innervation [46].

The broad GHSR distribution on both vagal and DRG neurons strongly suggests the presence of parallel central and peripheral mechanisms regulating ghrelin's downstream effects on energy expenditure. Our finding that sensory neuron specific GHSR knockout attenuates DIO development furthers our understanding of ghrelin's role in obesity development, and complements previous studies showing global GHSR ablation affords similar obesity resistance and improved glycemic regulation. This improved insulin sensitivity and glucose disposal manifests as diabetes resistance in HFD-fed animals, yet the absence of ghrelin signaling in whole body GHSR knockout mice results in hypoglycemia during fasting [25, 74]. Selective GHSR restoration in AgRP neurons or hindbrain Phox2b expressing neurons restores fasting glucose levels suggesting these neurons are sufficient to mediate ghrelin's glucoregulatory effects [29, 75]. However, Phox2b is expressed in both hindbrain and peripheral sensory

neurons [76, 77], and it is therefore impossible to delineate the central or peripheral mechanism mediating this effect. Our results demonstrating that peripheral, sensory neuron specific GHSR knockout has no effect on fasting glucose levels in chow-fed animals would suggest the improved glucoregulation in Phox2b GHSR-restored mice involves a central mechanism. Because GHSRs are ablated in both DRG and vagal neurons, we hypothesize that neurons downstream of the DMV and NTS, including Arc AgRP neurons [10, 11, 78], regulate glucose metabolism. On the other hand, the mild improvement of insulin sensitivity in HFD-fed AGKO mice may be secondary to their protection from diet-induced obesity.

Previous GHSR knockout studies have shown that, despite comparable food intake to WT mice, obesity resistance is due to a marked upregulation in energy expenditure mediated by increased sympathetic outflow to adipose tissue [25, 27, 61]. The dissociation between ghrelin-induced food intake and augmented energy expenditure suggests discrete nuclei regulate these effects. To this end, adipose tissue sympathetic outflow neurons are found in numerous hindbrain and forebrain nuclei [11, 79], and many of these nuclei concurrently integrate peripheral sensory neuron information to regulate energy expenditure [10, 80]. We have identified here a novel peripheral GHSR signaling mechanism that functions to decrease energy expenditure, and we hypothesize this circuit elicits its effects through two possible mechanisms. First, ghrelin signaling on sensory neurons may decrease energy expenditure through short feedback loops at the level of the spinal column. In support of this, sensory-sympathetic cross talk at the level of the spinal cord exists in gastrointestinal system [81], and spinal column damage impairs normal gastric function despite intact vagal signaling [82]. Second, and more plausibly, ghrelin-mediated energy expenditure may be mediated through sensory integration in hindbrain nuclei. Previous work has demonstrated fourth ventricular ghrelin injections is

sufficient to decrease energy expenditure and elicit neuronal activity in several hindbrain nuclei that receive sensory neuron input including the DMV and NTS [66, 67]. As these neurons also send sympathetic projections to adipose tissue, it is likely that peripheral ghrelin signaling inhibits these neurons in WT animals. Hence, we find increased thermogenic gene expression in iBAT, eWAT, and iWAT pads in our AGKO knockout mice, possibly due to an upregulated sympathetic response, as shown by increased β3AR mRNA and TH protein levels. This upregulated energy expenditure paradigm following peripheral GHSR ablation is an important finding in the context of clinical approaches to combat obesity. Because our animals have normal glucose regulation and food intake while simultaneously resisting obesity, a treatment regimen targeting peripheral ghrelin signaling would prove beneficial as it has fewer side effects compared with non-specific GHSR antagonism and would circumvent the need to bypass the blood brain barrier. In turn, our results may provide a novel approach for obesity treatment.

The marked upregulation of thermogenic genes across iBAT, eWAT, and iWAT engender improved thermoregulation during an acute or chronic cold challenge and provides a mechanism for the elevated energy expenditure that attenuates obesity development. Although global and neuronal GHSR knockout mice have upregulated thermogenic genes in adipose tissues [25, 27, 74], to our knowledge this is the first demonstration that sensory neuron GHSR signaling functions to decrease expression of these genes. While the exact mechanism through which the absence of GHSR signaling increases adipose thermogenic gene expression necessitates further study, we propose a mechanism involving gut-brain crosstalk. We have shown here both vagal and DRG GHSR-positive neurons innervate the stomach and small intestine [**Fig. 1**], and nutrient activation of gut afferents is sufficient to increase iBAT temperature [9]. Because endogenous ghrelin signaling inhibits these enteric sensory neurons

[41, 83], it is likely that the absence of GHSRs results in a chronic, uninhibited afferent activity that drives adipose thermogenic gene expression. In addition, the same study found that NTS NMDA blockade inhibited this nutrient-induced increase in iBAT activity [9], and, given the colocalization of gastric afferents in the NTS, it is likely that GHSR activation of these neurons would similarly decrease glutamatergic NTS neuron activity.

In sum, our results demonstrate a novel peripheral ghrelin signaling pathway that responds to energetic challenges and regulates metabolic homeostasis. As this pathway is independent of central ghrelin signaling, it strongly suggests the presence of multiple ghrelin-involved mechanisms that regulate whole body energy homeostasis. Hence, peripheral ghrelin signal intervention may provide novel therapeutic approaches that increase basal energy expenditure and prevent or reverse obesity.

## 4.6 Acknowledgements

This research was supported by NIH R01DK107544, R01DK078358, R01DK035254, R01HL107500, and American Diabetes Association 1-18-IBS-260 to B.X., and NIH DK116425-02 to M.A.T.

## 4.7 Disclosures

The authors have nothing to disclose, financial or otherwise.

## 4.8 References

[1] James, W. P. Obesity-a modern pandemic: the burden of disease. Endocrinol Nutr. 2013,60 Suppl 1:3-6.

[2] Ogden, C. L., Yanovski, S. Z., Carroll, M. D., Flegal, K. M. The epidemiology of obesity. Gastroenterology. 2007,132:2087-102.

[3] Flegal, K. M. Epidemiologic aspects of overweight and obesity in the United States. Physiol Behav. 2005,86:599-602.

[4] Cawley, J., Meyerhoefer, C. The medical care costs of obesity: an instrumental variables approach. J Health Econ. 2012,31:219-30.

[5] Dockray, G. J. Gastrointestinal hormones and the dialogue between gut and brain. J Physiol. 2014,592:2927-41.

[6] Thomas, M. A., Tran, V., Ryu, V., Xue, B., Bartness, T. J. AgRP knockdown blocks long-term appetitive, but not consummatory, feeding behaviors in Siberian hamsters. Physiol Behav. 2018,190:61-70.

[7] Popovic, V., Duntas, L. H. Brain somatic cross-talk: ghrelin, leptin and ultimate challengers of obesity. Nutr Neurosci. 2005,8:1-5.

[8] Moran, T. H. Gut peptides in the control of food intake. Int.J Obes.(Lond). 2009,33 Suppl 1:S7-10.

[9] Blouet, C., Schwartz, G. J. Duodenal lipid sensing activates vagal afferents to regulate non-shivering brown fat thermogenesis in rats. PloS one. 2012,7:e51898.

[10] Ryu, V., Bartness, T. J. Short and long sympathetic-sensory feedback loops in white fat. Am.J.Physiol Regul.Integr.Comp Physiol. 2014.

[11] Nguyen, N. L., Barr, C. L., Ryu, V., Cao, Q., Xue, B., Bartness, T. J. Separate and shared sympathetic outflow to white and brown fat coordinately regulates thermoregulation and beige adipocyte recruitment. Am J Physiol Regul Integr Comp Physiol. 2017,312:R132-R45.

[12] Kojima, M., Hosoda, H., Date, Y., Nakazato, M., Matsuo, H., Kangawa, K. Ghrelin is a growth-hormone-releasing acylated peptide from stomach. Nature. 1999,402:656-60.

[13] Ariyasu, H., Takaya, K., Tagami, T., Ogawa, Y., Hosoda, K., Akamizu, T., et al. Stomach is a major source of circulating ghrelin, and feeding state determines plasma ghrelin-like immunoreactivity levels in humans. J.Clin.Endocrinol.Metab. 2001,86:4753-8.

[14] Tschop, M., Wawarta, R., Riepl, R. L., Friedrich, S., Bidlingmaier, M., Landgraf, R., et al. Post-prandial decrease of circulating human ghrelin levels. J.Endocrinol.Invest. 2001,24:RC19-RC21.

[15] Kim, M. S., Yoon, C. Y., Park, K. H., Shin, C. S., Park, K. S., Kim, S. Y., et al. Changes in ghrelin and ghrelin receptor expression according to feeding status. NeuroReport. 2003,14:1317-20.

[16] Kamegai, J., Tamura, H., Shimizu, T., Ishii, S., Sugihara, H., Wakabayashi, I. Central effect of ghrelin, an endogenous growth hormone secretagogue, on hypothalamic peptide gene expression. Endocrinology. 2000,141:4797-800.

[17] Thomas, M. A., Ryu, V., Bartness, T. J. Central ghrelin increases food foraging/hoarding that is blocked by GHSR antagonism and attenuates hypothalamic paraventricular nucleus neuronal activation. Am J Physiol Regul Integr Comp Physiol. 2015:ajpregu 00216 2015.

[18] Cowley, M. A., Smith, R. G., Diano, S., Tschop, M., Pronchuk, N., Grove, K. L., et al. The distribution and mechanism of action of ghrelin in the CNS demonstrates a novel hypothalamic circuit regulating energy homeostasis. Neuron. 2003,37:649-61.

[19] Huda, M. S., Dovey, T., Wong, S. P., English, P. J., Halford, J., McCulloch, P., et al. Ghrelin restores 'lean-type' hunger and energy expenditure profiles in morbidly obese subjects but has no effect on postgastrectomy subjects. Int.J Obes.(Lond). 2009,33:317-25.

[20] Tokizawa, K., Onoue, Y., Uchida, Y., Nagashima, K. Ghrelin induces time-dependent modulation of thermoregulation in the cold. Chronobiology international. 2012,29:736-46.

[21] Broglio, F., Arvat, E., Benso, A., Gottero, C., Muccioli, G., Papotti, M., et al. Ghrelin, a natural GH secretagogue produced by the stomach, induces hyperglycemia and reduces insulin secretion in humans. J Clin Endocrinol Metab. 2001,86:5083-6.

[22] Reimer, M. K., Pacini, G., Ahren, B. Dose-dependent inhibition by ghrelin of insulin secretion in the mouse. Endocrinology. 2003,144:916-21.

[23] Zigman, J. M., Jones, J. E., Lee, C. E., Saper, C. B., Elmquist, J. K. Expression of ghrelin receptor mRNA in the rat and the mouse brain. J.Comp Neurol. 2006,494:528-48.

[24] Ueberberg, B., Unger, N., Saeger, W., Mann, K., Petersenn, S. Expression of ghrelin and its receptor in human tissues. Horm Metab Res. 2009,41:814-21.

[25] Zigman, J. M., Nakano, Y., Coppari, R., Balthasar, N., Marcus, J. N., Lee, C. E., et al. Mice lacking ghrelin receptors resist the development of diet-induced obesity. J.Clin.Invest. 2005,115:3564-72.

[26] Wortley, K. E., Anderson, K. D., Garcia, K., Murray, J. D., Malinova, L., Liu, R., et al. Genetic deletion of ghrelin does not decrease food intake but influences metabolic fuel preference. Proc.Natl.Acad.Sci.U.S.A. 2004,101:8227-32.

[27] Lee, J. H., Lin, L., Xu, P., Saito, K., Wei, Q., Meadows, A. G., et al. Neuronal Deletion of Ghrelin Receptor Almost Completely Prevents Diet-Induced Obesity. Diabetes. 2016,65:2169-78.

[28] Dezaki, K., Sone, H., Koizumi, M., Nakata, M., Kakei, M., Nagai, H., et al. Blockade of pancreatic islet-derived ghrelin enhances insulin secretion to prevent high-fat diet-induced glucose intolerance. Diabetes. 2006,55:3486-93.

[29] Wang, Q., Liu, C., Uchida, A., Chuang, J. C., Walker, A., Liu, T., et al. Arcuate AgRP neurons mediate orexigenic and glucoregulatory actions of ghrelin. Mol.Metab. 2014,3:64-72.

[30] Craig, A. D. Interoception: the sense of the physiological condition of the body. Curr Opin Neurobiol. 2003,13:500-5.

[31] Mayer, E. A. Gut feelings: the emerging biology of gut-brain communication. Nat Rev Neurosci. 2011,12:453-66.

[32] Garretson, J. T., Szymanski, L. A., Schwartz, G. J., Xue, B., Ryu, V., Bartness, T. J. Lipolysis sensation by white fat afferent nerves triggers brown fat thermogenesis. Mol Metab. 2016,5:626-34.

[33] Hill, J. O., Wyatt, H. R., Peters, J. C. Energy balance and obesity. Circulation. 2012,126:126-32.

[34] Lee, J., Cummings, B. P., Martin, E., Sharp, J. W., Graham, J. L., Stanhope, K. L., et al. Glucose sensing by gut endocrine cells and activation of the vagal afferent pathway is impaired in a rodent model of type 2 diabetes mellitus. Am J Physiol Regul Integr Comp Physiol. 2012,302:R657-66.

[35] Naznin, F., Toshinai, K., Waise, T. M., NamKoong, C., Md Moin, A. S., Sakoda, H., et al. Diet-induced obesity causes peripheral and central ghrelin resistance by promoting inflammation. J Endocrinol. 2015,226:81-92.

[36] Cummings, D. E., Overduin, J. Gastrointestinal regulation of food intake. J Clin Invest. 2007,117:13-23.

[37] Geliebter, A. Gastric distension and gastric capacity in relation to food intake in humans. Physiol Behav. 1988,44:665-8.

[38] Yox, D. P., Brenner, L., Ritter, R. C. CCK-receptor antagonists attenuate suppression of sham feeding by intestinal nutrients. Am J Physiol. 1992,262:R554-61.

[39] van de Wall, E. H., Duffy, P., Ritter, R. C. CCK enhances response to gastric distension by acting on capsaicin-insensitive vagal afferents. Am J Physiol Regul Integr Comp Physiol. 2005,289:R695-703.

[40] Cui, X., Nguyen, N. L., Zarebidaki, E., Cao, Q., Li, F., Zha, L., et al. Thermoneutrality decreases thermogenic program and promotes adiposity in high-fat diet-fed mice. Physiological reports. 2016,4.

[41] Date, Y., Murakami, N., Toshinai, K., Matsukura, S., Niijima, A., Matsuo, H., et al. The role of the gastric afferent vagal nerve in ghrelin-induced feeding and growth hormone secretion in rats. Gastroenterology. 2002,123:1120-8.

[42] Le Roux, C. W., Neary, N. M., Halsey, T. J., Small, C. J., Martinez-Isla, A. M., Ghatei, M. A., et al. Ghrelin does not stimulate food intake in patients with surgical procedures involving vagotomy. J Clin Endocrinol.Metab. 2005,90:4521-4.

[43] Mano-Otagiri, A., Ohata, H., Iwasaki-Sekino, A., Nemoto, T., Shibasaki, T. Ghrelin suppresses noradrenaline release in the brown adipose tissue of rats. J.Endocrinol. 2009,201:341-9.

[44] Brookes, S. J., Spencer, N. J., Costa, M., Zagorodnyuk, V. P. Extrinsic primary afferent signalling in the gut. Nat Rev Gastroenterol Hepatol. 2013,10:286-96.

[45] Asakawa, A., Inui, A., Kaga, T., Yuzuriha, H., Nagata, T., Ueno, N., et al. Ghrelin is an appetite-stimulatory signal from stomach with structural resemblance to motilin. Gastroenterology. 2001,120:337-45.

[46] Dass, N. B., Munonyara, M., Bassil, A. K., Hervieu, G. J., Osbourne, S., Corcoran, S., et al. Growth hormone secretagogue receptors in rat and human gastrointestinal tract and the effects of ghrelin. Neuroscience. 2003,120:443-53.

[47] Cui, C., Ohnuma, H., Daimon, M., Susa, S., Yamaguchi, H., Kameda, W., et al. Ghrelin infused into the portal vein inhibits glucose-stimulated insulin secretion in Wistar rats. Peptides. 2008,29:1241-6.

[48] Romanovsky, A. A., Kulchitsky, V. A., Simons, C. T., Sugimoto, N., Szekely, M. Cold defense mechanisms in vagotomized rats. Am J Physiol. 1997,273:R784-9.

[49] Fukuda, H., Mizuta, Y., Isomoto, H., Takeshima, F., Ohnita, K., Ohba, K., et al. Ghrelin enhances gastric motility through direct stimulation of intrinsic neural pathways and capsaicin-sensitive afferent neurones in rats. Scand J Gastroenterol. 2004,39:1209-14.

[50] Cui, J., Zaror-Behrens, G., Himms-Hagen, J. Capsaicin desensitization induces atrophy of brown adipose tissue in rats. Am.J.Physiol. 1990,259:R324-R32.

[51] Cui, J., Himms-Hagen, J. Long-term decrease in body fat and in brown adipose tissue in capsaicin-desensitized rats. Am.J.Physiol. 1992,262:R568-R73.

[52] Jiang, H., Betancourt, L., Smith, R. G. Ghrelin amplifies dopamine signaling by cross talk involving formation of growth hormone secretagogue receptor/dopamine receptor subtype 1 heterodimers. Mol Endocrinol. 2006,20:1772-85.

[53] Zurborg, S., Piszczek, A., Martinez, C., Hublitz, P., Al Banchaabouchi, M., Moreira, P., et al. Generation and characterization of an Advillin-Cre driver mouse line. Mol Pain. 2011,7:66.

[54] Hasegawa, H., Abbott, S., Han, B. X., Qi, Y., Wang, F. Analyzing somatosensory axon projections with the sensory neuron-specific Advillin gene. J Neurosci. 2007,27:14404-14.

[55] Paxinos, G., Franklin, K. B. J. The Mouse Brain in Stereotaxic Coordinates. 2nd ed. New York: Academic Press; 2007.

[56] Livak, K. J., Schmittgen, T. D. Analysis of relative gene expression data using real-time quantitative PCR and the 2(-Delta Delta C(T)) Method. Methods. 2001,25:402-8.

[57] Tomasik, P. J., Sztefko, K., Pizon, M. The effect of short-term cold and hot exposure on total plasma ghrelin concentrations in humans. Horm Metab Res. 2005,37:189-90.

[58] Verbalis, J. G., Stricker, E. M., Robinson, A. G., Hoffman, G. E. Cholecystokinin activates cFos expression in hypothalamic oxytocin and corticotropin releasing hormone neurons. Journal of Neuroendocrinology. 1991,3:205-13.

[59] Cummings, D. E., Clement, K., Purnell, J. Q., Vaisse, C., Foster, K. E., Frayo, R. S., et al. Elevated plasma ghrelin levels in Prader Willi syndrome. Nat.Med. 2002,8:643-4.

[60] DelParigi, A., Tschop, M., Heiman, M. L., Salbe, A. D., Vozarova, B., Sell, S. M., et al. High circulating ghrelin: a potential cause for hyperphagia and obesity in prader-willi syndrome. J Clin.Endocrinol.Metab. 2002,87:5461-4.

[61] Pfluger, P. T., Kirchner, H., Gunnel, S., Schrott, B., Perez-Tilve, D., Fu, S., et al. Simultaneous deletion of ghrelin and its receptor increases motor activity and energy expenditure. Am.J.Physiol Gastrointest.Liver Physiol. 2008,294:G610-G8.

[62] Krashes, M. J., Koda, S., Ye, C., Rogan, S. C., Adams, A. C., Cusher, D. S., et al. Rapid, reversible activation of AgRP neurons drives feeding behavior in mice. J Clin.Invest. 2011,121:1424-8.

[63] Gropp, E., Shanabrough, M., Borok, E., Xu, A. W., Janoschek, R., Buch, T., et al. Agouti-related peptide-expressing neurons are mandatory for feeding. Nat.Neurosci. 2005,8:1289-91.

[64] Luquet, S., Perez, F. A., Hnasko, T. S., Palmiter, R. D. NPY/AgRP neurons are essential for feeding in adult mice but can be ablated in neonates. Science. 2005,310:683-5.

[65] Bagnasco, M., Tulipano, G., Melis, M. R., Argiolas, A., Cocchi, D., Muller, E. E. Endogenous ghrelin is an orexigenic peptide acting in the arcuate nucleus in response to fasting. Regul.Pept. 2003,111:161-7.

[66] Kinzig, K. P., Scott, K. A., Hyun, J., Bi, S., Moran, T. H. Lateral ventricular ghrelin and fourth ventricular ghrelin induce similar increases in food intake and patterns of

hypothalamic gene expression. Am.J Physiol Regul.Integr.Comp Physiol. 2006,290:R1565-R9.

[67] Faulconbridge, L. F., Grill, H. J., Kaplan, J. M., Daniels, D. Caudal brainstem delivery of ghrelin induces fos expression in the nucleus of the solitary tract, but not in the arcuate or paraventricular nuclei of the hypothalamus. Brain Research. 2008,1218:151-7.

[68] Faulconbridge, L. F., Cummings, D. E., Kaplan, J. M., Grill, H. J. Hyperphagic effects of brainstem ghrelin administration. Diabetes. 2003,52:2260-5.

[69] Rogers, R. C., Kita, H., Butcher, L. L., Novin, D. Afferent projections to the dorsal motor nucleus of the vagus. Brain Res.Bull. 1980,5:365-73.

[70] Kalia, M., Sullivan, J. M. Brainstem projections of sensory and motor components of the vagus nerve in the rat. J.Comp Neurol. 1982,211:248-65.

[71] Fyda, D. M., Cooper, K. E., Veale, W. L. Modulation of brown adipose tissue-mediated thermogenesis by lesions to the nucleus tractus solitarius in the rat. Brain Research. 1991,546:203-10.

[72] Olson, B. R., Freilino, M., Hoffman, G. E., Stricker, E. M., Sved, A. F., Verbalis, J. G. c-Fos Expression in Rat Brain and Brainstem Nuclei in Response to Treatments That Alter Food Intake and Gastric Motility. Mol.Cell Neurosci. 1993,4:93-106.

[73] Arnold, M., Mura, A., Geary, N., Langhans, W. Subdiaphragmatic vagal afferents are not necessary for the feeding-stimulatory effect of intraperitoneally administered ghrelin. 2004 Abstract Viewer/Itinerary Planner.Washington, DC: Society for Neuroscience (online). 2004:rogram.

[74] Sun, Y., Butte, N. F., Garcia, J. M., Smith, R. G. Characterization of adult ghrelin and ghrelin receptor knockout mice under positive and negative energy balance. Endocrinology. 2008,149:843-50.

[75] Scott, M. M., Perello, M., Chuang, J. C., Sakata, I., Gautron, L., Lee, C. E., et al. Hindbrain ghrelin receptor signaling is sufficient to maintain fasting glucose. PLoS.ONE. 2012,7:e44089.

[76] Young, H. M., Ciampoli, D., Hsuan, J., Canty, A. J. Expression of Ret-, p75(NTR)-, Phox2a-, Phox2b-, and tyrosine hydroxylase-immunoreactivity by undifferentiated neural crest-derived cells and different classes of enteric neurons in the embryonic mouse gut. Dev Dyn. 1999,216:137-52.

[77] Pattyn, A., Morin, X., Cremer, H., Goridis, C., Brunet, J. F. The homeobox gene Phox2b is essential for the development of autonomic neural crest derivatives. Nature. 1999,399:366-70.

[78] Bartness, T. J., Liu, Y., Shrestha, Y. B., Ryu, V. Neural innervation of white adipose tissue and the control of lipolysis. Front Neuroendocrinol. 2014,35:473-93.

[79] Bamshad, M., Aoki, V. T., Adkison, M. G., Warren, W. S., Bartness, T. J. Central nervous system origins of the sympathetic nervous system outflow to white adipose tissue. Am.J.Physiol. 1998,275:R291-R9.

[80] Bartness, T. J., Shrestha, Y. B., Vaughan, C. H., Schwartz, G. J., Song, C. K. Sensory and sympathetic nervous system control of white adipose tissue lipolysis. Mol.Cell Endocrinol. 2010,318:34-43.

[81] Browning, K. N., Travagli, R. A. Central nervous system control of gastrointestinal motility and secretion and modulation of gastrointestinal functions. Comprehensive Physiology. 2014,4:1339-68.

[82] Ebert, E. Gastrointestinal involvement in spinal cord injury: a clinical perspective. J Gastrointestin Liver Dis. 2012,21:75-82.

[83] de, L. G., Lur, G., Dimaline, R., Varro, A., Raybould, H., Dockray, G. J. EGR1 Is a target for cooperative interactions between cholecystokinin and leptin, and inhibition by ghrelin, in vagal afferent neurons. Endocrinology. 2010,151:3589-99.

## 5 CONCLUDING REMARKS

This dissertation serves as an important step forward in our understanding of how the orexigenic hormone ghrelin regulates whole body energy homeostasis. We approached these studies with a complementary focus on interrogating the behavioral and physiological mechanisms through which ghrelin mediates metabolism. We have expanded the known role of ghrelin in driving ingestive behaviors by demonstrating 1) central ghrelin signaling is necessary and sufficient to drive appetitive and consummatory behaviors, 2) central ghrelin acts through AgRP neurons to drive these behaviors, and 3) AgRP signaling is necessary for the long-term increases in food hoarding following an exogenous ghrelin challenge or fasting. Moreover, we have identified a novel peripheral sensory neuron ghrelin signaling pathway that is critical for metabolic regulation. The novelty of this work lies in the multifaceted behavior and physiology experimental paradigms that contrast with approaches aimed at a single outcome (e.g. food

intake). Hence, we have elucidated ghrelin's role in two discrete mechanisms that drive excessive weight gain.

Our finding that central GHSR activation is necessary and sufficient to drive ingestive behaviors and the chronic increases in food hoarding is regulated by AgRP peptide signaling complements previous studies in other laboratory rodent species [134, 180, 181]. The long-term behavioral adaptation in which animals, including humans, hoard food to prevent future caloric deficiencies is a major contributor to weight regain following dieting. Our results here serve as a critical step toward understanding the mechanism through which this is mediated. However, the downstream nuclei that regulate long-term food hoarding remain to be identified. AgRP neurons project to numerous nuclei involved in food intake and/or energy expenditure control [95], and advances in neuron specific circuit mapping is an attractive approach to interrogate the role of these projections in the context of appetitive behaviors. Discrete Arc→PVH projections are likely critical for driving food intake, and several studies have demonstrated selective activation of these projections drives food intake comparable to total AgRP neuronal activation [95]. We show here that central GHSR antagonism blocks appetitive and consummatory ingestive behaviors and PVH neuronal activity while leaving the Arc relatively unaffected [28]. Because redundant AgRP projections to downstream nuclei sufficient to drive food intake exist, it may be possible that non-PVH nuclei receiving AgRP neuron input are also sufficient to mediate other ingestive behaviors. Unfortunately, the genetic models required for neuron-specific mapping are available only in mice and, to a lesser extent, rats. It is therefore impossible to employ the spatial and temporal experimental resolution necessary to directly test this in Siberian hamsters.

In an evolutionary context, a dual physiological approach that simultaneously drives energy consumption and energy conservation would markedly increase an animal's survival

probability. However, these adaptive responses must be balanced as food foraging inherently requires energy expenditure. The mechanisms through which this balance is maintained and at what point animals stop appetitive behaviors in favor of conserving energy remains unclear, yet converging experimental and anecdotal evidence suggests unconstrained, elevated circulating ghrelin concentrations causes this switch. Central GHSR responsive neurons (i.e. within the Arc) may be more sensitive to circulating ghrelin or require significantly fewer neurons to be activated to elicit ingestive behaviors compared with peripheral GHSR neurons. Prolonged caloric restriction results in unimpeded stomach ghrelin production and AgRP neuron upregulation and may in turn reach a plateau at which point higher circulating ghrelin cannot further drive ingestive behaviors. Because GI-derived anorectic hormones that oppose ghrelin's peripheral sensory neuron effects would concurrently reach nadir, elevated ghrelin concentrations would maximally activate vagal and DRG sensory neurons causing a switch to energy conservation rather than ingestive behaviors. In support of this hypothesis, activation of as few as 400 AgRP neurons is sufficient to drive maximum food intake in mice [95], and we have observed very large ghrelin doses (~1mg/kg i.p.) cause Siberian hamsters to remain in their bottom hoarding cage rather than foraging for and gathering food for hoarding (Thomas and Bartness unpublished observations). By contrast, physiological ghrelin doses (~30 µg/kg i.p.) cause a robust increase in appetitive behaviors and drive long term behavioral adaptations [22, 28, 182]. Although the experimental and anecdotal evidence presented here would support this hypothesis, future work is clearly needed to fully elucidate this mechanism.

The presence of GHSRs on DRG and vagal neurons raises several important, unanswered questions. First, although DRG and vagal ghrelin signaling is necessary to mediate metabolic homeostasis, it is unclear how this information is integrated centrally and where any

hindbrain/forebrain crosstalk may or may not occur. Hindbrain nuclei including the NTS and DMV receive broad peripheral sensory neuron information from DRG and vagal sensory neurons, and these nuclei can elicit a metabolic response directly or relay this information to hypothalamic and forebrain nuclei for further processing [37, 39, 183-185]. In addition, these nuclei are integral in regulating sympathetic outflow to adipose tissues suggesting a possible mechanism through which sensory neuron ghrelin signaling can regulate adipose metabolism [38, 186-188]. These hindbrain nuclei may therefore serve to integrate peripheral GHSR signaling and then relay this information to other central nuclei or mount a metabolic response directly, and future work is needed to examine this hypothesis. Second, it is unclear if DRG and vagal sensory neurons act as redundant peripheral ghrelin signaling pathways or if they drive discrete metabolic effects. Previous work has demonstrated sensory neurons are critical for maintaining energy homeostasis and that non-vagal sensory neurons are sufficient to mediate ghrelin's effects on gastric motility, but whether or not this seemingly redundant mechanism exists in the NTS or DMV is unknown. Our novel AGKO mouse model is an important step towards understanding how peripheral sensory neurons regulate metabolic homeostasis, but because it inherently deletes GHSRs on all sensory neurons (i.e. both DRG and vagal) it is unable to differentiate the discrete role of these pathways. Moreover, we are presently unable to comment on any changes in hindbrain NTS/DMV crosstalk or downstream changes that could account for our observed phenotype.

In sum, our work presented here will serve as a foundation from which future studies can build upon to fully elucidate ghrelin's role in metabolic control. The diverse behavioral and physiological effects of ghrelin make it an attractive target for obesity reversal and prevention. By identifying the mechanism through which ghrelin drives acute and long-term changes in

appetitive and consummatory behaviors as well as how it regulates metabolism through peripheral signaling pathways, we have provided clinically relevant information that can be used to progress drug or behavioral therapies.

## REFERENCES

[1] Ng, M., Fleming, T., Robinson, M., Thomson, B., Graetz, N., Margono, C., et al. Global, regional, and national prevalence of overweight and obesity in children and adults during 1980-2013: a systematic analysis for the Global Burden of Disease Study 2013. Lancet. 2014,384:766-81.
[2] Finkelstein, E. A., Trogdon, J. G., Cohen, J. W., Dietz, W. Annual medical spending attributable to obesity: payer-and service-specific estimates. Health Aff.(Millwood.). 2009,28:822-31.
[3] Kojima, M., Hosoda, H., Date, Y., Nakazato, M., Matsuo, H., Kangawa, K. Ghrelin is a growth-hormone-releasing acylated peptide from stomach. Nature. 1999,402:656-60.
[4] Zhang, Y., Proenca, R., Maffei, M., Barone, M., Leopold, L., Friedman, J. M. Positional cloning of the mouse obese gene and its human homologue. Nature. 1994,372:425-32.
[5] Le, M. J., Devos, M. Metabolic correlates of the meal onset in the free food intake of rats. Physiol Behav. 1970,5:805-14.
[6] Bailey, C. J., Atkins, T. W., Conner, M. J., Manley, C. G., Matty, A. J. Diurnal variations of food consumption, plasma glucose and plasma insulin concentrations in lean and obese hyperglycaemic mice. Hormone Research. 1975,6:380-6.
[7] Ahlers, I., Ahlersova, E., Smajda, B., Sedlakova, A. Circadian rhythm of serum and tissue lipids in fed and fasted rats. Physiol Bohemoslov. 1980,29:525-33.
[8] Lu, X. Y., Shieh, K. R., Kabbaj, M., Barsh, G. S., Akil, H., Watson, S. J. Diurnal rhythm of agouti-related protein and its relation to corticosterone and food intake. Endocrinology. 2002,143:3905-15.
[9] Sanchez, J., Oliver, P., Pico, C., Palou, A. Diurnal rhythms of leptin and ghrelin in the systemic circulation and in the gastric mucosa are related to food intake in rats. Pflugers Arch. 2004,448:500-6.
[10] Buettner, C., Pocai, A., Muse, E. D., Etgen, A. M., Myers, M. G., Jr., Rossetti, L. Critical role of STAT3 in leptin's metabolic actions. Cell Metab. 2006,4:49-60.
[11] Scherer, T., O'hare, J., Diggs-Andrews, K., Schweiger, M., Cheng, B., Lindtner, C., et al. Brain insulin controls adipose tissue lipolysis and lipogenesis. Cell Metab. 2011,13:183-94.
[12] Jequier, E. Leptin signaling, adiposity, and energy balance. Ann.N.Y.Acad.Sci. 2002,967:379-88.
[13] Popovic, V., Duntas, L. H. Brain somatic cross-talk: ghrelin, leptin and ultimate challengers of obesity. Nutr Neurosci. 2005,8:1-5.
[14] Beneke, W. M., Davis, C. H. Relationship of hunger, use of a shopping list and obesity to food purchases. Int.J.Obes. 1985,9:391-9.
[15] Dodd, D. K., Stalling, R. B., Bedell, J. Grocery purchases as a function of obesity and assumed food deprivation. Int.J Obes. 1977,1:43-7.
[16] Mela, D. J., Aaron, J. I., Gatenby, S. J. Relationships of consumer characteristics and food deprivation to food purchasing behavior. Physiol Behav. 1996,60:1331-5.
[17] Ransley, J. K., Donnelly, J. K., Botham, H., Khara, T. N., Greenwood, D. C., Cade, J. E. Use of supermarket receipts to estimate energy and fat content of food purchased by lean and overweight families. Appetite. 2003,41:141-8.
[18] Betley, J. N., Xu, S., Cao, Z. F., Gong, R., Magnus, C. J., Yu, Y., et al. Neurons for hunger and thirst transmit a negative-valence teaching signal. Nature. 2015,521:180-5.
[19] Wood, A. D., Bartness, T. J. Food deprivation-induced increases in hoarding by Siberian hamsters are not photoperiod-dependent. Physiol Behav. 1996,60:1137-45.

[20] Woods, S. C., Decke, E., Vasselli, J. R. Metabolic hormones and regulation of body weight. Psychol.Rev. 1974,81:26-43.
[21] Atrens, D. M., Sinden, J. D., Penicaud, L., Devos, M., Magnen, J. Hypothalamic modulation of energy expenditure. Physiology and Behavior. 1985,35:15-20.
[22] Keen-Rhinehart, E., Bartness, T. J. Peripheral ghrelin injections stimulate food intake, foraging and food hoarding in Siberian hamsters. Am.J.Physiol. 2005,288:R716-R22.
[23] Keen-Rhinehart, E., Bartness, T. J. Leptin inhibits food-deprivation-induced increases in food intake and food hoarding. Am.J.Physiol Regul.Integr.Comp Physiol. 2008,295:R1737-R46.
[24] Asakawa, A., Inui, A., Yuzuriha, H., Ueno, N., Katsuura, G., Fujimiya, M., et al. Characterization of the effects of pancreatic polypeptide in the regulation of energy balance. Gastroenterology. 2003,124:1325-36.
[25] Lejeune, M. P., Westerterp, K. R., Adam, T. C., Luscombe-Marsh, N. D., Westerterp-Plantenga, M. S. Ghrelin and glucagon-like peptide 1 concentrations, 24-h satiety, and energy and substrate metabolism during a high-protein diet and measured in a respiration chamber. Am J Clin Nutr. 2006,83:89-94.
[26] Teubner, B. J., Bartness, T. J. PYY(3-36) into the arcuate nucleus inhibits food deprivation-induced increases in food hoarding and intake. Peptides. 2013,47:20-8.
[27] Kamegai, J., Tamura, H., Shimizu, T., Ishii, S., Sugihara, H., Wakabayashi, I. Central effect of ghrelin, an endogenous growth hormone secretagogue, on hypothalamic peptide gene expression. Endocrinology. 2000,141:4797-800.
[28] Thomas, M. A., Ryu, V., Bartness, T. J. Central ghrelin increases food foraging/hoarding that is blocked by GHSR antagonism and attenuates hypothalamic paraventricular nucleus neuronal activation. Am J Physiol Regul Integr Comp Physiol. 2015:ajpregu 00216 2015.
[29] Cowley, M. A., Smith, R. G., Diano, S., Tschop, M., Pronchuk, N., Grove, K. L., et al. The distribution and mechanism of action of ghrelin in the CNS demonstrates a novel hypothalamic circuit regulating energy homeostasis. Neuron. 2003,37:649-61.
[30] Huda, M. S., Dovey, T., Wong, S. P., English, P. J., Halford, J., McCulloch, P., et al. Ghrelin restores 'lean-type' hunger and energy expenditure profiles in morbidly obese subjects but has no effect on postgastrectomy subjects. Int.J Obes.(Lond). 2009,33:317-25.
[31] Tokizawa, K., Onoue, Y., Uchida, Y., Nagashima, K. Ghrelin induces time-dependent modulation of thermoregulation in the cold. Chronobiology international. 2012,29:736-46.
[32] Billington, C. J., Bartness, T. J., Briggs, J., Levine, A. S., Morley, J. E. Glucagon stimulation of brown adipose tissue growth and thermogenesis. Am.J.Physiol. 1987,252:R160-R5.
[33] Youngstrom, T. G., Bartness, T. J. Catecholaminergic innervation of white adipose tissue in the Siberian hamster. Am.J.Physiol. 1995,268:R744-R51.
[34] Murphy, K. T., Schwartz, G. J., Nguyen, N. L., Mendez, J. M., Ryu, V., Bartness, T. J. Leptin-sensitive sensory nerves innervate white fat. Am.J.Physiol Endocrinol.Metab. 2013,304:E1338-E47.
[35] Yasuda, T., Masaki, T., Kakuma, T., Yoshimatsu, H. Centrally administered ghrelin suppresses sympathetic nerve activity in brown adipose tissue of rats. Neuroscience Letters. 2003,349:75-8.
[36] Minokoshi, Y., Alquier, T., Furukawa, N., Kim, Y. B., Lee, A., Xue, B., et al. AMP-kinase regulates food intake by responding to hormonal and nutrient signals in the hypothalamus. Nature. 2004,428:569-74.

[37] Bamshad, M., Aoki, V. T., Adkison, M. G., Warren, W. S., Bartness, T. J. Central nervous system origins of the sympathetic nervous system outflow to white adipose tissue. Am.J.Physiol. 1998,275:R291-R9.
[38] Youngstrom, T. G., Bartness, T. J. White adipose tissue sympathetic nervous system denervation increases fat pad mass and fat cell number. Am.J.Physiol. 1998,275:R1488-R93.
[39] Bowers, R. R., Festuccia, W. T. L., Song, C. K., Shi, H., Migliorini, R. H., Bartness, T. J. Sympathetic innervation of white adipose tissue and its regulation of fat cell number. Am.J.Physiol. 2004,286:R1167-R75.
[40] Landsberg, L., Young, J. B. The role of the sympathoadrenal system in modulating energy expenditure. Clin.Endocrinol.Metab. 1984,13:475-99.
[41] Astrup, A. Thermogenesis in human brown adipose tissue and skeletal muscle induced by sympathomimetic stimulation. Acta Endocrinol.Suppl (Copenh). 1986,278:1-32.
[42] Amir, S. Stimulation of the paraventricular nucleus with glutamate activates interscapular brown adipose tissue thermogenesis in rats. Brain Research. 1990,508:152-5.
[43] Cui, X., Nguyen, N. L., Zarebidaki, E., Cao, Q., Li, F., Zha, L., et al. Thermoneutrality decreases thermogenic program and promotes adiposity in high-fat diet-fed mice. Physiological reports. 2016,4.
[44] Nakazato, M., Murakami, N., Date, Y., Kojima, M., Matsuo, H., Kangawa, K., et al. A role for ghrelin in the central regulation of feeding. Nature. 2001,409:194-8.
[45] Date, Y., Nakazato, M., Murakami, N., Kojima, M., Kangawa, K., Matsukura, S. Ghrelin acts in the central nervous system to stimulate gastric acid secretion. Biochem.Biophys.Res.Commun. 2001,280:904-7.
[46] Hosoda, H., Kojima, M., Kangawa, K. Ghrelin and the regulation of food intake and energy balance. Mol.Interv. 2002,2:494-503.
[47] Lawrence, C. B., Snape, A. C., Baudoin, F. M., Luckman, S. M. Acute central ghrelin and GH secretagogues induce feeding and activate brain appetite centers. Endocrinology. 2002,143:155-62.
[48] Panksepp, J. Central metabolic and humoral factors involved in the neural regulation of feeding. Pharmacology,Biochemistry,and Behavior. 1975,3:107-19.
[49] Sclafani, A., Kirchgessner, A. L. The role of the medial hypothalamus in the control of food intake: An update. In: Ritter RC, Ritter S, Barnes CD, eds. Feeding Behavior: Neural and Humoral Controls. Orlando, FL: Academic Press; 1986. p. 27-66.
[50] Palkovits, M. Hypothalamic regulation of the food intake. Ideggyogy.Sz. 2003,56:288-302.
[51] Schwartz, G. J. Brainstem integrative function in the central nervous system control of food intake. Forum Nutr. 2010,63:141-51.
[52] Cone, R. D., Cowley, M. A., Butler, A. A., Fan, W., Marks, D. L., Low, M. J. The arcuate nucleus as a conduit for diverse signals relevant to energy homeostasis. Int.J Obes.Relat Metab Disord. 2001,25 Suppl 5:S63-S7.
[53] Barth, S. W., Riediger, T., Lutz, T. A., Rechkemmer, G. Peripheral amylin activates circumventricular organs expressing calcitonin receptor a/b subtypes and receptor-activity modifying proteins in the rat. Brain Research. 2004,997:97-102.
[54] Dumont, Y., Moyse, E., Fournier, A., Quirion, R. Distribution of peripherally injected peptide YY ([125I] PYY (3-36)) and pancreatic polypeptide ([125I] hPP) in the CNS: enrichment in the area postrema. J.Mol.Neurosci. 2007,33:294-304.
[55] Lin, Y., Matsumura, K., Fukuhara, M., Kagiyama, S., Fujii, K., Iida, M. Ghrelin acts at the nucleus of the solitary tract to decrease arterial pressure in rats. Hypertension. 2004,43:977-82.

[56] Miceli, M. O. Abdominal vagus and regulation of ingestive behavior and body weight in golden hamsters. Am.J.Physiol. 1985,248:R686-R97.
[57] Date, Y., Murakami, N., Toshinai, K., Matsukura, S., Niijima, A., Matsuo, H., et al. The role of the gastric afferent vagal nerve in ghrelin-induced feeding and growth hormone secretion in rats. Gastroenterology. 2002,123:1120-8.
[58] Koda, S., Date, Y., Murakami, N., Shimbara, T., Hanada, T., Toshinai, K., et al. The role of the vagal nerve in peripheral PYY3-36-induced feeding reduction in rats. Endocrinology. 2005,146:2369-75.
[59] Brookes, S. J., Spencer, N. J., Costa, M., Zagorodnyuk, V. P. Extrinsic primary afferent signalling in the gut. Nat Rev Gastroenterol Hepatol. 2013,10:286-96.
[60] Yox, D. P., Brenner, L., Ritter, R. C. CCK-receptor antagonists attenuate suppression of sham feeding by intestinal nutrients. Am J Physiol. 1992,262:R554-61.
[61] van de Wall, E. H., Duffy, P., Ritter, R. C. CCK enhances response to gastric distension by acting on capsaicin-insensitive vagal afferents. Am J Physiol Regul Integr Comp Physiol. 2005,289:R695-703.
[62] Blouet, C., Schwartz, G. J. Duodenal lipid sensing activates vagal afferents to regulate non-shivering brown fat thermogenesis in rats. PloS one. 2012,7:e51898.
[63] Rogers, R. C., Kita, H., Butcher, L. L., Novin, D. Afferent projections to the dorsal motor nucleus of the vagus. Brain Res.Bull. 1980,5:365-73.
[64] Bernardis, L. L. The dorsomedial hypothalamic nucleus in autonomic and neuroendocrine homeostasis. Can.J Neurol.Sci. 1975,2:45-60.
[65] Swanson, L. W., Kuypers, H. G. The paraventricular nucleus of the hypothalamus: cytoarchitectonic subdivisions and organization of projections to the pituitary, dorsal vagal complex, and spinal cord as demonstrated by retrograde fluorescence double-labeling methods. J Comp Neurol. 1980,194:555-70.
[66] Kirchgessner, A. L., Sclafani, A. Histochemical identification of a PVN-hindbrain feeding pathway. Physiology and Behavior. 1988,42:529-43.
[67] Kinzig, K. P., Scott, K. A., Hyun, J., Bi, S., Moran, T. H. Lateral ventricular ghrelin and fourth ventricular ghrelin induce similar increases in food intake and patterns of hypothalamic gene expression. Am.J Physiol Regul.Integr.Comp Physiol. 2006,290:R1565-R9.
[68] Faulconbridge, L. F., Grill, H. J., Kaplan, J. M., Daniels, D. Caudal brainstem delivery of ghrelin induces fos expression in the nucleus of the solitary tract, but not in the arcuate or paraventricular nuclei of the hypothalamus. Brain Research. 2008,1218:151-7.
[69] Emanuel, A. J., Ritter, S. Hindbrain catecholamine neurons modulate the growth hormone but not the feeding response to ghrelin. Endocrinology. 2010,151:3237-46.
[70] Scott, M. M., Perello, M., Chuang, J. C., Sakata, I., Gautron, L., Lee, C. E., et al. Hindbrain ghrelin receptor signaling is sufficient to maintain fasting glucose. PLoS.ONE. 2012,7:e44089.
[71] Traebert, M., Riediger, T., Whitebread, S., Scharrer, E., Schmid, H. A. Ghrelin acts on leptin-responsive neurones in the rat arcuate nucleus. J.Neuroendocrinol. 2002,14:580-6.
[72] Olszewski, P. K., Grace, M. K., Billington, C. J., Levine, A. S. Hypothalamic paraventricular injections of ghrelin: effect on feeding and c-Fos immunoreactivity. Peptides. 2003,24:919-23.
[73] Farooqi, I. S., Keogh, J. M., Yeo, G. S., Lank, E. J., Cheetham, T., O'Rahilly, S. Clinical spectrum of obesity and mutations in the melanocortin 4 receptor gene. N.Engl.J.Med. 2003,348:1085-95.

[74] Masuda, A., Oishi, T. Effects of photoperiod and temperature on body weight, food intake, food storage, and pelage color in Djungarian hamster, Phodopus sungorus. Journal of Experimental Zoology. 1988,248:133-9.
[75] Vander Wall, S. B. Food hoarding in animals. Chicago: Univ. Chicago Press; 1990.
[76] Bartness, T. J., Clein, M. R. Effects of food deprivation and restriction, and metabolic blockers on food hoarding in Siberian hamsters. Am.J.Physiol. 1994,266:R1111-R7.
[77] Bartness, T. J., Demas, G. E. Comparative studies of food intake: Lessons from non-traditionally studied species. In: Stricker EM, Woods SC, eds. Food and Fluid Intake. New York: Plenum; 2004. p. 423-67.
[78] Day, D. E., Bartness, T. J. Fasting-induced increases in hoarding are dependent on the foraging effort level. Physiology and Behavior. 2003,78:655-68.
[79] Day, D. E., Bartness, T. J. Effects of foraging effort on body fat and food hoarding by Siberian hamsters. J.Exp.Zool. 2001,289:162-71.
[80] Date, Y., Kojima, M., Hosoda, H., Sawaguchi, A., Mondal, M. S., Suganuma, T., et al. Ghrelin, a novel growth hormone-releasing acylated peptide, is synthesized in a distinct endocrine cell type in the gastrointestinal tracts of rats and humans. Endocrinology. 2000,141:4255-61.
[81] Wren, A. M., Small, C. J., Ward, H. L., Murphy, K. G., Dakin, C. L., Taheri, S., et al. The novel hypothalamic peptide ghrelin stimulates food intake and growth hormone secretion. Endocrinology. 2000,141:4325-8.
[82] Gutierrez, J. A., Solenberg, P. J., Perkins, D. R., Willency, J. A., Knierman, M. D., Jin, Z., et al. Ghrelin octanoylation mediated by an orphan lipid transferase. Proc.Natl.Acad.Sci.U.S.A. 2008,105:6320-5.
[83] Muller, T. D., Nogueiras, R., Andermann, M. L., Andrews, Z. B., Anker, S. D., Argente, J., et al. Ghrelin. Mol Metab. 2015,4:437-60.
[84] Ariyasu, H., Takaya, K., Tagami, T., Ogawa, Y., Hosoda, K., Akamizu, T., et al. Stomach is a major source of circulating ghrelin, and feeding state determines plasma ghrelin-like immunoreactivity levels in humans. J.Clin.Endocrinol.Metab. 2001,86:4753-8.
[85] Tschop, M., Wawarta, R., Riepl, R. L., Friedrich, S., Bidlingmaier, M., Landgraf, R., et al. Post-prandial decrease of circulating human ghrelin levels. J.Endocrinol.Invest. 2001,24:RC19-RC21.
[86] Dimitropoulos, A., Feurer, I. D., Roof, E., Stone, W., Butler, M. G., Sutcliffe, J., et al. Appetitive behavior, compulsivity, and neurochemistry in Prader-Willi syndrome. Ment.Retard.Dev.Disabil.Res.Rev. 2000,6:125-30.
[87] DelParigi, A., Tschop, M., Heiman, M. L., Salbe, A. D., Vozarova, B., Sell, S. M., et al. High circulating ghrelin: a potential cause for hyperphagia and obesity in prader-willi syndrome. J Clin.Endocrinol.Metab. 2002,87:5461-4.
[88] Cummings, D. E., Purnell, J. Q., Frayo, R. S., Schmidova, K., Wisse, B. E., Weigle, D. S. A preprandial rise in plasma ghrelin levels suggests a role in meal initiation in humans. Diabetes. 2001,50:1714-9.
[89] Yang, J., Brown, M. S., Liang, G., Grishin, N. V., Goldstein, J. L. Identification of the acyltransferase that octanoylates ghrelin, an appetite-stimulating peptide hormone. Cell. 2008,132:387-96.
[90] Teubner, B. J., Bartness, T. J. Anti-ghrelin Spiegelmer inhibits exogenous ghrelin-induced increases in food intake, hoarding, and neural activation, but not food deprivation-induced increases. Am.J.Physiol Regul.Integr.Comp Physiol. 2013,305:R323-R33.

[91] Teubner, B. J., Garretson, J. T., Hwang, Y., Cole, P. A., Bartness, T. J. Inhibition of ghrelin O-acyltransferase attenuates food deprivation-induced increases in ingestive behavior. Horm.Behav. 2013,63:667-73.
[92] Barnett, B. P., Hwang, Y., Taylor, M. S., Kirchner, H., Pfluger, P. T., Bernard, V., et al. Glucose and weight control in mice with a designed ghrelin O-acyltransferase inhibitor. Science. 2010,330:1689-92.
[93] Theander-Carrillo, C., Wiedmer, P., Cettour-Rose, P., Nogueiras, R., Perez-Tilve, D., Pfluger, P., et al. Ghrelin action in the brain controls adipocyte metabolism. J Clin.Invest. 2006,116:1983-93.
[94] Reimer, M. K., Pacini, G., Ahren, B. Dose-dependent inhibition by ghrelin of insulin secretion in the mouse. Endocrinology. 2003,144:916-21.
[95] Betley, J. N., Cao, Z. F., Ritola, K. D., Sternson, S. M. Parallel, redundant circuit organization for homeostatic control of feeding behavior. Cell. 2013,155:1337-50.
[96] Kim, M. S., Yoon, C. Y., Park, K. H., Shin, C. S., Park, K. S., Kim, S. Y., et al. Changes in ghrelin and ghrelin receptor expression according to feeding status. NeuroReport. 2003,14:1317-20.
[97] Tups, A., Helwig, M., Khorooshi, R. M., Archer, Z. A., Klingenspor, M., Mercer, J. G. Circulating ghrelin levels and central ghrelin receptor expression are elevated in response to food deprivation in a seasonal mammal (Phodopus sungorus). J.Neuroendocrinol. 2004,16:922-8.
[98] Zigman, J. M., Jones, J. E., Lee, C. E., Saper, C. B., Elmquist, J. K. Expression of ghrelin receptor mRNA in the rat and the mouse brain. J.Comp Neurol. 2006,494:528-48.
[99] Ueberberg, B., Unger, N., Saeger, W., Mann, K., Petersenn, S. Expression of ghrelin and its receptor in human tissues. Horm Metab Res. 2009,41:814-21.
[100] Sun, Y., Wang, P., Zheng, H., Smith, R. G. Ghrelin stimulation of growth hormone release and appetite is mediated through the growth hormone secretagogue receptor. Proc.Natl.Acad.Sci.U.S.A. 2004,101:4679-84.
[101] Shrestha, Y. B., Wickwire, K., Giraudo, S. Effect of reducing hypothalamic ghrelin receptor gene expression on energy balance. Peptides. 2009,30:1336-41.
[102] Holubova, M., Spolcova, A., Demianova, Z., Sykora, D., Fehrentz, J. A., Martinez, J., et al. Ghrelin agonist JMV 1843 increases food intake, body weight and expression of orexigenic neuropeptides in mice. Physiol Res. 2013,62:435-44.
[103] Ramirez, V. T., van Oeffelen, W., Torres-Fuentes, C., Chruscicka, B., Druelle, C., Golubeva, A. V., et al. Differential functional selectivity and downstream signaling bias of ghrelin receptor antagonists and inverse agonists. FASEB J. 2018:fj201800655R.
[104] Salome, N., Hansson, C., Taube, M., Gustafsson-Ericson, L., Egecioglu, E., Karlsson-Lindahl, L., et al. On the central mechanism underlying ghrelin's chronic pro-obesity effects in rats: new insights from studies exploiting a potent ghrelin receptor antagonist. J Neuroendocrinol. 2009,21:777-85.
[105] Skibicka, K. P., Hansson, C., Egecioglu, E., Dickson, S. L. Role of ghrelin in food reward: impact of ghrelin on sucrose self-administration and mesolimbic dopamine and acetylcholine receptor gene expression. Addict.Biol. 2011.
[106] Skibicka, K. P., Hansson, C., Alvarez-Crespo, M., Friberg, P. A., Dickson, S. L. Ghrelin directly targets the ventral tegmental area to increase food motivation. Neuroscience. 2011,180:129-37.

[107] Lee, J. H., Lin, L., Xu, P., Saito, K., Wei, Q., Meadows, A. G., et al. Neuronal Deletion of Ghrelin Receptor Almost Completely Prevents Diet-Induced Obesity. Diabetes. 2016,65:2169-78.
[108] Wortley, K. E., del Rincon, J. P., Murray, J. D., Garcia, K., Iida, K., Thorner, M. O., et al. Absence of ghrelin protects against early-onset obesity. J Clin Invest. 2005,115:3573-8.
[109] Sun, Y., Butte, N. F., Garcia, J. M., Smith, R. G. Characterization of adult ghrelin and ghrelin receptor knockout mice under positive and negative energy balance. Endocrinology. 2008,149:843-50.
[110] Wang, Q., Liu, C., Uchida, A., Chuang, J. C., Walker, A., Liu, T., et al. Arcuate AgRP neurons mediate orexigenic and glucoregulatory actions of ghrelin. Mol.Metab. 2014,3:64-72.
[111] Young, H. M., Ciampoli, D., Hsuan, J., Canty, A. J. Expression of Ret-, p75(NTR)-, Phox2a-, Phox2b-, and tyrosine hydroxylase-immunoreactivity by undifferentiated neural crest-derived cells and different classes of enteric neurons in the embryonic mouse gut. Dev Dyn. 1999,216:137-52.
[112] Pattyn, A., Morin, X., Cremer, H., Goridis, C., Brunet, J. F. The homeobox gene Phox2b is essential for the development of autonomic neural crest derivatives. Nature. 1999,399:366-70.
[113] Zhang, W., Lin, T. R., Hu, Y., Fan, Y., Zhao, L., Stuenkel, E. L., et al. Ghrelin stimulates neurogenesis in the dorsal motor nucleus of the vagus. J.Physiol. 2004,559:729-37.
[114] Le Roux, C. W., Neary, N. M., Halsey, T. J., Small, C. J., Martinez-Isla, A. M., Ghatei, M. A., et al. Ghrelin does not stimulate food intake in patients with surgical procedures involving vagotomy. J Clin Endocrinol.Metab. 2005,90:4521-4.
[115] Mano-Otagiri, A., Ohata, H., Iwasaki-Sekino, A., Nemoto, T., Shibasaki, T. Ghrelin suppresses noradrenaline release in the brown adipose tissue of rats. J.Endocrinol. 2009,201:341-9.
[116] Asakawa, A., Inui, A., Kaga, T., Yuzuriha, H., Nagata, T., Ueno, N., et al. Ghrelin is an appetite-stimulatory signal from stomach with structural resemblance to motilin. Gastroenterology. 2001,120:337-45.
[117] Dass, N. B., Munonyara, M., Bassil, A. K., Hervieu, G. J., Osbourne, S., Corcoran, S., et al. Growth hormone secretagogue receptors in rat and human gastrointestinal tract and the effects of ghrelin. Neuroscience. 2003,120:443-53.
[118] Cui, C., Ohnuma, H., Daimon, M., Susa, S., Yamaguchi, H., Kameda, W., et al. Ghrelin infused into the portal vein inhibits glucose-stimulated insulin secretion in Wistar rats. Peptides. 2008,29:1241-6.
[119] Romanovsky, A. A., Kulchitsky, V. A., Simons, C. T., Sugimoto, N., Szekely, M. Cold defense mechanisms in vagotomized rats. Am J Physiol. 1997,273:R784-9.
[120] Mani, B. K., Walker, A. K., Lopez Soto, E. J., Raingo, J., Lee, C. E., Perello, M., et al. Neuroanatomical characterization of a growth hormone secretagogue receptor-green fluorescent protein reporter mouse. J Comp Neurol. 2014,522:3644-66.
[121] Mondal, M. S., Date, Y., Yamaguchi, H., Toshinai, K., Tsuruta, T., Kangawa, K., et al. Identification of ghrelin and its receptor in neurons of the rat arcuate nucleus. Regul.Pept. 2005,126:55-9.
[122] Hewson, A. K., Dickson, S. L. Systemic administration of ghrelin induces Fos and Egr-1 proteins in the hypothalamic arcuate nucleus of fasted and fed rats. J Neuroendocrinol. 2000,12:1047-9.

[123] Campbell, J. N., Macosko, E. Z., Fenselau, H., Pers, T. H., Lyubetskaya, A., Tenen, D., et al. A molecular census of arcuate hypothalamus and median eminence cell types. Nat Neurosci. 2017,20:484-96.
[124] Hamilton, C. L., Ciaccia, P. J., Lewis, D. O. Feeding behavior in monkeys with and without lesions of the hypothalamus. Am.J Physiol. 1976,230:818-30.
[125] Takasaki, Y. Studies on brain lesion by administration of monosodium L-glutamate to mice. I. Brain lesions in infant mice caused by administration of monosodium L-glutamate. Toxicology. 1978,9:293-305.
[126] Merchenthaler, I. Neurons with access to the general circulation in the central nervous system of the rat: a retrograde tracing study with fluoro-gold. Neuroscience. 1991,44:655-62.
[127] Tamura, H., Kamegai, J., Shimizu, T., Ishii, S., Sugihara, H., Oikawa, S. Ghrelin Stimulates GH But Not Food Intake in Arcuate Nucleus Ablated Rats. Endocrinology. 2002,143:3268-75.
[128] Luquet, S., Perez, F. A., Hnasko, T. S., Palmiter, R. D. NPY/AgRP neurons are essential for feeding in adult mice but can be ablated in neonates. Science. 2005,310:683-5.
[129] Dailey, M. J., Bartness, T. J. Arcuate nucleus destruction does not block food deprivation-induced increases in food foraging and hoarding. Brain Res. 2010,1323:94-108.
[130] Wang, L., Saint-Pierre, D. H., Tache, Y. Peripheral ghrelin selectively increases Fos expression in neuropeptide Y - synthesizing neurons in mouse hypothalamic arcuate nucleus. Neuroscience Letters. 2002,325:47-51.
[131] Day, D. E., Bartness, T. J. Agouti-related protein increases food hoarding, but not food intake by Siberian hamsters. Am.J.Physiol. 2004,286:R38-R45.
[132] Day, D. E., Keen-Rhinehart, E., Bartness, T. J. Role of NPY and its receptor subtypes in foraging, food hoarding, and food intake by Siberian hamsters. Am.J Physiol Regul.Integr.Comp Physiol. 2005,289:R29-R36.
[133] Teubner, B. J., Keen-Rhinehart, E., Bartness, T. J. Third ventricular coinjection of subthreshold doses of NPY and AgRP stimulate food hoarding and intake and neural activation. Am.J.Physiol Regul.Integr.Comp Physiol. 2012,302:R37-R48.
[134] Krashes, M. J., Koda, S., Ye, C., Rogan, S. C., Adams, A. C., Cusher, D. S., et al. Rapid, reversible activation of AgRP neurons drives feeding behavior in mice. J Clin.Invest. 2011,121:1424-8.
[135] Atasoy, D., Betley, J. N., Su, H. H., Sternson, S. M. Deconstruction of a neural circuit for hunger. Nature. 2012,488:172-7.
[136] Chen, H. Y., Trumbauer, M. E., Chen, A. S., Weingarth, D. T., Adams, J. R., Frazier, E. G., et al. Orexigenic action of peripheral ghrelin is mediated by neuropeptide Y and agouti-related protein. Endocrinology. 2004,145:2607-12.
[137] Nguyen, N. L., Barr, C. L., Ryu, V., Cao, Q., Xue, B., Bartness, T. J. Separate and shared sympathetic outflow to white and brown fat coordinately regulates thermoregulation and beige adipocyte recruitment. Am J Physiol Regul Integr Comp Physiol. 2017,312:R132-R45.
[138] Dailey, M. J., Bartness, T. J. Appetitive and consummatory ingestive behaviors stimulated by PVH and perifornical area NPY injections. Am.J.Physiol Regul.Integr.Comp Physiol. 2009,296:R877-R92.
[139] Wood, A. D., Bartness, T. J. Partial lipectomy, but not PVN lesions, increases food hoarding by Siberian hamsters. Am.J.Physiol. 1997,272:R783-R92.
[140] Garfield, A. S., Li, C., Madara, J. C., Shah, B. P., Webber, E., Steger, J. S., et al. A neural basis for melanocortin-4 receptor-regulated appetite. Nat Neurosci. 2015,18:863-71.

[141] Krashes, M. J., Shah, B. P., Madara, J. C., Olson, D. P., Strochlic, D. E., Garfield, A. S., et al. An excitatory paraventricular nucleus to AgRP neuron circuit that drives hunger. Nature. 2014,507:238-42.
[142] Krashes, M. J., Shah, B. P., Koda, S., Lowell, B. B. Rapid versus delayed stimulation of feeding by the endogenously released AgRP neuron mediators GABA, NPY, and AgRP. Cell Metab. 2013,18:588-95.
[143] Chen, Y., Lin, Y. C., Kuo, T. W., Knight, Z. A. Sensory detection of food rapidly modulates arcuate feeding circuits. Cell. 2015,160:829-41.
[144] Swanson, L. W., Hartman, B. K. The central adrenergic system. An immunofluorescence study of the location of cell bodies and their efferent connections in the rat utilizing dopamine-beta-hydroxylase as a marker. J Comp Neurol. 1975,163:467-505.
[145] Kelly, J., Alheid, G. F., Newberg, A., Grossman, S. P. GABA stimulation and blockade in the hypothalamus and midbrain: effects on feeding and locomotor activity. Pharmacology,Biochemistry,and Behavior. 1977,7:537-41.
[146] Naleid, A. M., Grace, M. K., Cummings, D. E., Levine, A. S. Ghrelin induces feeding in the mesolimbic reward pathway between the ventral tegmental area and the nucleus accumbens. Peptides. 2005,26:2274-9.
[147] Abizaid, A., Liu, Z. W., Andrews, Z. B., Shanabrough, M., Borok, E., Elsworth, J. D., et al. Ghrelin modulates the activity and synaptic input organization of midbrain dopamine neurons while promoting appetite. J Clin.Invest. 2006,116:3229-39.
[148] King, S. J., Isaacs, A. M., O'Farrell, E., Abizaid, A. Motivation to obtain preferred foods is enhanced by ghrelin in the ventral tegmental area. Horm.Behav. 2011,60:572-80.
[149] Weinberg, Z. Y., Nicholson, M. L., Currie, P. J. 6-Hydroxydopamine lesions of the ventral tegmental area suppress ghrelin's ability to elicit food-reinforced behavior. Neuroscience Letters. 2011,499:70-3.
[150] Faulconbridge, L. F., Cummings, D. E., Kaplan, J. M., Grill, H. J. Hyperphagic effects of brainstem ghrelin administration. Diabetes. 2003,52:2260-5.
[151] Gong, Y., Liu, Y., Liu, F., Wang, S., Jin, H., Guo, F., et al. Ghrelin fibers from lateral hypothalamus project to nucleus tractus solitaries and are involved in gastric motility regulation in cisplatin-treated rats. Brain Res. 2017,1659:29-40.
[152] Herman, M. A., Alayan, A., Sahibzada, N., Bayer, B., Verbalis, J., Dretchen, K. L., et al. micro-Opioid receptor stimulation in the medial subnucleus of the tractus solitarius inhibits gastric tone and motility by reducing local GABA activity. American journal of physiology. Gastrointestinal and liver physiology. 2010,299:G494-506.
[153] Sivarao, D. V., Krowicki, Z. K., Hornby, P. J. Role of GABAA receptors in rat hindbrain nuclei controlling gastric motor function. Neurogastroenterol Motil. 1998,10:305-13.
[154] Babic, T., Browning, K. N., Travagli, R. A. Differential organization of excitatory and inhibitory synapses within the rat dorsal vagal complex. American journal of physiology. Gastrointestinal and liver physiology. 2011,300:G21-32.
[155] Browning, K. N., Travagli, R. A. Mechanism of action of baclofen in rat dorsal motor nucleus of the vagus. American journal of physiology. Gastrointestinal and liver physiology. 2001,280:G1106-13.
[156] Herman, M. A., Cruz, M. T., Sahibzada, N., Verbalis, J., Gillis, R. A. GABA signaling in the nucleus tractus solitarius sets the level of activity in dorsal motor nucleus of the vagus cholinergic neurons in the vagovagal circuit. American journal of physiology. Gastrointestinal and liver physiology. 2009,296:G101-11.

[157] Cornejo, M. P., De Francesco, P. N., Garcia Romero, G., Portiansky, E. L., Zigman, J. M., Reynaldo, M., et al. Ghrelin receptor signaling targets segregated clusters of neurons within the nucleus of the solitary tract. Brain Struct Funct. 2018.
[158] Cui, R. J., Li, X., Appleyard, S. M. Ghrelin inhibits visceral afferent activation of catecholamine neurons in the solitary tract nucleus. J Neurosci. 2011,31:3484-92.
[159] Berthoud, H. R., Morrison, C. The brain, appetite, and obesity. Annu.Rev.Psychol. 2008,59:55-92.
[160] Schwartz, G. J., Moran, T. H., White, W. O., Ladenheim, E. E. Relationships between gastric motility and gastric vagal afferent responses to CCK and GRP in rats differ. Am.J.Physiol. 1997,272:R1726-R33.
[161] Berthoud, H. R., Sutton, G. M., Townsend, R. L., Patterson, L. M., Zheng, H. Brainstem mechanisms integrating gut-derived satiety signals and descending forebrain information in the control of meal size. Physiol Behav. 2006,89:517-24.
[162] Laughton, W. B., Powley, T. L. Localization of efferent function in the dorsal motor nucleus of the vagus. Am.J.Physiol. 1987,252:R13-R25.
[163] Williams, D. L., Kaplan, J. M., Grill, H. J. The role of the dorsal vagal complex and the vagus nerve in feeding effects of melanocortin-3/4 receptor stimulation. Endocrinology. 2000,141:1332-7.
[164] Fukuda, H., Mizuta, Y., Isomoto, H., Takeshima, F., Ohnita, K., Ohba, K., et al. Ghrelin enhances gastric motility through direct stimulation of intrinsic neural pathways and capsaicin-sensitive afferent neurones in rats. Scand J Gastroenterol. 2004,39:1209-14.
[165] Arnold, M., Mura, A., Langhans, W., Geary, N. Gut vagal afferents are not necessary for the eating-stimulatory effect of intraperitoneally injected ghrelin in the rat. J Neurosci. 2006,26:11052-60.
[166] Adachi, S., Takiguchi, S., Okada, K., Yamamoto, K., Yamasaki, M., Miyata, H., et al. Effects of ghrelin administration after total gastrectomy: a prospective, randomized, placebo-controlled phase II study. Gastroenterology. 2010,138:1312-20.
[167] Kitazawa, T., De, S. B., Verbeke, K., Depoortere, I., Peeters, T. L. Gastric motor effects of peptide and non-peptide ghrelin agonists in mice in vivo and in vitro. Gut. 2005,54:1078-84.
[168] Ang, D., Nicolai, H., Vos, R., Mimidis, K., Akyuz, F., Kindt, S., et al. Influence of ghrelin on the gastric accommodation reflex and on meal-induced satiety in man. Neurogastroenterol Motil. 2009,21:528-33, e8-9.
[169] Levin, F., Edholm, T., Schmidt, P. T., Gryback, P., Jacobsson, H., Degerblad, M., et al. Ghrelin stimulates gastric emptying and hunger in normal-weight humans. J Clin Endocrinol Metab. 2006,91:3296-302.
[170] Fujino, K., Inui, A., Asakawa, A., Kihara, N., Fujimura, M., Fujimiya, M. Ghrelin induces fasted motor activity of the gastrointestinal tract in conscious fed rats. J Physiol. 2003,550:227-40.
[171] Masuda, Y., Tanaka, T., Inomata, N., Ohnuma, N., Tanaka, S., Itoh, Z., et al. Ghrelin stimulates gastric acid secretion and motility in rats. Biochem Biophys Res Commun. 2000,276:905-8.
[172] Cummings, D. E., Overduin, J. Gastrointestinal regulation of food intake. J Clin Invest. 2007,117:13-23.
[173] Geliebter, A. Gastric distension and gastric capacity in relation to food intake in humans. Physiol Behav. 1988,44:665-8.

[174] Dockray, G. J. Gastrointestinal hormones and the dialogue between gut and brain. J Physiol. 2014,592:2927-41.
[175] Li, H., Zhang, J. B., Xu, C., Tang, Q. Q., Shen, W. X., Zhou, J. Z., et al. Effects and mechanisms of auricular vagus nerve stimulation on high-fat-diet--induced obese rats. Nutrition. 2015,31:1416-22.
[176] Cypess, A. M., White, A. P., Vernochet, C., Schulz, T. J., Xue, R., Sass, C. A., et al. Anatomical localization, gene expression profiling and functional characterization of adult human neck brown fat. Nat.Med. 2013,19:635-9.
[177] Depoortere, I., De Winter, B., Thijs, T., De Man, J., Pelckmans, P., Peeters, T. Comparison of the gastroprokinetic effects of ghrelin, GHRP-6 and motilin in rats in vivo and in vitro. Eur J Pharmacol. 2005,515:160-8.
[178] Xu, L., Depoortere, I., Tomasetto, C., Zandecki, M., Tang, M., Timmermans, J. P., et al. Evidence for the presence of motilin, ghrelin, and the motilin and ghrelin receptor in neurons of the myenteric plexus. Regul Pept. 2005,124:119-25.
[179] Bisschops, R., Vanden Berghe, P., Sarnelli, G., Janssens, J., Tack, J. CRF-induced calcium signaling in guinea pig small intestine myenteric neurons involves CRF-1 receptors and activation of voltage-sensitive calcium channels. American journal of physiology. Gastrointestinal and liver physiology. 2006,290:G1252-60.
[180] Kamegai, J., Tamura, H., Shimizu, T., Ishii, S., Sugihara, H., Wakabayashi, I. Chronic central infusion of ghrelin increases hypothalamic neuropeptide Y and agouti-related protein mRNA levels and body weight in rats. Diabetes. 2001,50:2438-43.
[181] Wirth, M. M., Giraudo, S. Q. Effect of agouti-related protein delivered to the dorsomedial nucleus of the hypothalamus on intake of a preferred versus a non-preferred diet. Brain Research. 2001,897:169-74.
[182] Thomas, M. A., Tran, V., Ryu, V., Xue, B., Bartness, T. J. AgRP knockdown blocks long-term appetitive, but not consummatory, feeding behaviors in Siberian hamsters. Physiol Behav. 2018,190:61-70.
[183] Bamshad, M., Song, C. K., Bartness, T. J. CNS origins of the sympathetic nervous system outflow to brown adipose tissue. Am.J.Physiol. 1999,276:R1569-R78.
[184] Bartness, T. J., Demas, G. E., Song, C. K. Central nervous system innervation of white adipose tissue. In: Klaus S, ed. Adipose Tissue. Georgetown, TX: Landes Bioscience; 2001. p. 116-30.
[185] Ryu, V., Bartness, T. J. Short and long sympathetic-sensory feedback loops in white fat. Am.J.Physiol Regul.Integr.Comp Physiol. 2014.
[186] Song, C. K., Jackson, R. M., Harris, R. B., Richard, D., Bartness, T. J. Melanocortin-4 receptor mRNA is expressed in sympathetic nervous system outflow neurons to white adipose tissue. Am.J.Physiol Regul.Integr.Comp Physiol. 2005,289:R1467-R76.
[187] Brito, M. N., Brito, N. A., Baro, D. J., Song, C. K., Bartness, T. J. Differential activation of the sympathetic innervation of adipose tissues by melanocortin receptor stimulation. Endocrinology. 2007,148:5339-53347.
[188] Brito, N. A., Brito, M. N., Bartness, T. J. Differential sympathetic drive to adipose tissues after food deprivation, cold exposure or glucoprivation. Am.J.Physiol Regul.Integr.Comp Physiol. 2008,294:R1445-R52.